MINISTRY OF SUPPLY

AERONAUTICAL RESEARCH COUNCIL
REPORTS AND MEMORANDA

All-Moving Wing-Tip Controls at Subsonic, Sonic, and Supersonic Speeds. A Discussion of Available Theoretical Methods and Their Application to a Delta Wing with Half-Delta Controls

By

H. H. B. M. THOMAS, B.Sc., A.F.R.Ae.S., and
K. W. MANGLER, Dr.Sc.nat., A.F.R.Ae.S.

All-Moving Wing-tip Controls at Subsonic, Sonic and Supersonic Speeds. A Discussion of Available Theoretical Methods and Their Application to a Delta Wing with Half-Delta Controls

By

H. H. B. M. Thomas, B.Sc., A.F.R.Ae.S., and K. W. Mangler, Dr.Sc.nat., A.F.R.Ae.S.

Summary.—Methods are now available to calculate throughout the speed range the performance of all-moving wing-tip controls on flat-plate wings in inviscid flow, neglecting the shock waves in the transonic regime. The theory, with all its limitations, seems likely to predict in broad outline the main features of this type of control, and should therefore be useful to designers who have hesitated to consider its adoption because of the lack on the one hand of experimental data and on the other of a reasonable analytical approach to the aerodynamics of the problem.

In this report, therefore, the theory has been developed and assembled in such a way as to be directly applicable to plan-forms, the spanwise sections of which consist of one segment only, and the case of half-delta controls on the tips of delta wings has been studied in some detail. Much of the theory applies also to plan-forms the spanwise sections of which consist, in part, of two or more segments, such as the swallow tail.

A numerical illustration for half-delta controls on a 60-deg delta wing has been used to compare with free-flight transonic measurements of rolling moment and hinge moment. The agreement is as good as could be expected.

---

1. *Introduction.*—Some unpublished work has shown that a case can be made for the consideration of all-moving wing-tip controls. An examination of the data reveals that while enough is known about such controls to encourage their use, much needs to be done before sufficient data exist to make the designer's problem one to be tackled confidently. The accumulation of data on the experimental side must necessarily take some considerable time, and so it is essential to consider how far theoretical study of the problem can supplement the experimental work.

In the present paper a start is made by considering the particular case of a delta wing with half-delta tip controls. The methods of calculation described are of general application, as indeed are some of the results particularly for the sonic and supersonic speeds.

Available theory enables us to calculate, at any rate approximately, most of the aerodynamic characteristics of interest. For all speed regimes, subsonic, supersonic, and transonic, the thickness of the wing and control is neglected, and the flow assumed to be inviscid. Such sweeping assumptions were considered justified because we are concerned here with the entire chordwise load, the whole chord being moved, and thus the problem has more in common with that of the two-dimensional lift and pitching moment than with that of the two-dimensional flap control. Experience has shown that these two quantities are much less affected by section shape and viscosity, than are the flap control characteristics. How far these hopes are realised is discussed in the concluding paragraphs of the text, where a comparison of the theoretical results and some experimental data is made throughout the Mach-number range. It should be noted that this limited comparison is not conclusive, since a number of further assumptions, and approximations are necessary to represent the conditions of the test. These are discussed in detail in Section 5.

For subsonic speeds the method of Multhopp is used, but alternative theories are mentioned in Section 2.2, some of which give as much information but others give only the spanwise lift distribution, and the quantities that can be derived therefrom. For all the subsonic theories some method of fairing the discontinuous incidence must be formulated. A number of fairings are considered and their merits briefly discussed. This is a problem to which further consideration could profitably be given.

The transonic properties are calculated on the basis of an extension of the so-called slender-wing theory, and the relevant analysis for a wing whose spanwise sections consist of one segment only (Fig. 1a) is given in Section 3.

At supersonic speeds the solution is readily obtained, and the pressure distribution is given in previous work. From these known results the local lift and pitching moment are obtained, as well as the overall lift, rolling moment, and hinge moments.

2. *Subsonic Theory.*—2.1. *Application of Multhopp's Method to the Problem.*—The problem of the all-moving wing-tip control is in effect the problem of calculating the lift distribution of a wing with (*a*) uniform incidence and (*b*) an incidence which is uniform and finite over the control span, and zero elsewhere. The incidence in (*b*) may be symmetrical or antisymmetrical. If we are prepared to accept the approximation of the flat plate in inviscid flow the method of calculating lift distribution due to Multhopp[1] is well suited to the problem as it deals directly with the two quantities of most interest, namely, the sectional lift and the sectional pitching moment. The sectional pitching moment is of course readily related to the hinge moment about any given hinge.

In common with any other lifting-surface theory, that of Multhopp cannot strictly be applied where there are discontinuities in incidence, and so some fairing of the incidence is advisable. The problem of what form this fairing should take has been considered to some extent in the present application, and the findings are noted in a later paragraph.

2.1.1. *The scope of Multhopp's method.*—In its present form Multhopp's method is designed to give the sectional lift and moment over a wing, with a rough approximation to the chordwise pressure distribution.

From a solution for the wing at uniform incidence, we can obtain the local lift-coefficient slope (a_{1i}) and the rate of change of the local pitching moment with incidence (m_{1i}), and hence the rate of change with incidence of the local hinge moment (b_{1i}) if desired. A spanwise integration over the span of the control gives the overall value of b_1.

Similarly from a solution with the control only at unit incidence we have the corresponding derivatives with respect to control deflection, that is, a_{2i}, m_{2i}, and b_2.

2

From the two sets of derivatives we can obtain the derivative m_l, the rate of change of the pitching moment with respect to control deflection at constant lift coefficient, since

$$m_l = m_{2l} - m_{1l}\frac{a_{2l}}{a_{1l}}.$$

This derivative enters into the calculation of aeroelastic effects.

2.1.2. Methods of fairing the discontinuous incidence.—As indicated earlier, the theory does not allow of discontinuity of incidence and some fairing to produce a continuous incidence distribution is necessary, but the question naturally arises as to how this should be done, and the extent to which different methods affect the results obtained. Multhopp suggests a method of fairing which depends on the relative location of the end of the control and the nearest pivotal stations. This method results in no fairing for a control ending halfway between two pivotal stations, and so the process is not a gradual one as the span of the control changes.

A few solutions of the same configuration with various methods of fairing ranging from no fairing (which means accepting the fairing implied by the interpolation functions which are a feature of Multhopp's method) to a fairing extending over the wing semi-span are given in Figs. 9 to 13 and 39. Examination of the results suggests that in the case of moving wing-tip control at any rate this aspect of the problem needs further investigation.

The effect of the fairing on the calculated loading and aerodynamic centre is clearly

    (*a*) reduced by increase of the number of spanwise pivotal stations

    (*b*) most pronounced in the neighbourhood of the inboard end of the control.

It seems to become less important as the span ratio of the control approaches 50 per cent, but in this connection it is necessary to note that the fairing is reflected in the loading as illustrated by Fig. 13, and the curve in Fig. 39 marked 'fairing of NACA TN 2282', which show an increased load inboard of the control. The same feature is illustrated by a comparison of Figs. 10 and 12.

The above methods of fairing the incidence are arbitrary. A rather more logical method, can be developed along the lines suggested by De Young in his use of Weissinger's method for finding the spanwise loading due to a control. The incidence is so arranged as to give agreement of the approximate lifting-surface theory with an exact solution in the limiting case of a very slender wing ($A \rightarrow 0$). Work is proceeding on the limiting form of the Multhopp method, but whilst it is possible to formulate the procedure for calculating the loading of a wing as the aspect ratio approaches zero, it is not yet clear how far the Multhopp procedure is reliable in dealing with the limiting case. It may be possible to discuss this aspect of the problem more fully in a later note.

In the meantime some check on the degree of approximation involved by the fairing is obtained by comparing results by different methods, and by calculation of the incidence corresponding to the various solutions at points along the three-quarter chord-line.

2.2. Other Theoretical Methods.—Other lifting-surface theories[2,3] can, of course, be applied to the problem of the wing with an all-moving wing-tip control, and the procedure to be followed in each case is fairly straightforward, apart from the incidence-fairing problem. Certain of these theories only yield limited data, and of these the most highly developed is the application of Weissinger's 7-point method by De Young[4,5]. He constructed charts for the influence functions which greatly reduce the work involved. His method of fairing the incidence has been mentioned above, but he calculates the incidence distribution for only a limited number of cases, although in the Weissinger method the coefficients required in the limiting case of $A \rightarrow 0$ (the $p_{\nu n}$ coefficients in De Young's notation) are independent of plan-form shape, and so the calculation can be further pre-digested and put into chart form. It is necessary here to note that the slender-wing theory as applied by De Young[7] is probably valid only for wings which are uni-sectional spanwise. Nevertheless, since additional calculations had to be made for the control-span ratios considered

here, it is thought worthwhile collecting the data so obtained, and presenting the values of γ/ξ (G/δ in De Young's notation). The incidence distribution to be used in any specific example for an outboard aileron can be obtained by substitution of (γ/ξ) from these charts (Figs. 35 and 37) in the following equations of Weissinger's theory:

Antisymmetrical

$$\left.\begin{aligned}
\frac{a_3}{\xi} &= 10\cdot4524\left(\frac{\gamma_3}{\xi}\right) - 3\cdot6954\left(\frac{\gamma_2}{\xi}\right) \\[2mm]
\frac{a_2}{\xi} &= -2\quad\left(\frac{\gamma_3}{\xi}\right) + 5\cdot6568\left(\frac{\gamma_2}{\xi}\right) - 2\left(\frac{\gamma_1}{\xi}\right) \\[2mm]
\frac{a_1}{\xi} &= \qquad\qquad\quad -1\cdot5308\left(\frac{\gamma_2}{\xi}\right) + 4\cdot3296\left(\frac{\gamma_1}{\xi}\right)
\end{aligned}\right\} \quad \dots \quad \dots \quad \dots \quad \dots \quad (1)$$

Symmetrical

$$\left.\begin{aligned}
\frac{a_3}{\xi} &= \quad 10\cdot4524\left(\frac{\gamma_3}{\xi}\right) - 3\cdot8284\left(\frac{\gamma_2}{\xi}\right) \qquad\qquad\qquad - 0\cdot2938\left(\frac{\gamma_0}{\xi}\right) \\[2mm]
\frac{\alpha_2}{\xi} &= -\quad 2\cdot0720\left(\frac{\gamma_3}{\xi}\right) + 5\cdot6568\left(\frac{\gamma_2}{\xi}\right) - 2\cdot3888\left(\frac{\gamma_1}{\xi}\right) \\[2mm]
\frac{a_1}{\xi} &= \qquad\qquad\qquad\quad -1\cdot8284\left(\frac{\gamma_2}{\xi}\right) + 4\cdot3296\left(\frac{\gamma_1}{\xi}\right) - 1\cdot7022\left(\frac{\gamma_0}{\xi}\right) \\[2mm]
\frac{a_0}{\xi} &= -\quad 0\cdot2242\left(\frac{\gamma_3}{\xi}\right) \qquad\qquad\qquad - 3\cdot1548\left(\frac{\gamma_1}{\xi}\right) + 4\left(\frac{\gamma_0}{\xi}\right)
\end{aligned}\right\} \quad \dots \quad \dots \quad (2)$$

The suffix here refers to the pivotal station in the Multhopp system, that is, numbering from the centre section as zero (De Young follows Weissinger and numbers from the wing tip).

Having determined the faired-incidence distribution we can, by use of the charts prepared in Refs. 4 and 5 for the influence functions, $p_{\nu n}$, readily set up the system of four equations for symmetric incidence, or three equations for the antisymmetric incidence (loading known to be zero at the centre section).

These are

$$a_\nu = \sum_{n=0\,\text{or}\,1}^{3} p_{\nu n}\gamma_n, \qquad \nu = 0, 1, 2, 3$$
$$\text{or} \quad 1, 2, 3$$

according to the type of incidence distribution. Solution of these equations yields the γ distribution, which is, of course, all that we can obtain from a Weissinger calculation. The results for one aileron-wing combination are compared with the Multhopp solution in Fig. 39.

Additional points can be obtained by a process of Fourier interpolation, explained in Ref. 4 for antisymmetric loading, and in Ref. 6 for symmetric loading. Figs. 36, 38 give data additional to the original references which are useful for the interpolation.

This method gives a quick and probably generally good approximation to the span loading, the lift, and the rolling moment.

Another method, which yields the same data, albeit not with comparable accuracy, deserves mention. It is an application by Sivells[7] of some lifting-line calculations due to Gdaliahu. Since on the basis of these calculations we can establish equality of the lift and approximate equality of the moment arising from a lift distribution due to twist, and a certain distribution derived from that due to uniform incidence, we may assume that these distributions are themselves approximately equal. This procedure yields simple relationships between the lift distribution due to twist (symmetric and antisymmetric) and that due to uniform incidence.

4

These are modified in Sivells' paper to include approximately the effect of sweep, and are further assumed to be improved by using the loading due to uniform incidence as determined either experimentally or by lifting-surface theory.

Evidently the method is not directly applicable to a discontinuous twist distribution, such as produced by deflection of a wing-tip control. To overcome this, Sivells suggests an arbitrary elliptic fairing of the incidence extending over the wing semi-span. This he admits is completely arbitrary and not necessarily the best. Comparison of results based on his method with those based on the other methods used herein indicates that this fairing is not particularly successful (*see* Fig. 39).

The direct relationship of the twist and the loading makes the calculation too dependent on the type of fairing used. It is perhaps a method that should be developed as a means of providing quick estimates when the span loading due to uniform incidence is known.

2.3. *Results*.—The calculations refer to three delta wings with all-moving half-delta wing-tip controls. The table below indicates the scope of the calculations:

Wing aspect ratio	Control span/wing span*
2·31 (equilateral triangle)	0·261 0·3354
1·848	0·261 0·3354
1·386	0·261 0·3354

The calculations are made for both symmetric and antisymmetric control deflection.

In addition, solutions are given for these three wings at incidence with controls undeflected, and certain cases are repeated with different methods of fairing the incidence for the deflected control condition.

The aspect ratios are so related that the results admit of two interpretations either as applying to three wings in an incompressible inviscid fluid or as applying to the wing of aspect ratio 2·31 at the three Mach numbers, 0, 0·6 and 0·8.

To obtain any of the derivatives listed in Table 2 for a delta wing of aspect ratio A at a Mach number of M we multiply the value of that derivative for the wing of aspect ratio $A\sqrt{(1-M^2)}$ by the factor $\{\sqrt{(1-M^2)}\}^{-1}$.

2.3.1. *Overall results*.—From the basic data, the overall lift pitching moment about the wing apex, and rolling moment can be calculated by the interpolation formulae of Multhopp[1]. In terms of γ and μ these quantities are

$$C_L = \frac{\pi A}{m+1} \sum_{-(m-1)/2}^{(m-1)/2} \gamma_n \cos \frac{n\pi}{(m+1)} \qquad \qquad (4)$$

$$C_M = \frac{\pi A^2}{2(m+1)} \sum_{-(m-1)/2}^{(m-1)/2} \left(\mu_n \frac{2c_n}{b} - \gamma_n \xi_{nc/4} \right) \cos \frac{n\pi}{m+1}. \qquad (5)$$

* These control-span ratios are dictated by the comparison we shall make later with the experimental results.

These become for symmetrical loading :

$$C_L = \frac{2\pi A}{m+1} \left[\frac{\gamma_0}{2} + \sum_1^{(m-1)/2} \gamma_n \cos \frac{n\pi}{m+1} \right] \quad \cdots \quad \cdots \quad \cdots \quad \cdots \quad \cdots \quad (6)$$

$$C_M = \frac{\pi A^2}{m+1} \left[\sum_1^{(m-1)/2} \left(\mu_n \frac{2c_n}{b} - \gamma_n \xi_{nc/4} \right) \cos \frac{n\pi}{m+1} + \frac{1}{2} \left(\mu_0 \frac{2c_0}{b} - \gamma_0 \xi_{0c/4} \right) \right] ; \quad \cdots \quad (7)$$

with the rolling-moment coefficient,

$$C_l = \frac{\pi A}{2(m+1)} \sum_1^{(m-1)/2} \gamma_n \sin 2\theta_n$$

$$= \frac{\pi A}{2(m+1)} \sum_1^{(m-1)/2} \gamma_n \sin \frac{2n\pi}{m+1} . \quad \cdots \quad \cdots \quad \cdots \quad \cdots \quad \cdots \quad \cdots \quad (8)$$

Since, of course, unit control deflection or incidence is always assumed, these are directly the derivatives

$$\frac{\partial C_L}{\partial \alpha} \text{ or } a_1 , \qquad \frac{\partial C_L}{\partial \xi} \text{ or } a_2 , \qquad \frac{\partial C_M}{\partial \alpha} \text{ or } m_1 ,$$

$$\frac{\partial C_M}{\partial \xi} \text{ or } m_2 , \quad \text{and } \frac{\partial C_l}{\partial \xi} \text{ or } l_\xi .$$

The hinge moment derivatives $\partial C_H/\partial \alpha$ or b_1, and $\partial C_H/\partial \xi$ or b_2 are not so readily calculated. The local hinge moment follows from the basic data, and an integration, which in the present calculations was performed graphically, over the span of the control gives the overall value. Thus

$$C_H = 2A \left(\frac{c_r}{c_{\xi r}} \right)^3 \int_{\eta_0}^1 \gamma \left(\frac{d}{\bar{c}} \right) d\eta , \qquad \cdots \quad \cdots \quad \cdots \quad \cdots \quad \cdots \quad \cdots \quad \cdots \quad (9)$$

where d is the distance between the local aerodynamic centre and the hinge line.

The hinge line assumed in the present calculations is at $0\cdot635$ of the root chord of the control, and is dictated by the comparison which we shall make later in the paper with some experimental results.

The results for the various configurations mentioned above are collected together in Tables 1 and 2, and illustrated by Figs. 2 to 15 and Figs. 31 to 33. A feature of the results which calls for comment is the appreciable effect of the fairing of the incidence distribution (*see* earlier remarks in Section 2.1). Another interesting result is that the hinge moment is of the same order of magnitude for symmetrical and antisymmetrical control deflection.

The large positive values of b_1 (Fig. 33) arise because of the further forward location of the local aerodynamic centre for the wing at incidence as the tip is approached as compared with the control-deflected condition (*cf.* Figs. 2 and 5).

If the results are interpreted as for a delta wing of aspect ratio $2\cdot31$ at various Mach numbers, it is seen that as Mach number is increased the overall lift, and pitching moment approach their sonic values, that is,

$$a_1 \rightarrow \frac{\pi A}{2} = 3\cdot63$$

$$- m_1 \rightarrow \frac{2\pi A}{3} = 4\cdot83 .$$

The control becomes more nearly balanced as the aerodynamic-centre locus moves aft on the wing, making b_2 (Fig. 32) numerically small for this hinge position. The derivative b_1 (Fig. 33) is also affected but not to such a marked degree. Figs. 32 and 33 also illustrate the low-speed interpretation of the hinge-moment results.

6

2.3.2. *Lift distributions and aerodynamic-centre locations.*—The spanwise lift distribution is presented in the form of γ, the non-dimensional circulation, of $C_{LL}c/2b$. This is not the most usual form of presentation but has the advantage that it applies equally to the two interpretations of the results, *viz.*, different wings at zero Mach number or the same wing at different Mach numbers.

The local aerodynamic centre is given as a fraction of the local chord measured from the leading edge of the chord, and this quantity is independent of the transformation to compressible flow.

For the wings at uniform incidence the results are presented in Figs. 2, 3 and 4. It is seen that the spanwise loading approaches the elliptic loading of the sonic and supersonic solutions as the Mach number approaches unity or on the low-speed interpretation of the results as the aspect ratio approaches zero. Similarly the locus of the aerodynamic centre moves aft towards the locus for sonic speeds, or zero aspect ratio.

In Figs. 5 to 15 the solutions in terms of γ and the aerodynamic-centre locus are displayed for various wing-tip control arrangements operated symmetrically and antisymmetrically. Fig. 9 gives the results for antisymmetric deflection of a half-delta wing-tip control of span ratio $0 \cdot 261$, fitted to a delta wing of aspect ratio $2 \cdot 31$ ($M = 0$). It demonstrates the extent to which the method of fairing the incidence affects the solution by comparing a solution based on the method of fairing proposed by Multhopp with the extreme case where no fairing was applied. As is to be expected, the loading, and the aerodynamic-centre locus in the neighbourhood of the inboard end of the control, are the most affected.

Figs. 14 and 15 show the effect of increasing the span ratio of the all-moving wing-tip control from $0 \cdot 261$ to $0 \cdot 335$ on the delta wing of aspect ratio $2 \cdot 31$ at zero Mach number. Fig. 15 refers to symmetric control deflection and Fig. 14 to antisymmetric deflection. An interesting feature of both these figures is the very small effect of the increased span ratio on the aerodynamic centre except near the inboard end of the control.

For the same wing at a Mach number of $0 \cdot 6$ or a delta wing of aspect ratio $1 \cdot 848$ at low speed, we have the span loading and aerodynamic-centre locus shown in Figs. 5 to 8. Fig. 5 compares results for antisymmetric deflection of the smaller span control with those for the previous condition (i.e., $A = 2 \cdot 31$; $M = 0$). It is seen that the effect of changing the Mach number by $0 \cdot 6$ or reducing the aspect ratio to $1 \cdot 848$ is small on both γ and h.

Similar remarks apply to the results for $M = 0 \cdot 8$, $A = 2 \cdot 31$ or $M = 0$, $A = 1 \cdot 386$ (also illustrated by Fig. 5).

Fig. 12 demonstrates the effect of fairing on the results for symmetric deflection of a control of the larger span ratio ($0 \cdot 335$), and suggests that for this span ratio the effect is not marked, and is particularly small on the aerodynamic-centre locus.

The results for symmetric deflection of the larger span control at the three Mach numbers 0, $0 \cdot 6$, and $0 \cdot 8$ (or on the alternative interpretation for $A = 2 \cdot 31$, $1 \cdot 848$ and $1 \cdot 386$) are compared in Fig. 8. The relatively small differences in the values of both γ and h, taken in conjunction with the previous results for antisymmetrical deflection of the control, indicate that the effects of compressibility (or low aspect ratio) on γ and h are in the main confined to Mach numbers near sonic (or aspect ratios near zero). If this is generally true, it represents a considerable saving of labour because only few subsonic results are required. Indeed a reasonable approximation could be obtained by taking the values of γ and h at only one Mach number, and assuming that these apply in the range of Mach number 0 to $0 \cdot 8$ (say), the appropriate factor being used when these are converted into lift, pitching moment, etc.

2.3.3. *Spanwise variation of the derivatives a_1, a_2, m_1 and m_2.*—For certain reasons (Section 2.3.2), it is convenient to present the results in the form of curves of γ and h, but the interpretation of these in terms of the delta wing of aspect ratio $2 \cdot 31$ at various Mach numbers is worth considering in greater detail. Accordingly the results discussed in Section 2.3.2 have been converted into the more familiar sectional derivatives, a_{1l}, a_{2l}, m_{1l}, and m_{2l}. These are collected together

and presented in the form of a carpet plotting, together with the sonic and supersonic results (*see* Figs. 25 to 30), to give an overall picture of the speed effect. The sonic values are obtained in a manner similar to that used for the subsonic values, from the basic data of Figs. 16 and 17. At supersonic speeds the sectional derivatives can be evaluated in a closed analytic form (equations (37) to (50)).

3. *Sonic Theory.*—For the sonic range ($M \sim 1$) we employ the linearized-potential theory as outlined in Ref. 9. We have to solve first a two-dimensional problem in the (y,z) plane and these 'sectional' solutions, which contain x as a parameter, are afterwards connected, by means of the boundary conditions on the wing, to form a solution of our three-dimensional problem (slender-wing theory). At first we consider a wing with one aileron only. The case of a wing with two ailerons, deflected either in the same or in opposite directions, is then dealt with by linear combination of two such solutions.

3.1. *Solution for One Aileron.*—In this paper we consider only plan-forms, for which at the chordwise station x the wing extends for $- y_l(x) \leqslant y \leqslant + y_l(x)$ (*see* Fig. 1). The more general type of wing (*see* Fig. 1b) can be dealt with by suitable extension of the theory of Ref. 9. The aileron is defined by $0 < y_0(x) \leqslant y \leqslant y_l(x)$. Any more general aileron shape can be obtained as a linear combination of solutions of the present type.

As has already become apparent in Ref. 9, it is not easy to derive the formulae for the pressure distribution in a direct way from the two-dimensional Laplace equation and the boundary conditions. For the sake of brevity we shall firstly state the solutions and show afterwards that all necessary conditions are satisfied. The uniqueness of our solutions can be proved in a similar way to that of Appendix I of Ref. 3, for the cases given there.

When using a similar notation as in Ref. 9, the pressure p and the enthalpy I can best be written as (ξ = aileron deflection):

$$\frac{p - p_\infty}{\rho V^2} = \frac{I}{V^2} = - \xi \frac{d}{dx} \mathscr{R} \{ y_l(x) F(y,z) \} . \quad \ldots \quad \ldots \quad \ldots \quad \ldots \quad \ldots \quad \ldots \quad (10)$$

The symbol $\mathscr{R}$ denotes the real part of the complex function

$$F = F(Z) , \qquad Z = y + iz , \quad \ldots \quad \ldots \quad \ldots \quad \ldots \quad \ldots \quad \ldots \quad \ldots \quad (11)$$

so that (10) satisfies the Laplace equation in y and z as required. We choose $F = 0$ for all points ahead of and behind the aileron and

$$y_l F(Z) = \frac{1}{\pi} \left[(Z - y_0) \log \frac{y_l^2 - Zy_0 + \sqrt{(y_l^2 - y_0^2)} \sqrt{(y_l^2 - Z^2)}}{y_l(y_0 - Z)} \right. $$
$$\left. + \sqrt{(y_l^2 - Z^2)} \cos^{-1} \frac{y_0}{y_l} \right] \quad \ldots \quad \ldots \quad \ldots \quad \ldots \quad \ldots \quad \ldots \quad \ldots \quad (12)$$

for all spanwise sections, which intersect the aileron, so that

$$y_l \frac{dF}{dZ} = \frac{1}{\pi} \left[\log \frac{y_l^2 - Zy_0 + \sqrt{(y_l^2 - y_0^2)} \sqrt{(y_l^2 - Z^2)}}{y_l(y_0 - Z)} - \frac{\sqrt{(y_l^2 - y_0^2)}}{\sqrt{(y_l^2 - Z^2)}} \right. $$
$$\left. - \frac{Z}{\sqrt{(y_l^2 - Z^2)}} \cos^{-1} \frac{y_0}{y_l} \right] . \quad \ldots \quad \ldots \quad \ldots \quad \ldots \quad \ldots \quad \ldots \quad (13)$$

The boundary conditions for $|Z| \to \infty$ are satisfied, since $F(Z)$ and dF/dZ vanish there.

8

From the Euler equation

$$\frac{\partial}{\partial z}\left(\frac{I}{V^2}\right) = -\frac{d}{dx}\frac{w}{V},$$

we find for the downwash $-w/V$ on the wing with (10) and (13):

$$\left(-\frac{w}{V}\right)_{z=0} = \int_{-\infty}^{x}\frac{\partial}{\partial z}\frac{I}{V^2}dx = -\xi\,\mathscr{R}\left\{iy_l\frac{dF}{dZ}\right\}_{z=0} = \begin{Bmatrix}\xi \\ 0\end{Bmatrix}\cdots \qquad \cdots \qquad \cdots \qquad \cdots \quad (14)$$

as required, since

$$\mathscr{R}\left\{iy_l\frac{dF}{dZ}\right\} = \begin{Bmatrix}i^2 \\ 0\end{Bmatrix}\text{ for }\begin{Bmatrix}y_0 < y < y_l \\ -y_l < y < y_0\end{Bmatrix}$$

(It can easily be seen that $\log(y_0 - y) = \log|y_0 - y| - i\pi$ for points on the aileron ($y_0 < y$) and $\log(y_0 - y) = \log|y_0 - y|$ for points on the wing outside the aileron.) The function $F(Z)$ vanishes for $y_0 = y_l$, i.e., there is no disturbance in the pressure field ahead of the aileron.

The non-dimensional load coefficient l for a uni-sectional wing with one deflected aileron is according to (10) and (12):

$$l = -\frac{4I}{V^2} = 4\xi\frac{d}{dx}\mathscr{R}\{y_lF(Z)\}_{z=0} \qquad \cdots \qquad \cdots \qquad \cdots \qquad \cdots \qquad \cdots \quad (15)$$

since $y_0(x)$ and $y_l(x)$ are in general functions of x, the load consists of two terms:

$$l(x,y) = -\frac{4\xi}{\pi}\frac{dy_0}{dx}\log\frac{y_l^2 - yy_0 + \sqrt{(y_l^2 - y_0^2)}\sqrt{(y_l^2 - y^2)}}{y_l|y_0 - y|}$$

$$+ \frac{4\xi}{\pi}\frac{dy_l}{dx}\left[\cos^{-1}\frac{y_0}{y_l} + \frac{y}{y_l}\sqrt{\left(1 - \frac{y_0^2}{y_l^2}\right)}\right]\frac{y_l}{\sqrt{(y_l^2 - y^2)}}\cdot \qquad \cdots \qquad \cdots \quad (16)$$

Since the second term tends to infinity for $y \to y_l$, this expression holds only if $y = y_l(x)$ describes the leading edge of the wing, i.e., for $dy_l/dx \geqslant 0$. According to the Kutta-Joukowsky condition the pressure must remain finite along the trailing edge. In order to achieve this we add for the rear part of the wing (where $dy_l/dx < 0$) in (10) the term

$$-\xi\frac{d}{dx}\mathscr{R}(y_lF^*) = \mathscr{R}\frac{\xi}{\pi}\left\{\cos^{-1}\frac{y_0}{y_l}\frac{y_l}{\sqrt{(y_l^2 - Z^2)}}\frac{dy_l}{dx}\right.$$

$$\left. + \sqrt{\left(1 - \frac{y_0^2}{y_l^2}\right)}\left(\frac{Z}{\sqrt{(y_l^2 - Z^2)}} + \frac{1}{i}\right)\frac{dy_l}{dx}\right\}, \cdots \qquad \cdots \qquad \cdots \qquad \cdots \quad (10a)$$

which is a combination of the pressure functions for the incidence case and the rolling-wing case in Ref. 9. Since

$$-\frac{d}{dx}\frac{w}{V} = \frac{\partial}{\partial z}\frac{I}{V^2}$$

still vanishes along the wing surface, all the boundary conditions are satisfied and the resulting pressure distribution remains finite along the trailing edge. We obtain for $dy_l/dx < 0$:

$$l(x,y) = -\frac{4\xi}{\pi}\frac{dy_0}{dx}\log\frac{y_l^2 - yy_0 + \sqrt{(y_l^2 - y_0^2)}\sqrt{(y_l^2 - y^2)}}{y_l|y_0 - y|}\cdot \qquad \cdots \qquad \cdots \quad (16a)$$

Thus the flow is deflected through the angle ξ either along the line $y = y_0(x)$ or in passing round the leading edge of the aileron. It follows this direction as long as

$$\frac{\partial}{\partial z}\left(\frac{I}{V^2}\right)_{z=0} = 0$$

9

on the wing. For an aileron, which is shaped as indicated in the adjoining figure (FIG. I (a)), we have no load on those parts of the wing which are either ahead of or behind the aileron. Only the shaded parts are loaded. The pressure tends to infinity along the leading edge KL of the aileron and is finite (or zero) along its trailing edge LM. A weaker (logarithmic) infinity occurs along the line KNM $(y = y_0(x))$.
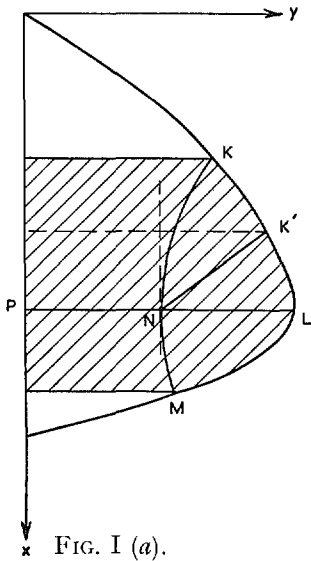
FIG. I (a).

Since the load on the forward part of the wing (up to the line PL where $y_l = s$) can also be written as in equation (15), this part of the load can easily be integrated, in order to find its contribution to the lift and the rolling moment due to a deflection of the aileron. The result depends only on the value of the function $F(Z)$ along the section PL and is therefore independent of the particular aileron shape. An aileron bounded by K'NM would produce the same lift and rolling moment as an aileron KNM. Obviously this does not apply for the pitching moment nor for an alteration of the line NM.
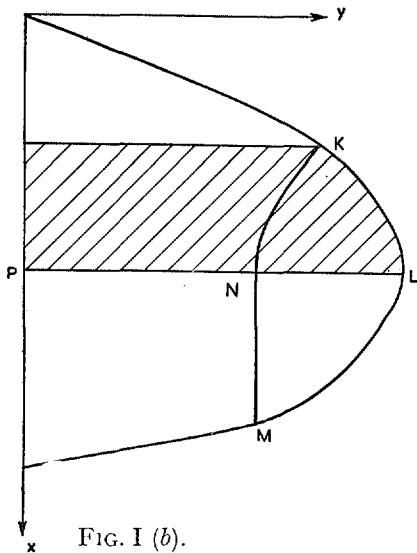
FIG. I (b).

If $y_0(x)$ is constant for all points behind the line PL (FIG. I (b)), only the forward part of the wing with $dy_l/dx \geqslant 0$ carries a load. For such plan-forms (*see* figure), the lift and the rolling moment depend only on the conditions along the line PL. The local lift coefficient $\tilde{C}_{LL}$, the lift C_L and the rolling moment C_l are functions of the ratio PN/PL only.
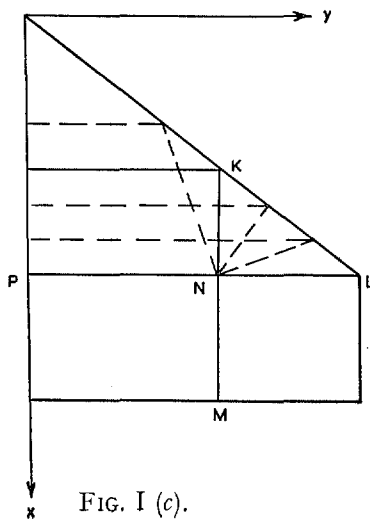
FIG. I (c).

The same applies for a delta wing and a cropped delta wing (FIG. I (c)), provided that y_0 is constant for all sections behind PL, so that the entire load is concentrated on the forward part of the wing.

10

3.2. *Forces and Moments for One Aileron.*—The forces and moments due to a deflection of the aileron can now be obtained by integrating the load distribution $l(x,y)$. We restrict our attention to such plan-forms, for which $y_0 = $ const in the rear part of the wing, where $dy_l/dx < 0$. Then we have no load on the rear part of the wing and the integration must be extended over the front part, where $dy_l/dx \geqslant 0$ up to the point, where $y_l = s = b/2$.

Thus we have for the rolling moment due to one aileron:

$$- \tfrac{1}{2}\rho V^2 \int \int ly\, dx\, dy = - \tfrac{1}{2}\rho V^2 SAb \frac{1}{8} \int \int \frac{ly\, dx\, dy}{s^3}$$

$$= - \xi \tfrac{1}{2}\rho V^2 SbA \frac{1}{8} \int_{-s}^{s} \left(\frac{yF_0(y)}{s^2} \right)_{y_l=s} dy , \quad .. \qquad .. \qquad .. \quad (17)$$

where (*cf.* equation (15)):

$$\pi F_0 = \pi F_0(y) \frac{y - y_0}{y_l} \log F_1 + \sqrt{\left(1 - \frac{y^2}{y_l^2} \right)} \cos^{-1} \frac{y_0}{y_l}$$

and

$$F_1 = \frac{y_l^2 - yy_0 + \sqrt{(y_l^2 - y_0^2)}\sqrt{(y_l^2 - y^2)}}{y_l|y_0 - y|} .$$

Since according to Appendix II, Section 2

$$\int_{-s}^{s} (ysF_0)_{y_l=s}\, dy = \tfrac{1}{6}(s^2 - y_0^2)^{3/2} ,$$

we obtain for the derivative l_ξ:

$$l_\xi = - \frac{d}{d\xi} \int \int \frac{ly\, dx\, dy}{Sb} = - \frac{A}{12} \left(1 - \frac{y_0^2}{s^2} \right)^{3/2} . \qquad .. \qquad .. \quad (18)$$

In order to obtain the pitching moment and the hinge moment it is convenient to calculate first the force produced by the aileron deflection on the entire wing, on the aileron and on the ' complementary ' aileron. This is the part of the wing on the other side, which is symmetric to the aileron, but remains undeflected. The latter force is required in order to combine two solutions for the case of two ailerons, which may be deflected either in the same or in opposite directions.

We integrate

$$\tfrac{1}{2}\rho V^2 \int \int l\, dx\, dy = \tfrac{1}{2}\rho V^2 SA \frac{1}{4} \int \int \frac{l\, dx\, dy}{s^2}$$

$$= \tfrac{1}{2}\rho V^2 SA\, \xi \int \left(\frac{sF_0}{s^2} \right)_{y_l=s} dy$$

between the appropriate limits and obtain (*cf.* Appendix II, Section 2) for the wing:

$$\frac{dC_L}{d\xi} = \frac{A}{2} \left[\cos^{-1} \frac{y_0}{s} - \frac{y_0}{s} \sqrt{\left(1 - \frac{y_0^2}{s^2} \right)} \right] ; \qquad .. \qquad .. \qquad .. \qquad .. \quad (19)$$

for the aileron:

$$\frac{dC_L}{d\xi} = \frac{A}{2\pi} \left[1 - \frac{y_0^2}{s^2} - 2\frac{y_0}{s} \sqrt{\left(1 - \frac{y_0^2}{s^2} \right)} \cos^{-1} \frac{y_0}{s} + \left(\cos^{-1} \frac{y_0}{s} \right)^2 \right] \quad .. \quad (20)$$

11

and for the complementary aileron:

$$\frac{dC_L}{d\xi} = \frac{A}{2\pi}\left[4\frac{y_0^2}{s^2}\log\left|\frac{s}{y_0}\right| - \left(1 - \frac{y_0^2}{s^2}\right) - 2\frac{y_0}{s}\sqrt{\left(1 - \frac{y_0^2}{s^2}\right)}\cos^{-1}\frac{y_0}{s}\right.$$

$$\left. + \left(\cos^{-1}\frac{y_0}{s}\right)^2\right]. \qquad \cdot\cdot \qquad \cdot\cdot \qquad \cdot\cdot \qquad \cdot\cdot \qquad \cdot\cdot \qquad \cdot\cdot \qquad (21)$$

The results (18) to (21) are proportional to the aspect ratio A of the wing. They depend only on the ratio y_0/s of the aileron span to the wing span at the maximum span $y_l = s$ as explained above. The results are independent of the shape of the forward part of the wing and the aileron (where $dy_l/dx > 0$). But when considering the pitching moment or hinge moments, we have to allow for the actual shape of the wing and the ailerons.

We consider only wing plan-forms with a straight leading edge $(y_l = x\cot\Lambda)$ and a moving wing tip $(y_0 = \text{const})$. Then we find for the pitching moment of the wing with respect to an axis through the apex of the wing $(x = 0)$:

$$\tfrac{1}{2}\rho V^2 \iint xl\,dx\,dy = \tfrac{1}{2}\rho V^2\, S\bar{c}A\,\frac{1}{4}\iint \frac{xl\,dx\,dy}{\bar{c}s^2}$$

$$= \tfrac{1}{2}\rho V^2\, S\bar{c}A\,\xi\int\frac{x}{\bar{c}}\frac{d}{dx}\int\frac{y_l F_0\,dy}{s^2}\,dx$$

or, when integrating by parts:

$$\frac{dC_M}{d\xi} = A\int\frac{x}{\bar{c}}\frac{d}{dx}\int\frac{y_l F_0\,dy}{s^2}\,dx$$

$$= \frac{1}{2}\left[\frac{dC_L}{d\xi} - A\int_{y_0}^s\left(\int\frac{y_l F\,dy}{s^2}\right)_{y_l=s}\frac{dy_l}{s}\right]A\tan\Lambda, \qquad \cdot\cdot \qquad \cdot\cdot \qquad (22)$$

where $x/\bar{c}$ has been expressed in terms of the aspect ratio, and y_l,

$$\frac{x}{\bar{c}} = \frac{y_l}{s}\frac{A}{2}\tan\Lambda. \qquad \cdot\cdot \qquad \cdot\cdot \qquad \cdot\cdot \qquad \cdot\cdot \qquad \cdot\cdot \qquad \cdot\cdot \qquad \cdot\cdot \qquad (23)$$

We use the last equation of Appendix II, Section 2 and find for the pitching-moment coefficient of the wing, due to the deflection of one aileron:

$$\frac{dC_M}{d\xi} = \frac{A\tan\Lambda}{2}\left[\frac{dC_L}{d\xi} - \frac{A}{6}\left\{\cos^{-1}\frac{y_0}{s} - 2\frac{y_0}{s}\sqrt{\left(1 - \frac{y_0^2}{s^2}\right)} + \frac{y_0^3}{s^3}\log\frac{s + \sqrt{(s^2 - y_0^2)}}{|y_0|}\right\}\right]$$

$$= \frac{A\tan\Lambda}{12}\left[2\cos^{-1}\frac{y_0}{s} - \frac{y_0}{s}\sqrt{\left(1 - \frac{y_0^2}{s^2}\right)} - \frac{y_0^3}{s^3}\log\frac{s + \sqrt{(s^2 - y_0^2)}}{|y_0|}\right]. \cdot\cdot \qquad \cdot\cdot \qquad (24)$$

This result holds for 'cropped' delta wings with a moving wing tip $(A = 4\cot\Lambda(1 - \lambda)/(1 + \lambda)$, $\lambda = \text{taper ratio})$.

It did not appear to be feasible to obtain a similar expression for the pitching moment of the aileron and the 'complementary' aileron. Instead, the chordwise integration, as required by (22), was carried out numerically, using the results of Appendix II for the spanwise integration.

It may be pointed out, that the spanwise load distribution over a wing with deflected aileron was calculated by De Young[8] by means of a different method, from which he obtained the forces and rolling moments, but not the pitching moments or the hinge moments.

3.3. *Results.*—Fig. 16 shows the spanwise distribution of the local lift coefficient C_{LL} for a delta wing of aspect ratio $A = 4 \cot \Lambda$ and various positions (y_0/s) of the aileron. The picture represents the load for the case of two ailerons deflected either in the same or in opposite directions. The corresponding positions of the local aerodynamic centre are shown in Fig. 17.

The overall forces and moments can be obtained as integrals over these spanwise distributions. But we preferred the more convenient way for performing the integration as described in the preceding section. Fig. 18 shows the rolling moment due to the deflection of two wing tips, as a function of y_0/s. The derivative l_ξ can for $0 \cdot 5 < y_0/s < 0 \cdot 9$ be approximated by a linear function of y_0/s:

$$- l_\xi = \frac{A}{12} \left[2^{3/2} - 3 \frac{y_0}{s} \right] \qquad \cdots \qquad \cdots \qquad \cdots \qquad \cdots \qquad \cdots \qquad (25)$$

(exact for $y_0/s = 1/\sqrt{2}$). Thus in the practically important range l_ξ is a linear function of the ratio flap span/wing span $(1 - y_0/s)$. The dependency of l_ξ on the ratio flap area/wing area (which equals $(1 - y_0/s)^2$) is more complicated. An increase in the area ratio produces a smaller increase in l_ξ than a corresponding increase in the span-ratio.

This shows that the relevant parameter describing the aileron efficiency is not the area of the moving tip, but rather its span $(1 - y_0/s)$.

Since the damping in roll for a delta wing at sonic speeds is $- l_p = \pi A/32$, we have

$$\frac{\xi l_\xi}{- l_p} = \xi \frac{16}{3\pi} \left(1 - \frac{y_0^2}{s^2} \right)^{3/2} , \qquad \cdots \qquad \cdots \qquad \cdots \qquad \cdots \qquad \cdots \qquad (26)$$

which, according to the simple theory of roll, must be equal to $pb/2V$ for a steady roll. Thus we can determine the aileron deflection required to produce a certain roll.

In order to estimate the hinge moments we represent the magnitude and position of the force on the aileron. Since the aileron angle is not always the same on both wing tips, we show in Figs. 19 and 20 the effects for one deflected aileron. Fig. 19 shows the force

$$\frac{1}{A} \frac{dC_L}{d\xi} = \frac{\pi}{2} \frac{(dC_L/d\xi)}{(dC_{L \, wing}/d\alpha)} = \frac{\pi}{2} \frac{a_2}{a_1}$$

for the deflected aileron, for the ' complementary ' aileron (*i.e.*, the part of the wing on the other side, which corresponds to the aileron and remains undeflected) and for the whole wing. The position of these forces in terms of the aileron root chord (measured from the apex of the aileron) is represented in Fig. 20. Figs. 21 and 22 show the forces and their position for the case of two ailerons deflected by the same angle ξ either in the same (elevator case) or in opposite directions. These results are obtained by combining the results in Figs. 19 and 20. Fig. 22 shows that the position of the force on the ailerons is always approximately 2/3 of the aileron root chord behind the aileron apex, whereas the position of the force on the entire wing is in the elevator case a little more forward. There is of course no resultant force in the aileron case, but only a couple.

13

4. *Supersonic Theory*.—The results given here are based on the linearised inviscid flow theory, and details of the calculations are given in the appendices, or in the references given therein.

Before quoting the expressions for the various aerodynamic characteristics it may be useful to give a brief discussion of how deflection of an all-moving tip affects the loading of a wing.

Referring to the diagrams, where ODC is the control, and OB, OB′ the Mach lines from the control apex, we note that only those parts of the wing which are shaded carry any load. It thus follows that the geometry of that part of the wing lying ahead of the line OA (normal through O to centre-line) plays no part in the derivatives with respect to control angle. When the speed is reduced to sonic the Mach cone degenerates into the plane through AO and normal to the flight direction.

In the special case of a delta wing with half-delta wing-tip control, which is the only configuration considered in detail here, we have the disposition of load as shown in the accompanying diagrams. The results which follow apply so long as there is no mutual interference of the port and starboard controls, that is, provided OB cuts the centre-line at a point behind the trailing edge of the root chord. The derivatives with respect to control angle apply with this restriction to all wings with unswept trailing edges, but it is clear that the wing geometry plays a much more important part in the derivatives with respect to incidence.
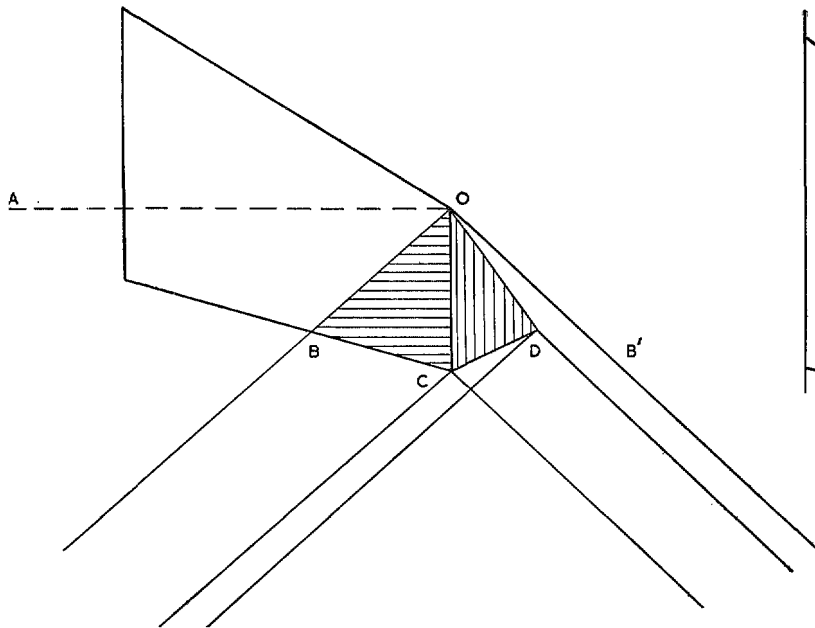
Fig. II (*a*) Subsonic leading edge.
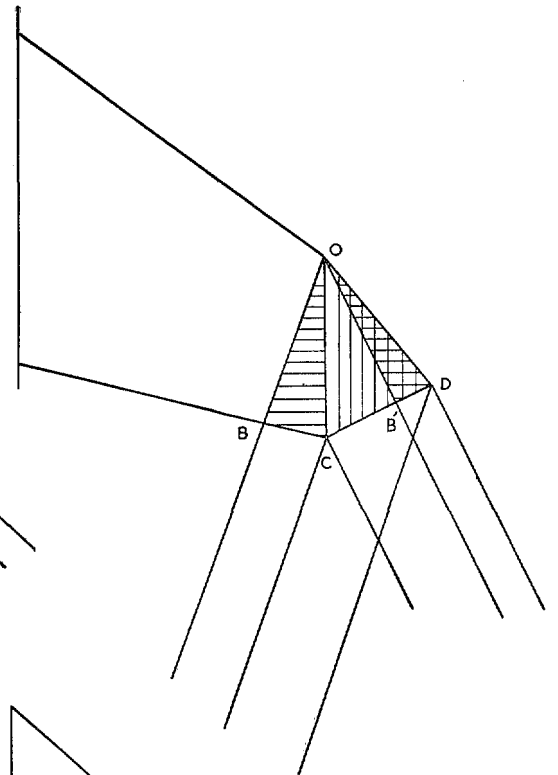
Fig. II (*b*) Supersonic leading edge.
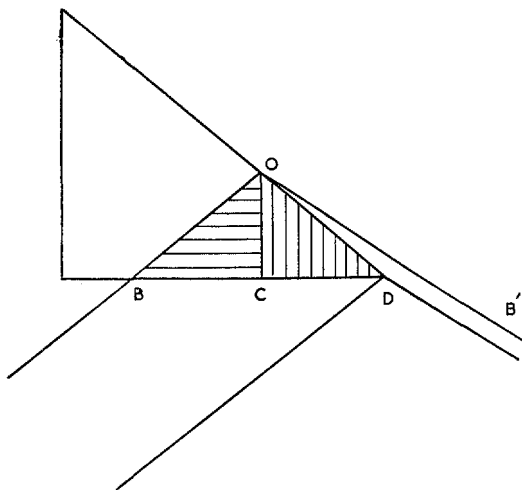
Fig. II (*c*) Subsonic leading edge.
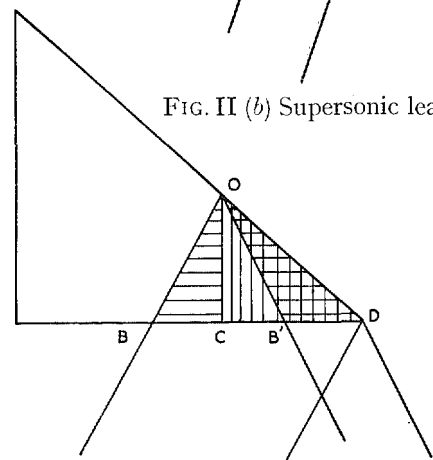
Fig. II (*d*) Supersonic leading edge.

14

4.1. *Overall Derivatives for Half-Delta Controls on a Delta Wing.*—For the delta wing with subsonic leading edges, we have for rate of change of the hinge moment with incidence, for an axis parallel to the trailing edge,

$$b_1 = \frac{A}{(1-\eta_0)^3 E\{\sqrt{(1-k^2)}\}} \left[(2\xi_h - 1)\{\tfrac{1}{2}\pi - \eta_0\sqrt{(1-\eta_0^2)} - \sin^{-1}\eta_0\} \right.$$

$$\left. + \frac{2}{3}\left\{\eta_0^3 \log\left(\frac{1+\sqrt{(1-\eta_0^2)}}{\eta_0}\right) - \frac{1}{4}\pi - \frac{\eta_0\sqrt{(1-\eta_0^2)}}{2} + \tfrac{1}{2}\sin^{-1}\eta_0\right\} \right]. \qquad .. \qquad .. \quad (27)$$

For notation, *see* Fig. 1, Appendix I, and list of symbols.

When the wing leading edge is supersonic we have for the same derivative,

$$b_1 = \frac{8}{3(1-\eta_0)^3\sqrt{(k^2-1)}} \left[\frac{A^3}{256}(1-\eta_0)(k-1)\left\{12\xi_h(1+\eta_0) - (k+1)(1+\eta_0+\eta_0^2)\tfrac{1}{4}A^2\right\} \right.$$

$$+ \frac{(k-1)\{(k+1)-3k\xi_h\}}{6k^2\beta} - \frac{(k-1)\beta A^3}{384k^2}\{(k+1)\beta\eta_0 - 3k\xi_h\}$$

$$- \frac{\sqrt{(k^2-1)}}{6\pi k^2}(\tfrac{1}{2}\pi - \sin^{-1}\beta\eta_0) - \frac{\sqrt{(k^2-1)}}{96\pi k^2}\beta\eta_0 A\sqrt{(16-A^2\beta^2\eta_0^2)}$$

$$\left. + \frac{\sqrt{(k^2-1)}}{192\pi k^2}\beta^3 A^3\eta_0^3 \log\left\{\frac{4+\sqrt{(16-\beta^2 A^2\eta_0^2)}}{\beta A\eta_0}\right\} \right]. \quad .. \qquad .. \qquad .. \qquad .. \qquad .. \quad (28)$$

Turning to the derivatives with respect to control angle we have:

Control with subsonic leading edge.

For a single control we have:

Lift:

$$a_2 = \frac{2(1-\eta_0)^2\sqrt{(\beta \tan\gamma)}}{\beta} \qquad .. \qquad .. \qquad .. \qquad .. \qquad .. \qquad .. \quad (29)$$

Pitching moment:

$$m_2 = \frac{4}{3}\frac{k^{1/2}}{\beta}(1-\eta_0)^2(2+\eta_0). \qquad .. \qquad .. \qquad .. \qquad .. \qquad .. \qquad .. \quad (30)$$

These relations imply symmetrical deflection of the two controls.

Hinge moment:

$$b_2 = -\frac{16k^{1/2}}{\pi(1+k)}\{\sqrt{k} + (1+k)\tan^{-1}\sqrt{k}\}(\tfrac{2}{3} - \xi_h') \quad .. \qquad .. \qquad .. \quad (31)$$

for an axis at $\xi_h'c_{\xi_r}$ of the control root chord and parallel to the trailing edge. Since no interference of the two controls is assumed, this applies to symmetrically or antisymmetrically deflected controls.

Rolling moment: In derivative form this is, for two controls,

$$l_\xi = -\frac{(1-\eta_0)^2}{3\beta\sqrt{k}}\{\eta_0(3k+1) + (3k-1)\}. \qquad .. \qquad .. \qquad .. \qquad .. \quad (32)$$

15

Control with supersonic leading edge.

The corresponding values for the control with supersonic leading edge are:

Lift:

$$a_2 = \frac{2(1-\eta_0)^2}{\beta} \quad .. \quad .. \quad .. \quad .. \quad .. \quad .. \quad .. \quad .. \quad (33)$$

Pitching moment:

$$m_2 = \frac{4}{3\beta}(1-\eta_0)^2(2+\eta_0) \quad .. \quad .. \quad .. \quad .. \quad .. \quad .. \quad (34)$$

Hinge moment:

$$b_2 = -\frac{8}{\beta}\left\{\frac{1}{2} + \frac{k}{\pi}\frac{\cos^{-1}(1/k)}{\sqrt{(k^2-1)}}\right\}\left(\frac{2}{3} - \xi_h'\right) \quad .. \quad .. \quad .. \quad .. \quad (35)$$

Rolling moment:

$$l_\xi = -\frac{2(1-\eta_0)^2(2\eta_0+1)}{3\beta} \quad \text{(two controls)} . \ .. \quad .. \quad .. \quad .. \quad (36)$$

4.2. *Sectional Values of the Derivatives (Half-Delta Controls on a Delta Wing).*—Performing the necessary chordwise integration we obtain the sectional derivatives a_{1l}, a_{2l}, m_{1l}, m_{2l} from which the locus of the aerodynamic centres is readily derived.

Wing and control with subsonic leading edge.

For the wing at incidence and control neutral we obtain:

Lift:

$$a_{1l} = \frac{A\sqrt{(1-\eta^2)}}{(1-\eta)} = A\sqrt{\left(\frac{1+\eta}{1-\eta}\right)} \quad .. \quad .. \quad .. \quad .. \quad .. \quad (37)$$

Pitching moment:

$$m_{1l} = \frac{A}{2(1-\eta)^2 E\{\sqrt{(1-k^2)}\}}\left\{\sqrt{(1-\eta^2)} + \eta^2\log\left(\frac{1+\sqrt{(1-\eta^2)}}{\eta}\right) - 2\eta\sqrt{(1-\eta^2)}\right\} \quad (38)$$

Wing and control with supersonic leading edge.

Again for the wing at incidence and control neutral we get:

Lift:

$$a_{1l} = \frac{A}{\pi(1-\eta)\sqrt{(k^2-1)}}\left[(1-\eta)\cos^{-1}\left\{\frac{(1-k^2\eta)}{k(1-\eta)}\right\} + (1+\eta)\cos^{-1}\left\{\frac{(1+k^2\eta)}{k(1+\eta)}\right\}\right] \quad (39)$$

Pitching moment:

$$m_{1l} = \frac{A}{\pi(1-\eta)^2\sqrt{(k^2-1)}}\left[\eta^2\sqrt{(k^2-1)}\log\left(\frac{1+\sqrt{(1-k^2\eta^2)}}{k\eta}\right)\right.$$
$$\left. + \frac{(1-\eta^2)}{2}\left\{\cos^{-1}\left(\frac{1+k^2\eta}{k(1+\eta)}\right) + \cos^{-1}\left(\frac{1-k^2\eta}{k(1-\eta)}\right)\right\}\right] . \quad .. \quad .. \quad .. \quad (40)$$

Considering now the wing at zero incidence with control deflected, we have the derivatives with respect to angle control.

16

Control with subsonic leading edge.

Lift:

$$a_{2l} = \frac{8}{\pi(1-\eta')(1+k)} \left[\tan\gamma \sqrt{\{(1-\eta')(1+k\eta')\}} \right.$$
$$\left. - (1+k)\eta' \log\left\{ \frac{\sqrt{(1+k\eta')} - \sqrt{(1-\eta')}}{\sqrt{\{(1+k)\eta'\}}} \right\} \right] \qquad \cdots \quad \cdots \quad \cdots \quad \cdots \quad (41)$$

over the span of the control, $0 \leqslant \eta' \leqslant 1$, and

$$a_{2l} = \frac{8}{\pi(1-\eta')(1+k)} \left[\tan\gamma \sqrt{\{(1-\eta')(1+k\eta')\}} \right.$$
$$\left. - (1+k)\eta' \log\left\{ \frac{\sqrt{(1-\eta')} - \sqrt{(1+k\eta')}}{\sqrt{\{-\eta'(1+k)\}}} \right\} \right] \qquad \cdots \quad \cdots \quad \cdots \quad \cdots \quad (42)$$

over that part of the fixed wing carrying induced load, i.e., for $-1/k \leqslant \eta' \leqslant 0$.

Pitching moment:

$$m_{2l} = \frac{2\tan\gamma}{\pi(k+1)(1-\eta')^2} \left[\sqrt{\{(1-\eta')(1+k\eta')\}}\{(1+k\eta') + (1-\eta')\} \right.$$
$$\left. + \eta'^2(1+k^2) \log\left\{ \frac{\sqrt{(1+k\eta')} - \sqrt{(1-\eta')}}{\sqrt{\{\eta'(1+k)\}}} \right\} \right] \quad \text{for } 0 \leqslant \eta' \leqslant 1, \quad \cdots \quad \cdots \quad (43)$$

and

$$m_{2l} = \frac{2\tan\gamma}{\pi(1+k)(1-\eta')^2} \left[\sqrt{\{(1-\eta')(1+k\eta')\}}\{(1+k\eta') + (1-\eta')\} \right.$$
$$\left. + \eta'^2(1+k^2) \log\left\{ \frac{\sqrt{(1-\eta')} - \sqrt{(1+k\eta')}}{\sqrt{\{-\eta'(1+k)\}}} \right\} \right] \quad \text{for } -1/k \leqslant \eta' \leqslant 0. \quad \cdots \quad (44)$$

Control with supersonic leading edge.

Lift:

$$a_{2l} = \frac{4\tan\gamma}{\pi(1-\eta')\sqrt{(k^2-1)}} \left[(1-\eta') \cos^{-1}\left\{ \frac{1-k^2\eta'}{k(1-\eta')} \right\} \right.$$
$$\left. + \eta'\sqrt{(k^2-1)} \log\left\{ \frac{1 + \sqrt{(1-k^2\eta'^2)}}{k\eta'} \right\} \right] \quad \text{for } 0 \leqslant \eta' \leqslant 1/k \qquad \cdots \quad \cdots \quad (45)$$

$$= \frac{4\tan\gamma}{\sqrt{(k^2-1)}} \qquad \text{for } 1/k \leqslant \eta' \leqslant 1 \qquad \cdots \quad \cdots \quad \cdots \quad \cdots \quad \cdots \quad \cdots \quad (46)$$

and for the fixed part of the wing affected by control deflection, $-1/k \leqslant \eta' \leqslant 0$, we have:

$$a_{2l} = \frac{4\tan\gamma}{\pi\sqrt{(k^2-1)}(1-\eta')} \left[(1-\eta') \cos^{-1}\left\{ \frac{1-k^2\eta'}{k(1-\eta')} \right\} \right.$$
$$\left. + \eta'\sqrt{(k^2-1)} \log\left\{ \frac{1 + \sqrt{(1-k^2\eta'^2)}}{k|\eta'|} \right\} \right] \qquad \cdots \quad \cdots \quad \cdots \quad \cdots \quad \cdots \quad (47)$$

17

Pitching moment:

$$m_{2l} = \frac{2 \tan \gamma}{\pi(1 - \eta')^2 \sqrt{(k^2 - 1)}} \left[(1 - \eta')^2 \cos^{-1}\left\{ \frac{1 - k^2\eta'}{k(1 - \eta')} \right\} \right.$$

$$- \eta'\sqrt{(k^2 - 1)} \log \left\{ \frac{1 + \sqrt{(1 - k^2\eta'^2)}}{k\eta'} \right\}$$

$$\left. + \eta'\sqrt{(k^2 - 1)}\sqrt{(1 - k^2\eta'^2)} \right] \quad \text{for } 0 \leqslant \eta' \leqslant 1/k \qquad .. \qquad .. \qquad .. \qquad .. \quad (48)$$

$$= \frac{2 \tan \gamma}{\sqrt{(k^2 - 1)}} \quad \text{for } 1/k \leqslant \eta' \leqslant 1 , \quad .. \qquad .. \qquad .. \qquad .. \qquad .. \qquad .. \qquad .. \quad (49)$$

and

$$m_{2l} = \frac{2 \tan \gamma}{\pi(1 - \eta')^2 \sqrt{(k^2 - 1)}} \left[(1 - \eta')^2 \cos^{-1}\left\{ \frac{1 - k^2\eta'}{k(1 - \eta')} \right\} \right.$$

$$- \eta'\sqrt{(k^2 - 1)} \log \left\{ \frac{1 + \sqrt{(1 - k^2\eta'^2)}}{k |\eta'|} \right\}$$

$$\left. + \eta'\sqrt{(k^2 - 1)}\sqrt{(1 - k^2\eta'^2)} \right] \quad \text{for } -1/k \leqslant \eta' \leqslant 0 . \qquad .. \qquad .. \qquad .. \quad (50)$$

The derivatives a_{2l} and m_{2l} are readily expressible in terms of the spanwise co-ordinate $\eta = y/s$ by use of the relationship $\eta' = (\eta - \eta_0)/(1 - \eta_0)$.

As mentioned earlier, these sectional derivatives have been calculated for the special case of an equilateral delta wing ($A = 2 \cdot 31$) with half-delta tip control of span ratios $0 \cdot 261$ and $0 \cdot 335$. The results for the smaller span ratio are given in Fig. 25 to 30, which include the subsonic and sonic results in a carpet plotting against M and η.

A feature common to all these figures is the peak in the local derivative as sonic speed is approached. This is particularly pronounced for the derivatives with respect to control angle (Figs. 27 to 30), and more so for symmetrical control deflection. Another interesting point is that the maximum value of $a_2(1 - \eta)$ (or the lift produced by control deflection), occurs at a value of η very near to $0 \cdot 85$ for all Mach numbers, and for both symmetrical and anti-symmetrical control deflection.

4.3. *Local Aerodynamic Centres.*—From the results of the preceding sections it is possible to evaluate the position of the local aerodynamic centres. It is both interesting and instructive to do this over the control span. The results for a delta wing of aspect ratio $2 \cdot 31$ with half-delta control at supersonic speeds are given in Figs. 23 and 24, where they are compared with those at subsonic speeds. These figures show the rearward movement of the local aerodynamic centre (over all but the tip of the control) as the Mach number increases. There is a large rearward shift between $M = 0 \cdot 8$ and $1 \cdot 0$, a small recovery between $M = 1 \cdot 0$ and $2 \cdot 0$, and a further shift above $M = 2 \cdot 0$ as the Mach cone crosses the leading edge, and more of the flow over the tip portion becomes two-dimensional in character. This movement of the aerodynamic centres, together with the changes in the loading of the tip control, are sufficient to cause a change in sign of the hinge moment due to control deflection (*see* Fig. 32) for an axis at $0 \cdot 635$ of the control root chord and parallel to the wing trailing edge. In this connection it is significant to note that the largest shift occurs near the peak in the loading (*see* above). For close balance of the control, whilst avoiding change of sign of b_2, it is clear that an inclined hinge is more likely to be successful. To exploit this particular advantage of the tip control further it may be better to combine an inclined hinge line with a different control plan-form. Further calculations, followed by experiment, are required to indicate suitable geometry.

18

5. *Comparison of Theoretical Results and Experiment.*—In Ref. 15 are described free-flight rocket-model tests of a 60 deg swept-back delta wing with half-delta tip ailerons over a speed range corresponding to $M = 0.69$ to 1.5, and covering an aileron angle range of ± 5 deg, at zero wing incidence*. The quantities measured are rolling moments, hinge moments, and damping-in-roll moments.

The model used in the investigation consisted of a sharp-nosed cylindrical body equipped with a cruciform arrangement of 60-deg swept-back delta wings (*see* Figs. 31 and 32), and so is not strictly comparable with the single wing arrangement of the theoretical investigation. In comparing the calculated and measured characteristics of the tip control we must bear in mind the interference effects of the body, and the damping wings. To these must be added the effect of wing thickness, viscosity, and the gap at the root of the control when deflected. Some unpublished work by P. R. Owen on a cruciform wing-plus-body arrangement with all-moving wings suggests that the interference effects reduce somewhat the control effectiveness. Wing thickness and viscosity are also expected to cause some reduction, although for the 3 per cent thick control these effects must be small. The gap at the control root must lead to some equalisation of pressure on the upper and lower surfaces of the control in the neighbourhood of its root chord, and thus to a further reduction of lift and rolling moment. It is therefore not surprising that the measured rolling moment (Fig. 31) is some 80 per cent of the theoretical value for the wing-aileron arrangement considered (equations 8, 25, 54 and 65). Some fairing of the linearised supersonic theory is necessary to produce a continuous curve through the sonic value of the rolling moment, but the interpolated curve is plausible and the trends of the experimental results are well reproduced.

Fig. 32 presents a comparison of measured and calculated hinge-moment characteristics. The calculated values refer in the main to an axis at 0.635 of the control root chord. Ref. 15, which gives results for three axis positions, one of which is at 0.640, became available only when the calculations were complete. However, the change in the value of b_2 on moving the hinge aft by 0.005 of the control root chord is small, as is illustrated by the two theoretical curves calculated only on the supersonic side. General considerations suggest that the change at subsonic speed would be of the order of 20 per cent of that at supersonic speeds. This suggests that the values for 0.635 control root chord hinge line are not reliable, and this is further confirmed by an examination of the data from the later tests[15], for different hinge-line locations (*see* Fig. 34).

A further point to bear in mind when assessing the value of the theoretical estimates is that the measured b_2 is a mean of the control-angle range 0 to -5 deg, and is accordingly not directly comparable with the theoretical b_2. It is of interest to note that the hinge-moment curves are rather non-linear.

Accepting the experimental curve for the 0.64 chord hinge line as the more reliable, we conclude that the theoretical curve is in as close agreement as we can expect in view of the difference in geometry and the limitations of the theory.

6. *Conclusions.*—The main conclusions to be drawn from the present investigation are as follows :

(*a*) The linearised subsonic, sonic, and supersonic theories are adequate means for making a comprehensive design study of the effects of wing and control plan-forms on the all-moving wing-tip control.

(*b*) In the calculation of the subsonic spanwise loading due to control deflection, and such quantities as are derived therefrom, *e.g.*, rolling moment, a reduction in labour can be effected with little loss of accuracy by use of simplified theory[4, 5, 6].

---

* At the time when the present investigation was undertaken only unpublished data for hinge axis at 0.635 of the control root chord were available ; hence the choice of this axis position in the calculations.

19

(c) The linearised solution at sonic speeds seems practicable for any wing-aileron or elevator combination.

(d) To improve the accuracy of the subsonic theory, a re-examination of the problem of the fairing of discontinuity in the incidence distribution should be attempted.

(e) One of the main advantages of the all-moving wing-tip control, namely, the possibility of close aerodynamic balance of the control, will imply an inclined hinge line and/or a special control plan-form.

(f) Some further calculations on the lines of the present investigation are desirable to sort out promising control plan-forms before starting any systematic experimental work.

LIST OF SYMBOLS

A Aspect ratio of wing $= (2s)^2/S$ $(- 4 \tan \gamma$ for delta wing)

C_H Hinge-moment coefficient $= \dfrac{H}{\frac{1}{2}\rho V^2 S_\xi \bar{c}_\xi}$

C_L Lift coefficient $= \dfrac{L}{\frac{1}{2}\rho V^2 S}$ overall

$\qquad\qquad\qquad = \dfrac{dL}{\frac{1}{2}\rho V^2 c\, dy}$ sectional (C_{LL})

C_M Pitching-moment coefficient $= \dfrac{M}{\frac{1}{2}\rho V^2 S \bar{c}}$ overall, about wing apex

$\qquad\qquad\qquad = \dfrac{dM}{\frac{1}{2}\rho V^2 c^2\, dy}$ sectional, about the leading edge

C_l Rolling-moment coefficient $= \dfrac{\text{Rolling moment}}{\rho V^2 S s}$

H Hinge moment

I Enthalpy of the unit volume of the flow around the wing

L Lift

L_W Lift produced on fixed part of wing by control deflection

L_ξ Lift produced on control by control deflection

M Wing pitching moment

S Gross wing area

S_ξ Area of one control

V Velocity of the undisturbed flow relative to the wing

$\left.\begin{array}{l} X \\ Y \end{array}\right\}$ Cartesian co-ordinates with control apex as origin

X_h Hinge-line location chordwise, measured from control apex

$Z = y + iz$

a_{1l}, a_1 Sectional and overall value of $\partial C_L / \partial \alpha$

a_{2l}, a_2 Sectional and overall value of $\partial C_L / \partial \xi$

b Wing span $= 2s$

$b_1 = \partial C_H / \partial \alpha$

$b_2 = \partial C_H / \partial \xi$

c Local wing chord

c_r Wing root chord

$\bar{c}$ Wing mean chord $= S/2s$

c_ξ Local control chord

$c_{\xi r}$ Control root chord

$\bar{c}_\xi$ Control mean chord $= \frac{\text{Control area}}{\text{Control span}}$

d Distance from hinge line to local aerodynamic centre

h Local aerodynamic centre as fraction of chord measured from leading edge

$k = \beta \tan \gamma = \dfrac{\tan \gamma}{\tan \mu}$

$l = \dfrac{\Delta p}{\frac{1}{2}\rho V^2} = \dfrac{4I}{V^2}$, non-dimensional load per unit area of the wing

$m = m_2 - m_1(a_2/a_1)$

m_{1l}, m_1 Sectional and overall values of $\partial C_M / \partial \alpha$

m_{2l}, m_2 Sectional and overall values of $\partial C_M / \partial \xi$

s Wing semi-span

$t = \beta Y/X$

$\left.\begin{array}{l} x \\ y \\ z \end{array}\right\}$ Cartesian co-ordinate with wing apex as origin (*see* Fig. 1).

y_l Value of y for wing leading edge

y_t Value of y for wing trailing edge

21

y_0 Value of y at the inboard end of the control

x_h Hinge-line co-ordinate with respect to wing apex

$x_{nc/4}$ Co-ordinate of quarter-chord point at nth pivotal station

α Wing incidence

β $\sqrt{(M^2 - 1)}$

γ Circulation (non-dimensional lift per unit span) $= cC_{LL}/2b$ (Section 2) or Semi-vertex angle of delta wing (Section 4 and Appendix 1)

η $=$ y/s

η_0 Value of η at inboard end of the control

η_a Span ratio of control $= 1 - \eta_0$

η' $=$ $Y/(\eta_a s)$.   Non-dimensional form of Y

μ (Subsonic theory, Section 2).   Pitching-moment   coefficient   per   unit   span $= C_M c/2b$

μ (Section 4).   Mach angle $= \tan^{-1} \dfrac{1}{\beta} = \tan^{-1} \dfrac{1}{\sqrt{(M^2 - 1)}}$

ξ Control deflection

ξ' $=$ $X/c_{\xi r}$.   Non-dimensional form of X

ξ_0' $=$ $X_{ac}/c_{\xi r}$.   Distance of aerodynamic centre of force behind control apex in terms of control root chord

$\xi_{nc/4}$ $=$ $\dfrac{x_{nc/2}}{s}$.   Non-dimensional form of $x_{nc/4}$

ξ_h $=$ x_h/c_r.   Non-dimensional form of x_h

REFERENCES

No.	Author	Title, etc.

Subsonic Theory

1 H. Multhopp .. .. .. Methods for calculating the lift distribution of wings (subsonic lifting-surface theory). R. & M. 2884. January, 1950.

2 V. M. Falkner .. .. .. The calculation of the aerodynamic loading on surfaces of any shape. R. & M. 1910. August, 1943.

3 H. C. Garner .. .. .. Methods of approaching an accurate three-dimensional potential solution for a wing. R. & M. 2721. October, 1948.

4 J. De Young .. .. .. Theoretical antisymmetrical span loading for wings of arbitrary plan-forms at subsonic speeds. N.A.C.A. Report 1056. 1951. (Supersedes NACA/TN/2140.)

5 J. De Young .. .. .. Theoretical symmetric span loading due to flap deflection for wings of arbitrary plan-form at subsonic speeds. N.A.C.A. Tech. Note 2278. January, 1951. (Superseded by NACA/Report/1071.)

6 J. De Young .. .. .. Theoretical symmetric span loading at subsonic speeds for wings having arbitrary plan-forms. N.A.C.A. Report 921. 1948.

7 J. C. Sivells .. .. .. An improved approximate method for calculating lift distributions due to twist. N.A.C.A. Tech. Note 2282. January, 1951.

Sonic Theory

8 J. De Young .. .. .. Spanwise loading for wings and control surfaces of low aspect ratio. N.A.C.A. Tech. Note 2011. January, 1950.

9 K. W. Mangler .. .. .. Calculation of the pressure distribution over a wing at sonic speed. R. & M. 2888. September, 1951.

Supersonic Theory

10 H. Multhopp .. .. .. A unified theory of supersonic wing flow, employing conical fields. R.A.E. Report Aero. 2415. A.R.C. 14,223. April, 1951.

11 R. A. Lagerstrom and M. E. Graham. Linearised theory of supersonic control surfaces. Douglas Aircraft Co. Report SM-13060. July, 1947. TPA3/TIB P32156. *J.Ae.Sci.* Vol. 16. No. 1. pp. 31 to 34. 1949.

12* J. H. Kainer and M. D. King .. The theoretical characteristics of triangular-tip control surfaces at supersonic speeds (Mach lines behind trailing edges). N.A.C.A. Tech. Note 2715. July, 1952.

13 W. A. Tucker and R. L. Nelson .. Theoretical characteristics in supersonic flow of two types of control surfaces on triangular wings. N.A.C.A. Report 939. 1949.

14 S. B. Gates .. .. .. Note on the transonic movement of wing aerodynamic centre. R. & M. 2785. May, 1949.

Experiment

15 C. W. Martz, J. D. Church and J. W. Goslee. Free-flight investigation to determine force and hinge-moment characteristics at zero angle of attack of a 60-deg. swept-back half-delta tip control on a 60-deg. swept-back delta wing at Mach numbers between 0·68 and 1·44. N.A.C.A. Research Memo. L51I14. NACA/TIB/2973. December, 1951.

16 D. W. Conner and E. B. May, Jr... Control effectiveness load and hinge-moment characteristics of a tip control surface on a delta wing at a Mach number of 1·9. N.A.C.A. Research Memo. L49H05. NACA/TIB/2190. October, 1949.

* This paper was received on completion of the present investigation.

APPENDIX I

Supersonic Theory

The usual linearised inviscid-flow theory is the basis of the calculations described in this section. For most of the simple wing shapes the problem can be readily treated by use of the Busemann conical theory, and we shall in particular be concerned with half-delta wing-tip controls fitted to delta wings, although certain of the results are of much wider applicability.

We will begin by quoting results for some of the overall derivatives as these for the most part have been derived previously by a number of authors[11, 12, 13].

I.1. *Overall Derivatives.*—Consider the delta wing at uniform incidence:

Wing with Subsonic Leading Edge.—When the wing lies inside the Mach cone from its apex the pressure difference across it is given by,

$$\frac{\Delta p}{\alpha q} = \frac{4 \tan^2 \gamma}{E\{\sqrt{(1 - k^2)}\}\sqrt{\{\tan^2 \gamma - (y^2/x^2)\}}}, \qquad \cdots \qquad \cdots \qquad \cdots \qquad (I.1)$$

where $k = \tan \gamma / \tan \mu$

μ = Mach angle

E = the complete elliptic integral of the second kind.

If we write

$$C = \frac{4\alpha q}{E\{\sqrt{(1 - k^2)}\}}$$

and

$$u = x \tan \gamma \, ,$$

we may write Δp in the form,

$$\Delta p = \frac{Cu \tan \gamma}{\sqrt{(u^2 - y^2)}} \cdot \qquad \cdots \qquad \cdots \qquad \cdots \qquad \cdots \qquad \cdots \qquad \cdots \qquad \cdots \qquad (I.2)$$

To find the hinge moment of the control we take moments, and integrate, thus,

$$H = - \int_{y_0}^{s} \int_{x_l}^{x_t} \Delta p(x - x_h) \, dx \, dy . \quad \cdots \qquad \cdots \qquad \cdots \qquad \cdots \qquad (I.3)*$$

Now

$$- \int_{x_l}^{x_t} \Delta p(x - x_h) \, dx = \frac{C}{\tan \gamma} \int_{u_l}^{u_t} \frac{u}{\sqrt{(u^2 - y^2)}} (u_h - u) \, du$$

$$= C \cot \gamma \left\{ \left(u_h - \frac{u_t}{2} \right) \sqrt{\left(u_t^2 - y^2 \right)} - \frac{y^2}{2} \log \left(\frac{u_t + \sqrt{(u_t^2 - y^2)}}{y} \right) \right\} ,$$

since $u_l = x_l \tan \gamma = y$.

Thus

$$H = C \cot \gamma \int_{y_0}^{s} \left[\left(x_h - \frac{x_t}{2} \right) \tan \gamma \sqrt{(x_t^2 \tan^2 \gamma - y^2)} \right.$$

$$\left. - \frac{y^2}{2} \log \left\{ \frac{x_t \tan \gamma + \sqrt{(x_t^2 \tan^2 \gamma - y^2)}}{y} \right\} \right] dy . \qquad \cdots \qquad \cdots \qquad (I.4)$$

---

* The use of polar co-ordinates might yield a rather neater solution here but as some of the integrals are common to this section and Section I.2, it is probably of not such advantage.

This applies to controls which lie ahead of the Mach cone from the trailing edge of the control root chord. We are here interested in the special case of the half-delta control, and for this $x_t = c_r$ and so $x_t \tan \gamma = c_r \tan \gamma = s$. With these relations H becomes

$$H = C \cot \gamma \int_{y_0}^{s} \left[\left(x_h - \frac{c_r}{2} \right) \tan \gamma \sqrt{(s^2 - y^2)} - \frac{y^2}{2} \log \left\{ \frac{s + \sqrt{(s^2 - y^2)}}{y} \right\} \right] dy$$

$$= C \left(x_h - \frac{c_r}{2} \right) \left| \frac{y}{2} \sqrt{(s^2 - y^2)} + \frac{s^2}{2} \sin^{-1} \frac{y}{s} \right|_{y_0}^{s} - \frac{C}{2} \cot \gamma \int_{y_0}^{s} y^2 \log \left\{ \frac{s + \sqrt{(s^2 - y^2)}}{y} \right\} dy$$

$$= C \left(x_h - \frac{c_r}{2} \right) \left\{ \frac{\pi s^2}{4} - \frac{y_0}{2} \sqrt{(s^2 - y_0^2)} - \frac{s^2}{2} \sin^{-1} \frac{y_0}{s} \right\}$$

$$+ \frac{C \cot \gamma}{2} \left[\frac{y_0^3}{3} \log \left\{ \frac{s + \sqrt{(s^2 - y^2)}}{y} \right\} - \frac{s}{3} \left\{ \frac{\pi s^2}{4} + \frac{y_0 \sqrt{(s^2 - y_0^2)}}{2} - \frac{s^2}{2} \sin^{-1} \frac{y_0}{s} \right\} \right] \quad .. \quad (I.5)$$

(*see* Appendix II).

If we write $\eta_0 = y_0/s$, and $\xi_h = x_h/c_r$, then

$$H = \frac{s^3 C}{A} \left[(2\xi_h - 1) \left\{ \frac{\pi}{2} - \eta_0 \sqrt{(1 - \eta_0^2)} - \sin^{-1} \eta_0 \right\} + \frac{2}{3} \left\{ \eta_0^3 \log \left(\frac{1 + \sqrt{(1 - \eta_0^2)}}{\eta_0} \right) - \frac{\pi}{4} \right. \right.$$

$$\left. \left. - \frac{\eta_0}{2} \sqrt{(1 - \eta_0^2)} + \tfrac{1}{2} \sin^{-1} \eta_0 \right\} \right]. \qquad .. \qquad .. \qquad .. \qquad .. \quad (I.6)$$

From this we have

$$b_1 = \frac{\partial C_H}{\partial a} = \frac{H}{\tfrac{1}{2} \rho V^2 S_\xi \bar{c}_\xi a} = \frac{H}{\tfrac{1}{2} \rho V^2 a \frac{(1 - \eta_0)^3}{4} s c_r^2}$$

$$= \frac{4 s^2 C}{\tfrac{1}{2} \rho V^2 a (1 - \eta_0)^3 c_r^2 A} \left[(2\xi_h - 1) \left\{ \frac{\pi}{2} - \eta_0 \sqrt{(1 - \eta_0^2)} - \sin^{-1} \eta_0 \right\} \right.$$

$$\left. + \frac{2}{3} \left\{ \eta_0^2 \log \left(\frac{1 + \sqrt{(1 - \eta_0^2)}}{\eta_0} \right) - \frac{\pi}{4} - \frac{\eta_0 \sqrt{(1 - \eta_0^2)}}{2} + \tfrac{1}{2} \sin^{-1} \eta_0 \right\} \right]. \qquad .. \qquad .. \quad (I.7)$$

But

$$\frac{s^2 C}{A} = \frac{\tfrac{1}{2} \rho V^2 a s c_r}{E\{\sqrt{(1 - k^2)}\}}$$

and

$$A = \frac{4s}{c_r}.$$

Thus,

$$b_1 = \frac{A}{(1 - \eta_0)^3 E\{\sqrt{(1 - k^2)}\}} \left[(2\xi_h - 1) \left\{ \frac{\pi}{2} - \eta_0 \sqrt{(1 - \eta_0^2)} - \sin^{-1} \eta_0 \right\} \right.$$

$$\left. + \frac{2}{3} \left\{ \eta_0^3 \log \left(\frac{1 + \sqrt{(1 - \eta_0^2)}}{\eta_0} \right) - \frac{\pi}{4} - \frac{\eta_0 \sqrt{(1 - \eta_0^2)}}{2} + \tfrac{1}{2} \sin^{-1} \eta_0 \right\} \right]. \qquad .. \qquad .. \quad (I.8)$$

25

Wing with Supersonic Leading Edge.—The calculation of the hinge moment for this case is considerably more complicated because we need two pressure distributions, one for the region between the leading edge and the Mach cone, and the other applying to the region behind the Mach cone. For the first region (between leading edge and Mach cone) the pressure distribution is given by

$$\left(\frac{\Delta p}{aq}\right)_1 = \frac{4 \tan \gamma}{\sqrt{(\beta^2 \tan^2 \gamma - 1)}}, \quad .. \qquad .. \qquad .. \qquad .. \qquad .. \qquad .. \qquad .. \quad (I.9)$$

where $\beta = \sqrt{(M^2 - 1)}$.

Behind the Mach cone we have, with $k = \beta \tan \gamma$,

$$\left(\frac{\Delta p}{aq}\right)_2 = \frac{4 \tan \gamma}{\pi\sqrt{(\beta^2 \tan^2 \gamma - 1)}} \left\{ \cos^{-1}\left(\frac{x + \beta ky}{kx + \beta y}\right) + \cos^{-1}\left(\frac{x - \beta ky}{kx - \beta y}\right) \right\}. \quad .. \quad (I.10)$$

For the derivation of these results, *see* Refs. 10 and 11. These results apply for a range of trailing edges, but we shall confine our attention to the delta wing with a half-delta control. For this simple geometry the hinge moment is given by

$$H = \int_{y_0}^{s} \int_{x_l}^{y \cot \mu} \left(\frac{\Delta p}{aq}\right)_1 aq(x_h - x) \, dx \, dy$$

$$+ \int_{y_0}^{c_r \tan \mu} \int_{y \cot \mu}^{x_t} \left(\frac{\Delta p}{aq}\right)_2 aq(x_h - x) \, dx \, dy . \quad .. \qquad .. \qquad .. \qquad .. \quad (I.11)$$

Also $x_l = y \cot \gamma$, $x_t = c_r$.

Therefore we can write,

$$H = \frac{4aq \tan \gamma}{\sqrt{(\beta^2 \tan^2 \gamma - 1)}} \left[\int_{y_0}^{s} \int_{y \cot \gamma}^{y \cot \mu} (x_h - x) \, dx \, dy \right.$$

$$+ \frac{1}{\pi} \int_{y_0}^{c_r \tan \mu} \int_{y \cot \mu}^{c_r} \left\{ \cos^{-1}\left(\frac{x + k\beta y}{kx + \beta y}\right) + \cos^{-1}\left(\frac{x - k\beta y}{kx - \beta y}\right) \right\} (x_h - x) \, dx \, dy \left. \right]$$

$$= \frac{4aq \tan \gamma}{\sqrt{(k^2 - 1)}} \left[\int_{y_0}^{s} \left| x_h x - \frac{x^2}{2} \right|_{y \cot \gamma}^{y \cot \mu} dy \right.$$

$$+ \frac{1}{\pi} \int_{y_0}^{c_r \tan \mu} \int_{y \cot \mu}^{c_r} \left\{ \cos^{-1}\left(\frac{x + k\beta y}{kx + \beta y}\right) + \cos^{-1}\left(\frac{x - k\beta y}{kx - \beta y}\right) \right\} (x_h - x) \, dx \, dy \left. \right]$$

$$= \frac{4aq \tan \gamma}{\sqrt{(k^2 - 1)}} \left[(\cot \mu - \cot \gamma) \int_{y_0}^{s} \left\{ x_h y - \frac{(\cot \mu + \cot \gamma)}{2} y^2 \right\} dy \right.$$

$$+ \frac{1}{\pi} \int_{y_0}^{c_r \tan \mu} \int_{y \cot \mu}^{c_r} \left\{ \cos^{-1}\left(\frac{x + k\beta y}{kx + \beta y}\right) + \cos^{-1}\left(\frac{x - k\beta y}{kx - \beta y}\right) \right\} (x_h - x) \, dx \, dy \left. \right]$$

$$= \frac{2}{3} \frac{aq \tan \gamma}{\sqrt{(k^2 - 1)}} \left[(s - y_0)(\cot \mu - \cot \gamma)\{3x_h (s + y_0) - (\cot \mu + \cot \gamma)(s^2 + sy_0 + y_0^2)\} \right.$$

$$+ \frac{1}{\pi} \int_{y_0}^{c_r \tan \mu} \int_{y \cot \mu}^{c_r} \left\{ \cos^{-1}\left(\frac{x + k\beta y}{kx + \beta y}\right) + \cos^{-1}\left(\frac{x - k\beta y}{kx - \beta y}\right) \right\} (x_h - x) \, dx \, dy \left. \right]. \quad .. \quad (I.12)$$

Consider the integration with respect to x:

$$\int_{y \cot \mu}^{c_r} \left\{ \cos^{-1}\left(\frac{x + k\beta y}{kx + \beta y}\right) + \cos^{-1}\left(\frac{x - k\beta y}{kx - \beta y}\right) \right\} (x_h - x)\, dx$$

$$= \frac{x_h}{k} \left| (kx - \beta y) \cos^{-1}\left(\frac{x - k\beta y}{kx - \beta y}\right) + (kx + \beta y) \cos^{-1}\left(\frac{x + k\beta y}{kx + \beta y}\right) \right|_{y \cot \mu = \beta y}^{c_r}$$

$$- \left| \frac{\beta^2 y^2 \sqrt{(k^2 - 1)}}{k^2} \log\{x + \sqrt{(x^2 - \beta^2 y^2)}\} + \frac{(kx - \beta y)}{2k^2}(2\beta y + kx - \beta y)\cos^{-1}\left(\frac{x - k\beta y}{kx - \beta y}\right) \right.$$

$$\left. + \frac{(kx + \beta y)(kx + \beta y - 2\beta y)}{2k^2} \cos^{-1}\left(\frac{kx + \beta y}{kx + \beta y}\right) \right|_{y \cot \mu}^{c_r}$$

$$= \left| \frac{(kx - \beta y)}{2k^2}(2kx_h - kx - \beta y)\cos^{-1}\left(\frac{x - k\beta y}{kx - \beta y}\right) \right.$$

$$+ \frac{(kx + \beta y)}{2k^2}(2kx_h - kx + \beta y)\cos^{-1}\left(\frac{x + k\beta y}{kx + \beta y}\right)$$

$$\left. - \frac{\beta^2 y^2}{k^2}(\sqrt{k^2 - 1})\log\{x + \sqrt{(x^2 - \beta^2 y^2)}\} \right|_{\beta y}^{c_r}$$

$$= \frac{(kc_r - \beta y)}{2k^2}(2kx_h - kc_r - \beta y)\cos^{-1}\left(\frac{c_r - k\beta y}{kc_r - \beta y}\right)$$

$$+ \frac{(kc_r + \beta y)}{2k^2}(2kx_h - kc_r + \beta y)\cos^{-1}\left(\frac{c_r + k\beta y}{kc_r + \beta y}\right)$$

$$- \frac{\pi(k - 1)}{2k^2}\beta y\{2kx_h - (k + 1)\beta y\} - \frac{\beta^2 y^2}{k^2}\sqrt{(k^2 - 1)}\log\left\{\frac{c_r + \sqrt{(c_r^2 - \beta^2 y^2)}}{\beta y}\right\}. \quad (I.13)$$

Integrating this again with respect to y, we have

$$\frac{c_r(2x_h - c_r)}{2}\left\{ \int_{y_0}^{c_r \tan \mu} \cos^{-1}\left(\frac{c_r - k\beta y}{kc_r - \beta y}\right)dy + \int_{y_0}^{c_r \tan \mu} \cos^{-1}\left(\frac{c_r + k\beta y}{kc_r + \beta y}\right)dy \right\}$$

$$+ 2\beta kx_h\left\{ \int_{y_0}^{c_r \tan \mu} y \cos^{-1}\left(\frac{c_r - k\beta y}{kc_r - \beta y}\right)dy - \int_{y_0}^{c_r \tan \mu} y \cos^{-1}\left(\frac{c_r + k\beta y}{kc_r + \beta y}\right)dy \right\}$$

$$+ \frac{\beta^2}{2k^2}\left\{ \int_{y_0}^{c_r \tan \mu} y^2 \cos^{-1}\left(\frac{c_r - k\beta y}{kc_r - \beta y}\right)dy + \int_{y_0}^{c_r \tan \mu} y^2 \cos^{-1}\left(\frac{c_r + k\beta y}{kc_r + \beta y}\right)dy \right\}$$

$$- \left| \frac{\pi(k - 1)\beta y^2}{6k^2}\{3kx_h - (k + 1)\beta y\} \right|_{y = y_0}^{c_r \tan \mu}$$

$$- \frac{\beta^2(k^2 - 1)^{1/2}}{k^2}\int_{y_0}^{c_r \tan \mu} y^2 \log\left\{\frac{c_r + \sqrt{(c_r^2 - \beta^2 y^2)}}{\beta y}\right\}dy.$$

27

The first three terms are zero since the integrals within the brackets clearly cancel and we are thus left with

$$F(y) = \frac{\pi(k-1)\beta}{6k^2}\left| y^2\{(k+1)\beta y - 3kx_h\}\right|_{y=y_0}^{c_r/\beta}$$

$$- \frac{(k^2-1)^{1/2}}{\beta k^2}\int_{y=y_0}^{c_r/\beta}\beta^2 y^2 \log\left\{\frac{c_r + \sqrt{(c_r^2 - \beta^2 y^2)}}{\beta y}\right\} d(\beta y)$$

$$= \frac{\pi(k-1)\beta}{6k^2}\left| y^2\{(k+1)\beta y - 3kx_h\}\right|_{y=y_0}^{c_r/\beta}$$

$$- \frac{(k^2-1)^{1/2}}{\beta k^2}\left[\left|\frac{\beta^3 y^3}{3}\log\left\{\frac{c_r + \sqrt{(c_r^2 - \beta^2 y^2)}}{\beta y}\right\}\right|_{y=y_0}^{c_r/\beta} - \frac{c_r}{3}\int_{y=y_0}^{c_r\tan\mu}\beta^3 y^3\frac{d(\beta y)}{\beta y\sqrt{(c_r^2 - \beta^2 y^2)}}\right]$$

so that

$$F(y) = \frac{\pi(k-1)}{6k^2}\frac{c_r^2}{\beta}\{(k+1)c_r - 3kx_h\} - \frac{\pi(k-1)}{6k^2}\beta y_0^2\{(k+1)\beta y_0 - 3kx_h\}$$

$$+ \frac{(k^2-1)^{1/2}}{\beta k^2}\left[\beta^3\frac{y_0^3}{3}\log\left\{\frac{c_r + \sqrt{(c_r^2 - \beta^2 y_0^2)}}{\beta y_0}\right\}\right.$$

$$\left.- \frac{c_r}{3}\left| - \tfrac{1}{2}\beta y\sqrt{(c_r^2 - \beta^2 y^2)} + \frac{c_r^2}{c}\sin^{-1}\frac{\beta y}{c_r}\right|_{y=y_0}^{c_r/\beta}\right]$$

$$= \frac{\pi(k-1)}{6k^2}\frac{c_r^2}{\beta}\{(k+1)c_r - 3kx_h\} - \frac{\pi(k-1)}{6k^2}\beta y_0^2\{(k+1)\beta y_0 - 3kx_h\}$$

$$+ \frac{\sqrt{(k^2-1)}}{k^2}\left[\frac{\beta^3 y_0^3}{3}\log\left\{\frac{c_r + \sqrt{(c_r^2 - \beta^2 y_0^2)}}{\beta y_0}\right\}\right.$$

$$\left.- \frac{c_r^3}{6}\frac{\pi}{2} - \frac{\beta c_r y_0}{6}\sqrt{(c_r^2 - \beta^2 y_0^2)} + \frac{c_r^3}{6}\sin^{-1}\frac{\beta y_0}{c_r}\right].$$

Inserting in the expression for H we now have,

$$H = \frac{2}{3}\frac{aq\tan\gamma}{\sqrt{(k^2-1)}}\left[(s-y_0)(\cot\mu - \cot\gamma)\{3x_h(s+y_0) - (\cot\mu + \cot\gamma)(s^2 + sy_0 + y_0^2)\}\right.$$

$$+ \frac{(k-1)}{6k^2}\frac{c_r^2}{\beta}\{(k+1)c_r - 3kx_h\} - \frac{(k-1)}{6k^2}\beta y_0^2\{(k+1)\beta y_0 - 3kx_h\}$$

$$- \frac{\sqrt{(k^2-1)}}{6k^2\pi}c_r^3\left(\frac{\pi}{2} - \sin^{-1}\frac{\beta y_0}{c_r}\right)$$

$$\left.- \frac{\sqrt{(k^2-1)}}{6k^2\pi}\beta c_r y_0\sqrt{(c_r^2 - \beta^2 y_0^2)} + \frac{\sqrt{(k^2-1)}}{3k^2\pi}\beta^3 y_0^3\log\left\{\frac{c_r + \sqrt{(c_r^2 - \beta^2 y_0^2)}}{\beta y_0}\right\}\right]. \quad (I.14)$$

We again write $\eta_0 = y_0/s$ and $\xi_h = x_h/c_r$.

Then using $A = 4s/c_r$, the hinge moment in terms of these non-dimensional quantities is

$$H = \frac{2}{3}\frac{aqc_r^3\tan\gamma}{\sqrt{(k^2-1)}}\left[\frac{A^2}{16}(1-\eta_0)(\cot\mu-\cot\gamma)\left\{3\xi_h(1+\eta_0)\right.\right.$$

$$\left.-(\cot\mu+\cot\gamma)(1+\eta_0+\eta_0^2)\frac{A}{4}\right\}$$

$$+\frac{(k-1)}{6k^2\beta}\left\{(k+1)-3k\xi_h\right\}-\frac{(k-1)A^3\beta}{384k^2}\left\{(k+1)\beta\eta_0-3k\xi_h\right\}$$

$$-\frac{\sqrt{(k^2-1)}}{6\pi k^2}\left(\frac{\pi}{2}-\sin^{-1}\beta\eta_0\right)-\frac{\sqrt{(k^2-1)}}{6\pi k^2}\beta\eta_0\frac{A}{4}\sqrt{\left(1-\frac{\beta^2\eta_0^2A^2}{16}\right)}$$

$$+\frac{\sqrt{(k^2-1)}}{3\pi k^2}\frac{\beta^3\eta_0^3A^3}{64}\log\left\{\frac{1+\sqrt{\left(1-\frac{\beta^2\eta_0^2A^2}{16}\right)}}{\frac{1}{4}(\beta\eta_0A)}\right\}\right],\quad\ldots\quad\ldots\quad\ldots\quad(I.15)$$

whence

$b_1 = \partial C_H/\partial\alpha$ is

$$b_1 = \frac{8}{3\sqrt{(k^2-1)}(1-\eta_0)^3}\left[\frac{A^2}{64}(1-\eta_0)(\cot\mu-\cot\gamma)\{12\xi_h(1+\eta_0)\right.$$

$$-(\cot\mu+\cot\gamma)(1+\eta_0+\eta_0^2)A\}$$

$$+\frac{(k-1)\{(k+1)-3k\xi_h\}}{6k^2\beta}-\frac{(k-1)\beta A^3}{384k^2}\{(k+1)\beta\eta_0-3k\xi_h\}$$

$$-\frac{\sqrt{(k^2-1)}}{6\pi k^2}\left(\frac{\pi}{2}-\sin^{-1}\beta\eta_0\right)-\frac{\sqrt{(k^2-1)}}{\pi\beta^2}\beta\eta_0\frac{A}{96}\sqrt{(16-A^2\beta^2\eta_0^2)}$$

$$+\frac{\sqrt{(k^2-1)}}{192\pi k^2}\beta^3A^3\eta_0^3\log\left\{\frac{4+\sqrt{(16-\beta^2A^2\eta_0^2)}}{\beta A\eta_0}\right\}\right].\quad\ldots\quad\ldots\quad(I.16)$$

Consider now the wing at zero incidence with the tip control deflected through an angle ξ.

In what follows we shall assume that the wing geometry is such that the Mach cone from the apex of the control does not intersect the wing root chord. The results therefore apply equally to symmetrical and antisymmetrical control deflection.

Control with Subsonic Leading Edge.—When the Mach cone from the apex of the control lies ahead of the leading edge of control the pressure difference produced by deflection of the control is given by

$$\frac{\Delta p}{q\xi} = \frac{8}{\pi\beta}\frac{k^{3/2}}{(1+k)}\sqrt{\left(\frac{1+t}{k-t}\right)}\qquad 0\leqslant k\leqslant 1,\quad\ldots\quad\ldots\quad\ldots\quad\ldots\quad(I.17)$$

where $k = \beta\tan\gamma$, and $t = \beta(Y/X)$, X and Y being co-ordinates relative to the control apex (*see* Fig. 1).

This result, which can be derived on the basis of the conical flow theory, is taken from Ref. 11. In the same paper the lift produced by this pressure distribution has been calculated.

The lift over the control alone is

$$L_\xi = \frac{16q\xi\bar{c}_\xi{}^2 k^{3/2}}{\pi\beta^2(1+k)}\{\sqrt{k} + (1+k)\tan^{-1}\sqrt{k}\} \quad .. \qquad .. \qquad .. \qquad .. \qquad .. \quad (I.18)$$

and that induced on the wing (*i.e.,* in region OBC of figure of section 4)

$$L_w = \frac{16q\xi\bar{c}_\xi{}^2 k^{3/2}}{\pi\beta^2(1+k)}\left\{\frac{\pi(1+k)}{2} - \sqrt{k} - (1+k)\tan^{-1}\sqrt{k}\right\} .. \quad .. \qquad .. \quad (I.19)$$

Thus the total lift produced by one control is

$$\frac{8q\xi\bar{c}_\xi{}^2 k^{3/2}}{\beta^2} = \frac{8q\xi\bar{c}_\xi{}^2 \tan\gamma k^{1/2}}{\beta} \quad . \quad .. \qquad .. \qquad .. \qquad .. \qquad .. \qquad .. \qquad .. \qquad .. \quad (I.20)$$

In terms of a_2 for a pair of controls this is (symmetrical deflection is implied here)

$$a_2 = \frac{4(1-\eta_0)^2 k^{1/2}}{\beta} = \frac{4(1-\eta^3)^2\sqrt{(\beta\tan\gamma)}}{\beta} \quad . \qquad .. \qquad .. \qquad .. \quad (I.21)$$

The aerodynamic centre of the lift on the control is at the point defined by

$$t_{ac} = \frac{3k-1}{4} + \frac{\sqrt{k}}{2\{\sqrt{k} + (1+k)\tan^{-1}\sqrt{k}\}} \qquad .. \qquad .. \qquad .. \qquad .. \quad (I.22)$$

and

$$X = \frac{2}{3}c_{\xi r},$$

since the pressure field is conical from the origin.

In the co-ordinates X, Y, this point is given by

$$\left.\begin{aligned} X &= \frac{2}{3}c_{\xi r}, \\[2mm] Y &= \frac{2c_{\xi r}}{3\beta}\left[\frac{3k-1}{4} + \frac{\sqrt{k}}{2\{\sqrt{k} + (1+k)\tan^{-1}\sqrt{k}\}}\right] \end{aligned}\right\} . \qquad .. \qquad .. \qquad .. \quad (I.23)$$

$c_{\xi r}$ may be replaced by $(1-\eta_0)c_r$ in these expressions. Together with the lift produced over the control these enable us to determine the hinge moment about any axis position. In particular for an axis position at right angles to the root chord of the wing we have

$$H = -\frac{16q\xi\bar{c}_\xi{}^2 k^{3/2}}{\pi\beta(1+k)}\{\sqrt{k} + (1+k)\tan^{-1}\sqrt{k}\}\left(\frac{2}{3} - \frac{X_h}{c_{\xi r}}\right)c_{\xi r}, \qquad .. \qquad .. \quad (I.24)$$

In derivative form this becomes,

$$b_2 = -\frac{16k^{1/2}}{\pi(1+k)}\{\sqrt{k} + (1+k)\tan^{-1}\sqrt{k}\}(\tfrac{2}{3} - \xi_h'). \qquad .. \qquad .. \qquad .. \quad (I.25)$$

Pitching moment.

The aerodynamic centre of the total lift produced by the control is defined by

$$\left.\begin{aligned} X &= \tfrac{2}{3}c_{\xi r} = \tfrac{2}{3}(1-\eta_0)c_r \\[2mm] Y &= \frac{2}{3}c_{\xi r}\frac{3k-1}{4} \end{aligned}\right\} . \quad .. \qquad .. \qquad .. \qquad .. \qquad .. \qquad .. \qquad .. \quad (I.26)$$

Combining this result with the equation for the total lift (I.20), we obtain the pitching moment produced by one control,

$$M = 8q\xi\bar{c}_\xi{}^2 \frac{\tan\gamma k^{1/2}}{\beta} \times \{\tfrac{2}{3} c_{\xi r} + (c_r - c_{\xi r})\} \dots \qquad \dots \qquad \dots \qquad \dots \qquad \dots \text{(I.27)}$$

For symmetrical deflection of the two wing-tip controls we have in derivative form,

$$m_2 = \frac{\partial C_M}{\partial \xi} = \frac{8}{3} \frac{k^{1/2}}{\beta} (1 - \eta_0)^2 (2 + \eta_0), \dots \qquad \dots \qquad \dots \qquad \dots \qquad \dots \text{(I.28)}$$

the moment being referred to the apex of the wing.

Rolling moment.

From equation (I.26) and the expression for the total lift produced by the control (equation (I.20)), we obtain in a similar way the rolling moment produced by antisymmetrical control deflection.

In the usual derivative form this is, for a pair of controls,

$$l_\xi = - \frac{(1 - \eta_0)^2}{3\beta\sqrt{k}} \{\eta_0(3k + 1) + (3k - 1)\} \dots \qquad \dots \qquad \dots \qquad \dots \text{(I.29)}$$

Some numerical values are plotted in Fig. 18. These results are valid only when the two Mach cones from the control apex do not intersect, and the limit for a delta wing of aspect ratio 2·31 is indicated.

Control with Supersonic Leading Edge.—Again, from Ref. 11 we have in the generally narrow region of the control ahead of the Mach cone the pressure distribution

$$\frac{\Delta p}{q} = \frac{4\xi}{\beta} \frac{k}{\sqrt{(k^2 - 1)}}; \qquad k = \beta\tan\gamma > 1, \dots \qquad \dots \qquad \dots \qquad \dots \text{(I.30)}$$

and inside the Mach cone from the apex of the control,

$$\frac{\Delta p}{q} = \frac{4\xi}{\beta} \frac{k}{\pi\sqrt{(k^2 - 1)}} \cos^{-1}\left(\frac{1 - kt}{k - t}\right) \qquad \dots \qquad \dots \qquad \dots \qquad \dots \qquad \dots \text{(I.31)}$$

$$k > 1, \quad -1 \leqslant t \leqslant 1, \quad \text{and} \quad t = \beta Y/X.$$

For $k = 1$,

$$\frac{\Delta p}{q} = \frac{4\xi}{\pi\beta} \sqrt{\left(\frac{1 + t}{1 - t}\right)} \cdot \qquad \dots \qquad \dots \qquad \dots \qquad \dots \qquad \dots \qquad \dots \text{(I.31a)}$$

It is of interest to note that by superposition of two solutions it can be demonstrated that the lift coefficient of the aileron based on the aileron area must have the two-dimensional value. Detailed integration gives the two separate contributions.

Lift.

The lift induced on the wing is

$$L_w = \frac{2q\xi}{\beta^2} c_{\xi r}{}^2 k \left[\frac{1}{2} - \frac{k}{\pi} \frac{\cos^{-1}(1/k)}{\sqrt{(k^2 - 1)}}\right] \cdot \qquad \dots \qquad \dots \qquad \dots \qquad \dots \qquad \dots \text{(I.32)}$$

The lift on the control alone is,

$$L_\xi = \frac{2q\xi}{\beta^2} c_{\xi r}{}^2 k \left[\frac{1}{2} + \frac{k}{\pi} \frac{\cos^{-1}(1/k)}{\sqrt{(k^2 - 1)}}\right] \cdot \qquad \dots \qquad \dots \qquad \dots \qquad \dots \qquad \dots \text{(I.33)}$$

31

In addition, we get the total lift which, in coefficient form based on aileron area, has the two-dimensional value

$$C_L = \frac{4\xi}{\beta} = \frac{4\xi}{\sqrt{(M^2 - 1)}} \cdot \qquad \cdots \qquad \cdots \qquad \cdots \qquad \cdots \qquad \cdots \qquad \cdots \qquad \cdots \quad (\text{I.34})$$

Thus, based on the wing area, we have for symmetrical deflection for a pair of controls,

$$a_2 = \frac{4(1 - \eta_0)^2}{\sqrt{(M^2 - 1)}} \cdot \qquad \cdots \qquad \cdots \qquad \cdots \qquad \cdots \qquad \cdots \qquad \cdots \qquad \cdots \quad (\text{I.35})$$

<u>Hinge moment of control.</u>

As in the preceding case the aerodynamic centres of the above loads are readily established. For the control lift the co-ordinates of the aerodynamic centre are,

and

$$
\begin{aligned}
X &= \tfrac{2}{3} c_{\xi\,r} = \tfrac{2}{3}(1 - \eta_0)c_r \\
Y &= \frac{2}{3}\frac{(1 - \eta_0)}{\beta} c_r \left\{ \frac{k}{2} + \frac{\sqrt{(k^2 - 1)}}{\pi\sqrt{(k^2 - 1)} + 2k\cos^{-1}(1/k)} \right\} \\
&= \frac{2}{3}\frac{c_{\xi\,r}}{\beta} \left\{ \frac{k}{2} + \frac{\sqrt{(k^2 - 1)}}{\pi\sqrt{(k^2 - 1)} + 2k\cos^{-1}(1/k)} \right\}
\end{aligned}
\right\} \quad \cdots \qquad \cdots \qquad \cdots \quad (\text{I.36})
$$

Taken together with the lift produced on the control itself (equation (I.33)), these give the hinge moment about any axis position. In particular for the axis perpendicular to the centre-line we have

$$H = -\frac{2q\xi}{\beta^2} c_{\xi\,r}^2 k \left\{ \frac{1}{2} + \frac{k}{\pi}\frac{\cos^{-1}(1/k)}{\sqrt{(k^2 - 1)}} \right\} \left(\tfrac{2}{3} - \xi_h' \right) c_{\xi\,r} \cdot \quad \cdots \qquad \cdots \qquad \cdots \quad (\text{I.37})$$

Or in derivative form,

$$b_2 = -\frac{8}{\beta} \left\{ \frac{1}{2} + \frac{k}{\pi}\frac{\cos^{-1}(1/k)}{\sqrt{(k^2 - 1)}} \right\} (2 - \xi_h') \cdot \quad \cdots \qquad \cdots \qquad \cdots \qquad \cdots \quad (\text{I.37}a)$$

<u>Pitching moment.</u>

The co-ordinates of the aerodynamic centre of the total lift are

and

$$
\begin{aligned}
X &= \tfrac{2}{3} c_{\xi\,r} = \tfrac{2}{3}(1 - \eta_0)c_r \\
Y &= \frac{2}{3}\frac{k}{2\beta} c_{\xi\,r} = \frac{\tan\gamma}{3} c_{\xi\,r}
\end{aligned}
\right\} \cdot \quad \cdots \qquad \cdots \qquad \cdots \qquad \cdots \qquad \cdots \qquad \cdots \qquad \cdots \quad (\text{I.38})
$$

In terms of x, y, the co-ordinates are

and

$$
\begin{aligned}
x &= c_r \left[1 - \frac{(1 - \eta_0)}{3} \right] = \frac{c_r}{3}(2 + \eta_0) \\
y &= \eta_0 s + Y = \frac{c_r}{3}\tan\gamma(2\eta_0 + 1)
\end{aligned}
\right\} \cdot \quad \cdots \qquad \cdots \qquad \cdots \qquad \cdots \quad (\text{I.38}a)
$$

Thus the pitching moment produced by deflection of one control is (from equations (I.38a) and (I.34)):

$$M = \frac{q\xi}{\beta^2} c_{\xi\,r}^2 k \frac{c_r}{3}(2 + \eta_0) , \qquad \cdots \qquad \cdots \qquad \cdots \qquad \cdots \qquad \cdots \qquad \cdots \quad (\text{I.39})$$

with reference to the apex of the wing.

32

For symmetrical control deflection we have, for two controls,

$$m_2 = \frac{\partial C_M}{\partial \xi} = \frac{8}{3\beta}(1 - \eta_0)^2(2 + \eta_0) . \quad .. \quad .. \quad .. \quad .. \quad .. \quad (I.39a)$$

Rolling moment.

Equations (I.34) and (I.38a) enable us to evaluate another interesting quantity, namely, the rolling moment due to antisymmetrically deflected controls.

In derivative form this is given by the following relatively simple relation for a pair of ailerons,

$$l_\xi = -\frac{2(1 - \eta_0)^2(2\eta_0 + 1)}{3\beta} . \quad .. \quad .. \quad .. \quad .. \quad .. \quad .. \quad .. \quad (I.40)$$

Numerical results for $M = 2 \cdot 5$ are shown in Fig. 18, with the same limitations as for equation (I.29).

I.2. *Sectional Values of the Derivatives.*—To give data corresponding to those given in the other two sections of this note we now consider the local or sectional derivatives. This implies an integration in the chordwise direction, which is a natural direction at subsonic speeds, but not at supersonic speeds where the pressure distribution is composed of conical fields. Accordingly some of the integration is tedious, and is mostly dealt with in Appendix II.

Wing and Control inside Mach Cone (Subsonic Leading Edge).—*Wing at Incidence, Control Neutral.*—The pressure distribution is given in Section I.1 and the integrations for this case are given in Ref. 14. Integrating we have for the lift

$$\frac{dL}{dy} = \int_{x_l}^{x_t} \Delta p \, dx$$

$$= \frac{4aq}{E\{\sqrt{(1 - k^2)}\}} s\sqrt{(1 - \eta^2)} . \quad .. \quad .. \quad .. \quad .. \quad .. \quad .. \quad (I.41)$$

In derivative form this is

$$a_{1l}(1 - \eta) = \frac{4s}{Ec_r}\sqrt{(1 - \eta^2)} = \frac{A}{E}\sqrt{(1 - \eta^2)} . \quad .. \quad .. \quad .. \quad .. \quad (I.41a)$$

The sonic solution is obtained by making $E \to 1$, and so is

$$a_{1l}(1 - \eta) = A\sqrt{(1 - \eta^2)} . \quad .. \quad .. \quad .. \quad .. \quad .. \quad .. \quad .. \quad (I.41b)$$

Pitching moment.

This again can be readily deduced from the results of Ref. 14, and

$$\frac{dM}{dy} = \int_{x_l}^{x_t} \Delta p(x - x_l) \, dx$$

$$= \frac{4aq}{E} \frac{s^2}{\tan \gamma} \left\{ \frac{\sqrt{(1 - \eta^2)}}{2} + \frac{\eta^2}{2} \log \left(\frac{1 + \sqrt{(1 - \eta^2)}}{\eta} \right) - \sqrt{(1 - \eta^2)} \right\} . \quad .. \quad .. \quad (I.42)$$

So that

$$m_{1l} = \frac{\partial C_m}{\partial a} = \frac{4}{E}\left(\frac{s}{c}\right)^2 \frac{1}{\tan \gamma} \left\{ \frac{\sqrt{(1 - \eta^2)}}{2} + \frac{\eta^2}{2} \log \left(\frac{1 + \sqrt{(1 - \eta^2)}}{\eta} \right) - \eta\sqrt{(1 - \eta^2)} \right\} \quad (I.43)$$

or in terms of aspect ratio

$$m_{1l}(1 - \eta)^2 = \frac{A}{2E\{\sqrt{(1 - k^2)}\}} \left\{ \sqrt{(1 - \eta^2)} + \eta^2 \log \left(\frac{1 + \sqrt{(1 - \eta^2)}}{\eta} \right) - 2\eta\sqrt{(1 - \eta^2)} \right\} . \quad (I.43a)$$

Wing and Control with Supersonic Leading Edge.—Wing at Incidence, Control Neutral.—For the region between the wing leading edge and the Mach cone we have the pressure distribution given by equation (I.9), and behind the Mach cone we have that defined by equation (I.10).

Lift.

The sectional lift is given by a chordwise integration thus,

$$\frac{dL}{dy} = \int_{x_l}^{y\cot\mu} \varDelta p_1\, dx + \int_{y\cot\mu}^{x_t} \varDelta p_2\, dx . \quad \ldots \quad \ldots \quad \ldots \quad \ldots \quad \ldots \quad \ldots \quad (I.44)$$

Now $x_t = y \cot\gamma$, and $y \cot\mu = \beta y$.

Thus,

$$\int_{x_l}^{y\cot\mu} \varDelta p_1\, dx = \frac{4aq\tan\gamma}{\sqrt{(k^2-1)}}\,(\cot\mu - \cot\gamma)y ,$$

and

$$\int_{y\cot\mu}^{x} \varDelta p_2\, dx = \frac{4aq\tan\gamma}{\pi\sqrt{(k^2-1)}} \int_{y\cot\mu}^{x_t} \left\{ \cos^{-1}\left(\frac{x+k\beta y}{kx+\beta y}\right) + \cos^{-1}\left(\frac{x-k\beta y}{kx-\beta y}\right) \right\} dx$$

$$= \frac{4aq\tan\gamma}{\pi k\sqrt{(k^2-1)}} \left| (kx-\beta y)\cos^{-1}\left(\frac{x-k\beta y}{kx-\beta y}\right)\right.$$

$$\left. + (kx+\beta y)\cos^{-1}\left(\frac{x+k\beta y}{kx+\beta y}\right) \right|_{y\cot\mu}^{x_t}$$

by Appendix II, and on inserting the limits we have,

$$\int_{y\cot\mu}^{x_t} \varDelta p_2\, dx = \frac{4aq\tan\gamma}{\pi k\sqrt{(k^2-1)}} \left\{ (kx_t-\beta y)\cos^{-1}\left(\frac{x_t-k\beta y}{kx_t-\beta y}\right)\right.$$

$$\left. + (kx_t+\beta y)\cos^{-1}\left(\frac{x_t+k\beta y}{kx_t+\beta y}\right) - \pi\beta y(k-1) \right\} .$$

For a delta wing $x_t = c_r$, and so finally we get for this wing,

$$\frac{dL}{dy} = \frac{4aq\tan\gamma}{\pi k\sqrt{(k^2-1)}} \left[(kc_r-\beta y)\cos^{-1}\left(\frac{c_r-k\beta y}{kc_r-\beta y}\right) + (kc_r+\beta y)\cos^{-1}\left(\frac{c_r+k\beta y}{kc_r+\beta y}\right) \right]$$

$$= \frac{4aq\tan\gamma c_r}{\pi\sqrt{(k^2-1)}} \left[(1-\eta)\cos^{-1}\left\{\frac{(1-\eta k^2)}{k(1-\eta)}\right\} + (1+\eta)\cos^{-1}\left\{\frac{(1+\eta k^2)}{k(1+\eta)}\right\} \right]. \quad \ldots \quad (I.45)$$

In the derivative form this is

$$a_{1l}(1-\eta) = \frac{4\tan\gamma}{\pi\sqrt{(k^2-1)}} \left[(1-\eta)\cos^{-1}\left\{\frac{(1-k^2\eta)}{k(1-\eta)}\right\} + (1+\eta)\cos^{-1}\left\{\frac{(1+k^2\eta)}{k(1+\eta)}\right\} \right], \quad \ldots \quad (I.46)$$

which can be expressed in terms of the wing aspect ratio A by writing $\tan\gamma = A/4$ and $k = \beta\tan\gamma = \beta A/4$.

Pitching moment.

The pitching moment locally about the leading edge of the chord is given by

$$\frac{dM}{dy} = \int_{x_l}^{\beta y} \varDelta p_1 x\, dx + \int_{\beta y}^{x_t} \varDelta p_2 x\, dx . \quad \ldots \quad \ldots \quad \ldots \quad \ldots \quad \ldots \quad \ldots \quad (I.47)$$

34

But

$$\int_{x_l}^{\beta y} \Delta p_l \, x \, dx = \frac{4aq \tan \gamma}{\sqrt{(k^2 - 1)}} \int_{x_l}^{\beta y} x \, dx$$

$$= \frac{2aq \tan \gamma}{\sqrt{(k^2 - 1)}} \left(\beta^2 y^2 - x_l^2 \right)$$

$$= \frac{2aq \tan \gamma}{\sqrt{(k^2 - 1)}} \left(\beta^2 y^2 - y^2 \cot^2 \gamma \right) ,$$

and

$$\int_{\beta y}^{x_t} \Delta p_2 x \, dx = \int_{\beta y}^{x_t} \frac{4aq \tan \gamma}{\pi \sqrt{(k^2 - 1)}} \left\{ \cos^{-1} \left(\frac{x + k\beta y}{kx + \beta y} \right) + \cos^{-1} \left(\frac{x - k\beta y}{kx - \beta y} \right) \right\} x \, dx$$

$$= \frac{4aq \tan \gamma}{\pi \sqrt{(k^2 - 1)}} \left| \frac{\beta^2 y^2 \sqrt{(k^2 - 1)}}{k^2} \log \left\{ x + \sqrt{(x^2 - \beta^2 y^2)} \right\} \right.$$

$$\left. + \frac{(k^2 x^2 - \beta^2 y^2)}{2k^2} \left\{ \cos^{-1} \left(\frac{x + k\beta y}{kx + \beta y} \right) + \cos^{-1} \left(\frac{x - k\beta y}{kx - \beta y} \right) \right\} \right|_{\beta y}^{x_t}$$

$$= \frac{4aq \tan \gamma}{\pi \sqrt{(k^2 - 1)}} \left[\frac{\beta^2 y^2 \sqrt{(k^2 - 1)}}{k^2} \log \left(\frac{x_t + \sqrt{(x_t^2 - \beta^2 y^2)}}{\beta y} \right) \right.$$

$$\left. + \frac{(k^2 x_t^2 - \beta^2 y^2)}{2k^2} \left\{ \cos^{-1} \left(\frac{x_t + k\beta y}{kx_t + \beta y} \right) + \cos^{-1} \left(\frac{x_t - k\beta y}{kx_t - \beta y} \right) \right\} - \frac{\beta^2 y^2 \pi (k^2 - 1)}{2k^2} \right] .$$

For the particular case of the delta wing $x_t = c_r$, so that if we set $y = \eta s$ and note that $s/c_r = \tan \gamma$ and that $k = \beta \tan \gamma$, we may write

$$\int_{\beta y}^{x_t} \Delta p_2 x \, dx = \frac{4aq c_r^2 \tan \gamma}{\pi \sqrt{(k^2 - 1)}} \left[\eta^2 \sqrt{(k^2 - 1)} \log \left(\frac{1 + \sqrt{(1 - k^2 \eta^2)}}{k\eta} \right) \right.$$

$$\left. + \frac{(1 - \eta^2)}{2} \left\{ \cos^{-1} \left(\frac{1 + k^2 \eta}{k(1 + \eta)} \right) + \cos^{-1} \left(\frac{1 - k^2 \eta}{k(1 - \eta)} \right) \right\} - \frac{\pi (k^2 - 1)}{2} \eta^2 \right] .$$

Similarly,

$$\int_{x_l}^{\beta y} \Delta p_1 x \, dx = \frac{2aq \tan \gamma}{\sqrt{(k^2 - 1)}} c_r^2 \eta^2 (k^2 - 1) .$$

From which it follows that

$$\frac{dM}{dy} = \frac{4aq c_r^2 \tan \gamma}{\pi \sqrt{(k^2 - 1)}} \left[\eta^2 \sqrt{(k^2 - 1)} \log \left(\frac{1 + \sqrt{(1 - k^2 \eta^2)}}{k\eta} \right) \right.$$

$$\left. + \frac{(1 - \eta^2)}{2} \left\{ \cos^{-1} \left(\frac{1 + k^2 \eta}{k(1 + \eta)} \right) + \cos^{-1} \left(\frac{1 - k^2 \eta}{k(1 - \eta)} \right) \right\} \right] . \qquad \text{..} \qquad \text{.. (I.48)}$$

In derivative form this is

$$m_{1l} = \frac{\partial C_m}{\partial a} = \frac{4 \tan \gamma}{\pi (1 - \eta)^2 \sqrt{(k^2 - 1)}} \left[\eta^2 \sqrt{(k^2 - 1)} \log \left(\frac{1 + \sqrt{(1 - k^2 \eta^2)}}{k\eta} \right) \right.$$

$$\left. + \frac{(1 - \eta^2)}{2} \left\{ \cos^{-1} \left(\frac{1 + k^2 \eta}{k(1 + \eta)} \right) + \cos^{-1} \left(\frac{1 - k^2 \eta}{k(1 - \eta)} \right) \right\} \right] . \qquad \text{..} \qquad \text{.. (I.49)}$$

This result can be expressed in terms of β and A if we use the relations $A = 4 \tan \gamma$ and $k = \beta \tan \gamma = \beta A/4$.

Turning now to the effect of control deflection we again consider the two speed regimes separately.

35

Control with Subsonic leading Edge.—Wing at Zero Incidence, Control Deflected through an Angle ξ.—The pressure distribution is already given in the corresponding paragraph of Section I.1 (equation (I.17)), and it remains to perform the necessary chordwise integrations.

Lift.

For the local or sectional lift over the control we have

$$
\begin{aligned}
\frac{dL}{dy} &= \int_{X_l}^{X_t} \Delta p \, dX \\
&= \frac{8q\xi k^{3/2}}{\pi\beta(1+k)} \int_{X_l}^{X_t} \sqrt{\left(\frac{X+\beta Y}{kX-\beta Y}\right)} \, dX \\
&= \frac{8q\xi}{\pi(\beta+\cot\gamma)} \int_{X_l}^{X_t} \sqrt{\left(\frac{X+\beta Y}{X-Y\cot\gamma}\right)} \, dX \,, \qquad \cdots \quad \cdots \quad \cdots \quad (\text{I.50})
\end{aligned}
$$

which by the 4th integral of Appendix II,

$$
\begin{aligned}
&= \frac{8q\xi}{\pi(\beta+\cot\gamma)} \Bigg| \sqrt{\{(X+\beta Y)(X-Y\cot\gamma)\}} \\
&\quad - \frac{Y}{2}(\beta+\cot\gamma)\log\left\{\frac{\sqrt{(X+\beta Y)}-\sqrt{(X-Y\cot\gamma)}}{\sqrt{(X+\beta Y)}+\sqrt{(X-Y\cot\gamma)}}\right\}\Bigg|_{X_l=Y\cot\gamma}^{X_t} \\
&= \frac{8q\xi}{\pi(\beta+\cot\gamma)} \Bigg[\sqrt{\{(X_t+\beta Y)(X_t-Y\cot\gamma)\}} \\
&\quad - \frac{Y}{2}(\beta+\cot\gamma)\log\left\{\frac{\sqrt{(X_t+\beta Y)}-\sqrt{(X_t-Y\cot\gamma)}}{\sqrt{(X_t+\beta Y)}+\sqrt{(X_t-Y\cot\gamma)}}\right\}\Bigg] \,.
\end{aligned}
$$

For the delta wing $X_t = c_{\xi r}$.

In this case

$$
\begin{aligned}
\frac{dL}{dy} &= \frac{8q\xi c_{\xi r}}{\pi(\beta+\cot\gamma)} \Bigg[\sqrt{\{(1-\eta')(1+k\eta')\}} \\
&\quad - \frac{\eta'(\beta\tan\gamma+1)}{2\tan\gamma}\log\left\{\frac{\sqrt{(1+k\eta')}-\sqrt{(1-\eta')}}{\sqrt{(1+k\eta')}+\sqrt{(1-\eta')}}\right\}\Bigg] \,, \qquad \cdots \quad \cdots \quad (\text{I.51})
\end{aligned}
$$

where $\eta' = Y/s_\xi$, and so

$$
\begin{aligned}
\frac{dL}{dy} &= \frac{8q\xi c_{\xi r}}{\pi(1+k)} \Bigg[\tan\gamma\sqrt{\{(1-\eta')(1+k\eta')\}} \\
&\quad - \eta'(1+k)\log\left\{\frac{\sqrt{(1+k\eta')}-\sqrt{(1-\eta')}}{\sqrt{\{\eta'(k+1)\}}}\right\}\Bigg] \,.
\end{aligned}
$$

In derivative form we thus have

$$
\begin{aligned}
a_{2t}(1-\eta') &= \frac{8}{\pi(1+k)} \Bigg[\tan\gamma\sqrt{\{(1-\eta')(1+k\eta')\}} \\
&\quad - (1+k)\eta'\log\left\{\frac{\sqrt{(1+k\eta')}-\sqrt{(1-\eta')}}{\sqrt{\{\eta'(k+1)\}}}\right\}\Bigg] \,. \qquad \cdots \quad \cdots \quad (\text{I.51}a)
\end{aligned}
$$

By means of the transformation $\eta' = (\eta-\eta_0)/(1-\eta_0)$ we can express this in terms of η, the non-dimensional spanwise distance from the wing root chord.

36

For the part of the wing affected by control deflection the integration extends from the Mach cone to the trailing edge of the wing, thus for this part of the wing

$$-\frac{1}{k} \leqslant \eta' \leqslant 0; \quad \frac{dL}{dY} = \int_{|Y|\cot\mu}^{X_t} \Delta p \, dX$$

$$= \frac{8q\xi}{\pi(\beta+\cot\gamma)} \int_{|Y|\cot\mu}^{X_t} \sqrt{\left(\frac{X+\beta Y}{X-Y\cot\gamma}\right)} dX$$

$$= \frac{8q\xi}{\pi(\beta+\cot\gamma)} \left[\sqrt{\{(X_t - Y\cot\gamma)(X_t+\beta Y)\}}\right.$$

$$\left. - \frac{Y}{2}(\beta+\cot\gamma)\log\left\{\frac{\sqrt{(X_t - Y\cot\gamma)} - \sqrt{(X_t+\beta Y)}}{\sqrt{(X_t - Y\cot\gamma)} + \sqrt{(X_t+\beta Y)}}\right\}\right]. \qquad \text{.. (I.52)}$$

For the delta wing we set $X_t = c_{\xi r}$, and so obtain

$$\frac{dL}{dY} = \frac{8q\xi c_{\xi r}}{\pi(1+k)}\left[\tan\gamma\sqrt{\{(1+k\eta')(1-\eta')\}}\right.$$

$$\left. - \eta'(1+k)\log\left\{\frac{\sqrt{(1-\eta')} - \sqrt{(1+k\eta')}}{\sqrt{\{-\eta'(1+k)\}}}\right\}\right], \qquad \text{..} \qquad \text{..} \qquad (I.52a)$$

which in derivative form is

$$a_{2t}(1-\eta') = \frac{8}{\pi(1+k)}\left[\tan\gamma\sqrt{\{(1-\eta')(1+k\eta')\}}\right.$$

$$\left. - (1+k)\eta'\log\left\{\frac{\sqrt{(1-\eta')} - \sqrt{(1+k\eta')}}{\sqrt{\{-\eta'(1+k)\}}}\right\}\right]. \qquad \text{..} \qquad \text{..} \qquad \text{.. (I.53)}$$

This also can be expressed in terms of η by use of the transformation given above.

Pitching moment.

Taking moments about the leading edge and integrating chordwise we have, over the control

$$\frac{dM}{dy} = \int_{X_l}^{X_t} \Delta p(X - X_l)\, dX$$

$$= \frac{8q\xi}{\pi(\beta+\cot\gamma)}\int_{X_l}^{X_t}(X-X_l)\sqrt{\left(\frac{X+\beta Y}{X-Y\cot\gamma}\right)} dX. \qquad \text{..} \qquad \text{.. (I.54)}$$

Using the results of Appendix II, integrals 4 and 5, this can be written

$$\frac{dM}{dy} = \frac{8q\xi}{\pi(\beta+\cot\gamma)}\left[\frac{\sqrt{\{(X_t+\beta Y)(X_t-Y\cot\gamma)\}}}{4}\{(X_t+\beta Y)+(X_t-Y\cot\gamma)\}\right.$$

$$\left. + \frac{Y^2(\beta+\cot\gamma)^2}{8}\log\left\{\frac{\sqrt{(X_t+\beta Y)} - \sqrt{(X_t-Y\cot\gamma)}}{\sqrt{(X_t+\beta Y)} + \sqrt{(X_t-Y\cot\gamma)}}\right\}\right] . \text{..} \qquad \text{..} \qquad \text{.. (I.55)}$$

37

For delta wing with half-delta control $X_t = c_{\xi r}$, thus:

$$\frac{dM}{dy} = \frac{8q\xi c_{\xi r}^2}{\pi(\beta + \cot\gamma)}\left[\frac{\sqrt{\{(1 + k\eta')(1 - \eta')\}}}{4}\{(1 + k\eta') + (1 - \eta')\}\right.$$
$$\left. + \frac{\eta'^2 \tan^2\gamma(\beta + \cot\gamma)^2}{8}\log\left\{\frac{\sqrt{(1 + k\eta')} - \sqrt{(1 - \eta')}}{\sqrt{(1 + k\eta')} + \sqrt{(1 - \eta')}}\right\}\right]$$
$$= \frac{2q\xi c_{\xi r}^2}{\pi(\beta + \cot\gamma)}\left[\sqrt{\{(1 + k\eta')(1 - \eta')\}\{(1 + k\eta') + (1 - \eta')\}}\right.$$
$$\left. + \eta'^2(1 + k)^2\log\left\{\frac{\sqrt{(1 + k\eta')} - \sqrt{(1 - \eta')}}{\sqrt{\{\eta'(1 + k)\}}}\right\}\right]. \qquad .. \qquad .. \qquad .. \qquad .. \quad (I.56)$$

In derivative form this is

$$m_{2t} = \frac{\partial C_m}{\partial\xi} = \frac{2}{\pi(\beta + \cot\gamma)(1 - \eta')^2}\left[\sqrt{\{(1 + k\eta')(1 - \eta')\}\{(1 + k\eta') + (1 - \eta')\}}\right.$$
$$\left. + \eta'^2(1 + k)^2\log\left\{\frac{\sqrt{(1 + k\eta')} - \sqrt{(1 - \eta')}}{\sqrt{\{\eta'(1 + k)\}}}\right\}\right]. \qquad .. \qquad .. \qquad .. \quad (I.56a)$$

This can in turn be expressed in terms of η if desired.

Lift is induced over part of the wing $- 1/k \leqslant \eta' \leqslant 0$ and for this part of the span the local pitching moment is given by

$$\frac{dM}{dy} = \int_{|Y|\cot\mu}^{X_t} \Delta p(X - X_t)\, dX, \quad .. \qquad .. \qquad .. \qquad .. \qquad .. \qquad .. \qquad .. \qquad .. \quad (I.57)$$

where of course $|Y|\cot\mu = \beta|Y|$.

This yields

$$m_{2t} = \frac{2}{\pi(\beta + \cot\gamma)(1 - \eta')^2}\left[\sqrt{\{(1 + k\eta')(1 - \eta')\}\{(1 + k\eta') + (1 - \eta')\}}\right.$$
$$\left. + \eta'^2(1 + k)^2\log\left\{\frac{\sqrt{(1 - \eta')} - \sqrt{(1 + k\eta')}}{\sqrt{\{-\eta'(1 + k)\}}}\right\}\right]. \qquad .. \qquad .. \qquad .. \qquad .. \quad (I.58)$$

Control with Supersonic Leading Edge.—Wing at Zero Incidence, Control Deflected through an Angle ξ.—

Lift.

The pressure distribution is given in the corresponding paragraph of Section I.1, and we have for the sectional lift produced over the control by control deflection, using equations (I.30) and (I.31),

$$\frac{dL}{dY} = \int_{X_t}^{X_0} \frac{4q\xi}{\beta}\frac{k}{\sqrt{(k^2 - 1)}}\, dX + \int_{X_0}^{X_t} \frac{4q\xi}{\beta}\frac{k}{\pi\sqrt{(k^2 - 1)}}\cos^{-1}\left(\frac{1 - kt}{k - t}\right)dX, \quad .. \qquad .. \quad (I.59)$$

where $X_0 = \beta Y$ and $t = \beta Y/X$.

The necessary integration has been performed in Appendix II, and it follows that, for $0 \leqslant \eta' \leqslant 1/k$,

$$\frac{dL}{dy} = \frac{4q\xi k}{\pi\beta\sqrt{(k^2 - 1)}}\left[\left(\frac{kX_t - \beta Y}{k}\right)\cos^{-1}\left(\frac{X_t - k\beta Y}{kX_t - \beta Y}\right)\right.$$
$$\left. + \frac{\beta Y\sqrt{(k^2 - 1)}}{k}\log\left\{\frac{X_t + \sqrt{(X_t^2 - \beta^2 Y^2)}}{\beta Y}\right\}\right]. \quad .. \qquad .. \qquad .. \qquad .. \qquad .. \quad (I.60)$$

38

Or in derivative form, for $0 \leqslant \eta' \leqslant 1/k$,

$$a_{2l} = \frac{4 \tan \gamma}{\pi(1 - \eta')\sqrt{(k^2 - 1)}} \left[(1 - \eta') \cos^{-1} \left[\frac{1 - k^2\eta'}{k(1 - \eta')} \right] \right.$$
$$\left. + \eta'\sqrt{(k^2 - 1)} \log \left\{ \frac{1 + \sqrt{(1 - k^2\eta'^2)}}{k\eta'} \right\} \right] , \qquad .. \qquad .. \qquad .. \qquad .. \qquad (I.60a)$$

where $k = \beta \tan \gamma$.

For sections lying ahead of the Mach cone we have simply

$$a_{2l} = \frac{4 \tan \gamma}{\sqrt{(k^2 - 1)}} ; \qquad 1 \geqslant \eta' \geqslant \frac{1}{k} . \qquad .. \qquad .. \qquad .. \qquad .. \qquad .. \qquad .. \qquad .. \quad (I.61)$$

For that part of the wing affected by control deflection, that is, $- 1/k \leqslant \eta' \leqslant 0$, we have on performing the required integration and after reducing to non-dimensional form,

$$a_{2l} = \frac{4 \tan \gamma}{\pi(1 - \eta')\sqrt{(k^2 - 1)}} \left[(1 - \eta') \cos^{-1} \left\{ \frac{1 - k^2\eta'}{k(1 - \eta')} \right\} \right.$$
$$\left. + \eta'\sqrt{(k^2 - 1)} \log \left\{ \frac{1 + \sqrt{(1 - k^2\eta'^2)}}{k|\eta'|} \right\} \right] . \qquad .. \qquad .. \qquad .. \qquad .. \qquad .. \quad (I.62)$$

All these derivatives can, of course, be expressed in terms of η, the non-dimensional distance in terms of wing semi-span.

Pitching moment.

Over the control itself the local pitching moment about the leading edge is given by

$$\frac{dM}{dy} = \frac{4q\xi k}{\beta\sqrt{(k^2 - 1)}} \int_{X_l}^{X_0} (X - X_l) \, dx + \frac{4q\xi k}{\pi\beta\sqrt{(k^2 - 1)}} \int_{X_0 = \beta Y}^{X_t} \cos^{-1} \left(\frac{1 - kt}{k - t} \right) (X - X_l) \, dX . \quad (I.63)$$

On inserting from Appendix II, with the limits of integration, we have, after collecting terms,

$$\frac{dM}{dy} = \frac{4q\xi}{\beta} \frac{k}{\sqrt{(k^2 - 1)}} \left[\frac{(kX_t - \beta Y)^2}{2\pi k^2} \cos^{-1} \left(\frac{X_t - k\beta Y}{kX_t - \beta Y} \right) \right.$$
$$\left. - \frac{\beta^2 Y^2}{2\pi k^2} \sqrt{(k^2 - 1)} \log \left(\frac{X_t + \sqrt{(X_t^2 - \beta^2 Y^2)}}{\beta Y} \right) + \frac{\beta Y}{2k} \sqrt{(k^2 - 1)}\sqrt{(X_t^2 - \beta^2 Y^2)} \right]$$
$$= \frac{2q\xi k}{\pi\beta\sqrt{(k^2 - 1)}} \left[(X_t - Y \cot \gamma)^2 \cos^{-1} \left(\frac{X_t - k\beta Y}{kX_t - \beta Y} \right) \right.$$
$$- Y^2 \cot^2 \gamma \sqrt{(k^2 - 1)} \log \left(\frac{X_t + \sqrt{(X_t^2 - \beta^2 Y^2)}}{\beta Y} \right)$$
$$\left. + Y \cot \gamma \sqrt{(k^2 - 1)}\sqrt{(X_t^2 - \beta^2 Y^2)} \right] . \qquad .. \qquad .. \qquad .. \qquad .. \qquad .. \qquad .. \quad (I.64)$$

For delta wing, with half-delta control, $X_t = c_{\xi r}$, and $Y \cot \gamma = \eta' c_{\xi r}$. Thus for this combination, and for $0 \leqslant \eta' \leqslant 1/k$,

$$\frac{dM}{dy} = \frac{2q\xi k c_{\xi r}^2}{\pi\beta\sqrt{(k^2 - 1)}} \left[(1 - \eta')^2 \cos^{-1} \left\{ \frac{1 - k^2\eta'}{k(1 - \eta')} \right\} \right.$$
$$\left. - \eta'^2\sqrt{(k^2 - 1)} \log \left(\frac{1 + \sqrt{(1 - k^2\eta'^2)}}{k\eta'} \right) + \eta'\sqrt{(k^2 - 1)}\sqrt{(1 - k^2\eta'^2)} \right] . \, .. \qquad .. \quad (I.65)$$

39

In derivative form this is

$$m_{2l} = \frac{2\tan\gamma}{\pi(1-\eta')^2\sqrt{(k^2-1)}}\left[(1-\eta')^2\cos^{-1}\left\{\frac{1-k^2\eta'}{k(1-\eta')}\right\}\right.$$
$$\left. - \eta'^2\sqrt{(k^2-1)}\log\left(\frac{1+\sqrt{(1-k^2\eta'^2)}}{k\eta'}\right) + \eta'\sqrt{(k^2-1)}\sqrt{(1-k^2\eta'^2)}\right], \ .. \qquad (I.65a)$$

which is expressible in terms of η for all previous derivatives.

In the region of the wing defined by $-1/k \leqslant \eta' \leqslant 0$, where there is an induced lift behind the Mach cone, we have merely the integral from $X_0 = \beta\,|Y|$ to the wing trailing edge thus,

$$\frac{dM}{dy} = \int_{X_0-\beta|Y|}^{X_l} \frac{4q\xi k}{\pi\beta\sqrt{k^2-1})}\cos^{-1}\left(\frac{1-kt}{k-t}\right)(X-X_l)\,dX \ . .. \qquad \qquad .. \qquad .. \qquad .. \qquad .. \ (I.66)$$

Integration yields, for our special case,

$$\frac{dM}{dy} = \frac{2q\xi kc_{\xi r}^2}{\pi\beta\sqrt{(k^2-1)}}\left[(1-\eta')^2\cos^{-1}\left\{\frac{1-k^2\eta'}{k(1-\eta')}\right\}\right.$$
$$\left. - \eta'^2\sqrt{(k^2-1)}\log\left(\frac{1+\sqrt{(1-k^2\eta'^2)}}{k\,|\eta'|}\right) + \eta'\sqrt{(k^2-1)}\sqrt{(1-k^2)\eta'^2}\right], \ .. \qquad .. \ (I.67)$$

or in derivative form,

$$m_2 = \frac{2\tan\gamma}{\pi(1-\eta')^2\sqrt{(k^2-1)}}\left[(1-\eta')^2\cos^{-1}\left\{\frac{1-k^2\eta'}{k(1-\eta')}\right\}\right.$$
$$\left. - \eta'^2\sqrt{(k^2-1)}\log\left(\frac{1+\sqrt{(1-k^2\eta'^2)}}{k\,|\eta'|}\right) + \eta'\sqrt{(k^2-1)}\sqrt{(1-k^2\eta'^2)}\right] \ldots \qquad .. \ (I.68)$$

This is again expressible in terms of η by means of the relation given earlier.

For those sections which are ahead of the Mach cone we have simply

$$m_{2l} = \frac{2\tan\gamma}{\sqrt{(k^2-1)}} \qquad .. \qquad .. \qquad .. \qquad .. \qquad .. \qquad .. \qquad .. \qquad .. \qquad .. \qquad .. \ (I.69)$$

for $1/k \leqslant \eta' \leqslant 1$.

APPENDIX II

II.1.1. *Some Integrals Required in the Supersonic Theory.*

$$\int_{y_0}^{s} y^2 \log\left[\frac{s+\sqrt{(s^2-y^2)}}{y}\right]dy \ .$$

Integrating by parts we have

$$\left|\frac{y^3}{3}\log\left[\frac{s+\sqrt{(s^2-y^2)}}{y}\right]\right|_{y_0}^{s} + \frac{s}{3}\int_{y_0}^{s} y^3 \frac{dy}{y\sqrt{(s^2-y^2)}}$$

$$= -\frac{y_0^3}{y}\log\left\{\frac{s+\sqrt{(s^2-y_0^2)}}{y_0}\right\} + \frac{s}{3}\left|-\tfrac{1}{2}y\sqrt{(s^2-y^2)}+\frac{s^2}{2}\sin^{-1}\frac{y}{s}\right|_{y_0}^{s}$$

$$= -\frac{y_0^3}{3}\log\left\{\frac{s+\sqrt{(s^2-y_0^2)}}{y_0}\right\} + \frac{s}{3}\left\{\frac{\pi s^2}{4}+\tfrac{1}{2}y_0\sqrt{(s^2-y_0^2)}-\frac{s^2}{2}\sin^{-1}\frac{y_0}{s}\right\} \ .$$

40

II.1.2.
$$\int \cos^{-1}\left(\frac{x - \beta k y}{kx - \beta y}\right) dx \quad \text{and} \quad \int \cos^{-1}\left(\frac{x + \beta k y}{kx + \beta y}\right) dx .$$

With $c_1 = \beta y$ in the first integral and $- \beta y$ in the second, we may write both integrals in the form,
$$\int \cos^{-1}\left(\frac{x - kc_1}{kx - c_1}\right) dx .$$

To integrate this put
$$u = \frac{x - kc_1}{kx - c_1} \quad \text{or} \quad x = \frac{c_1(k - u)}{1 - ku} ,$$
so that
$$\frac{dx}{du} = \frac{c_1(k^2 - 1)}{(1 - ku)^2}$$
and the integrals become
$$c_1(k^2 - 1) \int \cos^{-1} u \, \frac{du}{(1 - ku)^2} .$$

Integrating this by parts we have
$$c_1(k^2 - 1)\left[+ \frac{\cos^{-1} u}{k(1 - ku)} + \frac{1}{k}\int \frac{du}{(1 - ku)\sqrt{(1 - u^2)}} \right]$$
$$= c_1(k^2 - 1)\left[+ \frac{\cos^{-1} u}{k(1 - ku)} + \frac{1}{k}\int \frac{dz}{\sqrt{\{(k^2 - 1)z^2 + 2z - 1\}}} \right]$$

with $(1 - ku) = 1/z$, so that finally we have
$$c_1(k^2 - 1)\left[+ \frac{\cos^{-1} u}{k(1 - ku)} + \frac{1}{k\sqrt{(k^2 - 1)}} \log\left\{ \frac{(k^2 - 1)z + 1}{\sqrt{(k^2 - 1)}} + \sqrt{\{(k^2 - 1)z^2 + 2z - 1\}} \right\} \right]$$

which apart from constant terms can be written
$$c_1(k^2 - 1)\left[+ \frac{\cos^{-1} u}{k(1 - ku)} + \frac{1}{k\sqrt{(k^2 - 1)}} \log\left\{ \frac{k(k - u) + k\sqrt{(k^2 - 1)}\sqrt{(1 - u^2)}}{(1 - ku)} \right\} \right]$$

or in terms of x,
$$\frac{1}{k}(kx - c_1)\cos^{-1}\frac{(x - kc_1)}{(kx - c_1)} + \frac{c_1\sqrt{(k^2 - 1)}}{k} \log\{x + \sqrt{(x^2 - c_1^2)}\} ,$$
since
$$\frac{k(k - u)}{1 - ku} = \frac{kx}{c_1}$$
and
$$\frac{\sqrt{(1 - u^2)}}{(1 - ku)} = \frac{1}{c_1}\sqrt{\left(\frac{x^2 - c_1^2}{k^2 - 1}\right)}$$

II.1.3. The integrals
$$\int x \cos^{-1}\left(\frac{x - k\beta y}{kx - \beta y}\right) dx \quad \text{and} \quad \int x \cos^{-1}\left(\frac{x + k\beta y}{kx + \beta y}\right) dx .$$

Again we write $c_1 = \beta y$ and $- \beta y$ respectively, so that both integrals can be considered in the form,
$$\int x \cos^{-1}\left(\frac{x - kc_1}{kx - c_1}\right) dx .$$

We make the same substitution as in (2) and obtain

$$c_1^2(k^2 - 1) \int (\cos^{-1} u) \frac{(k - u)}{(1 - ku)^3} du$$

$$= \frac{c_1^2(k^2 - 1)^2}{2k^2} \int \cos^{-1} u \, d\left(\frac{1}{(1 - ku)^2}\right) + \frac{c_1^2(k^2 - 1)}{k} \int \frac{\cos^{-1} u}{(1 - ku)^2} du \, .$$

The second integral is evaluated in (2), so we need only consider the first term. Integrating by parts we get

$$\frac{c_1^2(k^2 - 1)^2}{2k^2} \left\{\frac{\cos^{-1} u}{(1 - ku)^2}\right\} + \frac{c_1^2(k^2 - 1)^2}{2k^2} \int \frac{du}{(1 - ku)^2 \sqrt{(1 - u^2)}} \, .$$

To evaluate the remaining integral consider the function

$$f = \frac{\sqrt{(1 - u^2)}}{(1 - ku)} \, .$$

Then

$$\frac{df}{du} = \frac{k\sqrt{(1 - u^2)}}{(1 - ku)^2} - \frac{u}{(1 - ku)\sqrt{(1 - u^2)}}$$

$$= \frac{k - u}{(1 - ku)^2 \sqrt{(1 - u^2)}}$$

$$= \left(\frac{k^2 - 1}{k}\right) \frac{1}{(1 - ku)^2 \sqrt{(1 - u^2)}} + \frac{1}{k} \frac{1}{(1 - ku)\sqrt{(1 - u^2)}} \, .$$

Thus

$$\int \frac{du}{(1 - ku)^2 \sqrt{(1 - u^2)}} = \frac{k}{(k^2 - 1)} \frac{\sqrt{(1 - u^2)}}{(1 - ku)} - \frac{1}{k^2 - 1} \int \frac{du}{(1 - ku)\sqrt{(1 - u^2)}} \, ,$$

which in terms of x becomes (see (2)),

$$\frac{k}{c_1(k^2 - 1)^{3/2}} \sqrt{(x^2 - c_1^2)} - \frac{1}{(k^2 - 1)^{3/2}} \log\{x + \sqrt{(x^2 - c_1^2)}\} \, .$$

Collecting terms, we have finally

$$\int x \cos^{-1}\left(\frac{x - kc_1}{kx - c_1}\right) dx$$

$$= \frac{c_1^2 \sqrt{(k^2 - 1)}}{2k^2} \log\{x + \sqrt{(x^2 - c_1^2)}\} + \frac{c_1}{k^2}(kx - c_1) \cos^{-1}\left(\frac{x - kc_1}{kx - c_1}\right)$$

$$+ \frac{1}{2k^2}(kx - c_1)^2 \cos^{-1}\left(\frac{x - kc_1}{kx - c_1}\right) + \frac{c_1 \sqrt{(k^2 - 1)}}{2k} \sqrt{(x^2 - c_1^2)}$$

apart from a constant term.

On inserting βy and $- \beta y$ for c_1 we have the two integrals required.

42

II.1.4.
$$\int \sqrt{\left(\frac{x+c_1}{x-c_2}\right)}\, dx .$$

Let
$$u^2 = \frac{x+c_1}{x-c_2} ,$$

then
$$x - c_2 = \frac{(c_1+c_2)}{u^2-1} .$$

Then the integral is
$$\int u \frac{dx}{du}\, du$$

$$= \int \left[(x-c_2) + u\frac{dx}{du} - \frac{(c_1+c_2)}{u^2-1} \right] du$$

$$= u(x-c_2) - \frac{(c_1+c_2)}{2} \log\left(\frac{u-1}{u+1}\right) .$$

Or in terms of x it is
$$\sqrt{\{(x-c_2)(x+c_1)\}} - \frac{(c_1+c_2)}{2} \log\left\{ \frac{\sqrt{(x+c_1)} - \sqrt{(x-c_2)}}{\sqrt{(x+c_1)} + \sqrt{(x-c_2)}} \right\}$$

II.1.5.
$$\int X \sqrt{\left(\frac{X+c_1}{X-c_2}\right)}\, dX$$

Let
$$u^2 = \frac{X+c_1}{X-c_2} ,$$

so that
$$X - c_2 = \frac{(c_1+c_2)}{u^2-1} .$$

The integral becomes
$$\int X u \frac{dX}{du}\, du .$$

To evaluate this we note that
$$\frac{d}{du}\left\{ \frac{u}{2}(X-c_2)^2 \right\} = Xu\frac{dX}{du} - c_2 u\frac{dX}{du} + \frac{(X-c_2)^2}{2}$$

$$= Xu\frac{dX}{du} - c_2 u\frac{dX}{du} + \frac{(c_1+c_2)^2}{2(u^2-1)^2} .$$

Thus
$$\int Xu\frac{dX}{du}\, du = \frac{u}{2}(X-c_2)^2 + \left\{ u(X-c_2) - \frac{(c_1+c_2)}{2}\log\left(\frac{u-1}{u+1}\right) \right\} c_2$$

$$- \frac{(c_1+c_2)^2}{2} \int \frac{du}{(u^2-1)^2} .$$

This last integral is easily evaluated with the substitution
$$u = \sec\theta ,$$

and is
$$\int \frac{du}{(u^2-1)^2} = -\frac{1}{2}\left\{ \frac{u}{u^2-1} + \frac{1}{2}\log\left(\frac{u-1}{u+1}\right) \right\} .$$

Thus

$$\int Xu\frac{dX}{du}\,du = \frac{u(X-c_2)^2}{2} + c_2\left\{u(X-c_2) - \frac{(c_1+c_2)}{2}\log\left(\frac{u-1}{u+1}\right)\right\}$$

$$+ \frac{(c_1+c_2)^2}{4}\left[\frac{u}{u^2-1} + \frac{1}{2}\log\left(\frac{u-1}{u+1}\right)\right]$$

$$= \frac{u}{2}(X^2 - c_2{}^2) + \frac{u(c_1+c_2)^2}{4(u^2-1)} - \frac{(c_1+c_2)(3c_2-c_1)}{8}\log\left(\frac{u-1}{u+1}\right)$$

$$= \frac{\sqrt{\{(X+c_1)(X-c_2)\}}}{4}(2X + c_1 + 3c_2)$$

$$- \frac{(c_1+c_2)(3c_2-c_1)}{8}\log\left\{\frac{\sqrt{(X+c_1)} - \sqrt{(X-c_2)}}{\sqrt{(X+c_1)} + \sqrt{(X-c_2)}}\right\}.$$

II.2. *Some Integrals Required in the Sonic Theory.*—Here we use the following abbreviations:

$$F_0 = \frac{1}{\pi}\left[\frac{y-y_0}{y_l}\log F_1 + \sqrt{\left(1 - \frac{y^2}{y_l{}^2}\right)}\cos^{-1}\frac{y_0}{y_l}\right],$$

$$F_1 = \frac{y_l{}^2 - yy_0 + \sqrt{(y_l{}^2 - y_0{}^2)}\sqrt{(y_l{}^2 - y^2)}}{y_l|y_0 - y|}.$$

Then the following integrals can be checked by differentiation:

$$\int yy_l F_0\,dy = \frac{1}{6\pi}\left[(y-y_0{}^2)(2y+y_0)\log F_1 - (y_l{}^2 - y_0{}^2)^{3/2}\cos^{-1}\frac{y}{y_l}\right.$$

$$\left. - (y-y_0)\sqrt{(y_l{}^2 - y_0{}^2)}\sqrt{(y_l{}^2 - y^2)} - 2(y_l{}^2 - y^2)^{3/2}\cos^{-1}\frac{y_0}{y_l}\right]$$

$$\int y_l F_0\,dy = \frac{1}{2\pi}\left[(y-y_0)^2\log F_1 - \sqrt{(y_l{}^2 - y_0{}^2)}\sqrt{y_l{}^2 - y^2)} + y\sqrt{(y_l{}^2 - y^2)}\cos^{-1}\frac{y_0}{y_l}\right.$$

$$\left. + \cos^{-1}\frac{y}{y_l}\left\{y_0\sqrt{(y_l{}^2 - y_0{}^2)} - y_l{}^2\cos^{-1}\frac{y_0}{y_l}\right\}\right].$$

They enable us to calculate forces and moments acting on the wing, on the aileron and the 'complementary' aileron (*see* Section).

For the calculation of the pitching moment on a wing with a moving tip ($y_0 = $ const) and a straight leading edge ($y_l = x\cot\Lambda$, $dx = \tan\Lambda\,dy_l$), we require the integrals:

$$\frac{1}{s^3}\int\left(\int_{-y_l}^{y_l} y_l F_0\,dy\right)dy_l = \frac{1}{2\pi}\int\left\{\cos^{-1}\frac{y_0}{y_l} - \frac{y_0}{y_l}\sqrt{\left(1 - \frac{y_0{}^2}{y_l{}^2}\right)}\right\}\frac{y_l{}^2\,dy_l}{s^3}$$

$$= \frac{1}{\pi}\left[\frac{y_l{}^2}{2s^2}\left\{\frac{y_l}{3s}\cos^{-1}\frac{y_0}{y_l} - \frac{y_0}{s}\sqrt{\left(1 - \frac{y_0{}^2}{y_l{}^2}\right)}\right\}\right.$$

$$\left. + \frac{y_0 y_l{}^2}{6s^3}\left\{\sqrt{\left(1 - \frac{y_0{}^2}{y_l{}^2}\right)}\frac{y_0{}^2}{y_l{}^2}\log\frac{y_l + \sqrt{(y_l{}^2 - y_0{}^2)}}{|y_0|}\right\}\right]$$

and

$$\frac{1}{s^3}\int_{y_0}^{s}\left(\int_{-y_l}^{y_l} y_l F_0\,dy\right)dy_l = \frac{1}{6\pi}\left[\cos^{-1}\frac{y_0}{s} - 2\frac{y_0}{s}\sqrt{\left(1 - \frac{y_0{}^2}{s^2}\right)}\right.$$

$$\left. + \frac{y_0{}^3}{s^3}\log\frac{s + \sqrt{(s^2 - y_0{}^2)}}{|y_0|}\right]$$

44

TABLE 1

Low-Speed Results $(M = 0)$

Wing aspect ratio	Control span ratio s_ξ/s	Method of fairing	Antisymmetrical control deflection		Symmetrical control deflection			Incidence		
			$-l_\xi$	b_2	b_2	a_2	$-m_2$	a_1	$-m_1$	b_1
2·31	0·261	Multhopp .. unfaired	0·0788 0·0622	0·0925 0·0686	0·2257 0·0639	0·2704 0·2005	0·4371 0·3330	2·422	2·854	1·002
	0·3354	Multhopp ..	0·1124	0·1797	0·1961	0·4116	0·6480	2·422	2·854	0·8515
1·848	0·261	Multhopp .. unfaired	0·0680 0·0542	0·1143 0·0228	0·1382 0·0033	0·2391 0·1799	0·3903 0·3004	2·075	2·491	0·8038
	0·3354	Multhopp .. unfaired	0·0967 0·1077	0·1174 0·1663	0·1336 0·1823	0·3661 0·4126	0·5822 0·6529	2·075	2·491	0·6847
1·386	0·261	Multhopp .. elliptic fairing ..	0·0556 0·0518	0·0714 0·0536	0·0826 0·0493	0·2034 0·1858	0·3365 0·3116	1·684	2·062	0·5906
	0·3354	Multhopp .. elliptic fairing ..	0·0783 0·0852	0·0606 0·0830	0·0781 0·0840	0·3058 0·3418	0·4951 0·5459	1·684	2·062	0·4735

TABLE 2

Wing of Aspect Ratio 2·31 at Various Mach Numbers

M	s_ξ/s	Method of fairing	Antisymmetrical control deflection		Symmetrical control deflection			Incidence		
			$-l_\xi$	b_2	b_2	a_2	$-m_2$	a_1	$-m_1$	b_1
0	0·261	Multhopp .. unfaired	0·0788 0·0622	0·1925 0·0686	0·2257 0·0639	0·2704 0·2005	0·4371 0·3330	2·422	2·854	1·002
	0·3354	Multhopp ..	0·1124	0·1797	0·1961	0·4116	0·6480	2·422	2·854	0·8515
0·6	0·261	Multhopp .. unfaired	0·8850 0·0678	0·1429 0·0285	0·1728 0·0042	0·2988 0·2249	0·4879 0·3755	2·593	3·114	1·005
	0·3354	Multhopp .. unfaired	0·1208 0·1346	0·1468 0·2079	0·1670 0·2278	0·4516 0·5158	0·7278 0·8161	2·593	3·114	0·8559
0·8	0·261	Multhopp .. elliptic fairing ..	0·0927 0·0864	0·1190 0·0893	0·1377 0·0822	0·3389 0·3097	0·5609 0·5194	2·807	3·436	0·9843
	0·3354	Multhopp .. elliptic fairing ..	0·1306 0·1420	0·1010 0·1384	0·1302 0·1400	0·5096 0·5696	0·8252 0·9098	2·807	3·436	0·7892
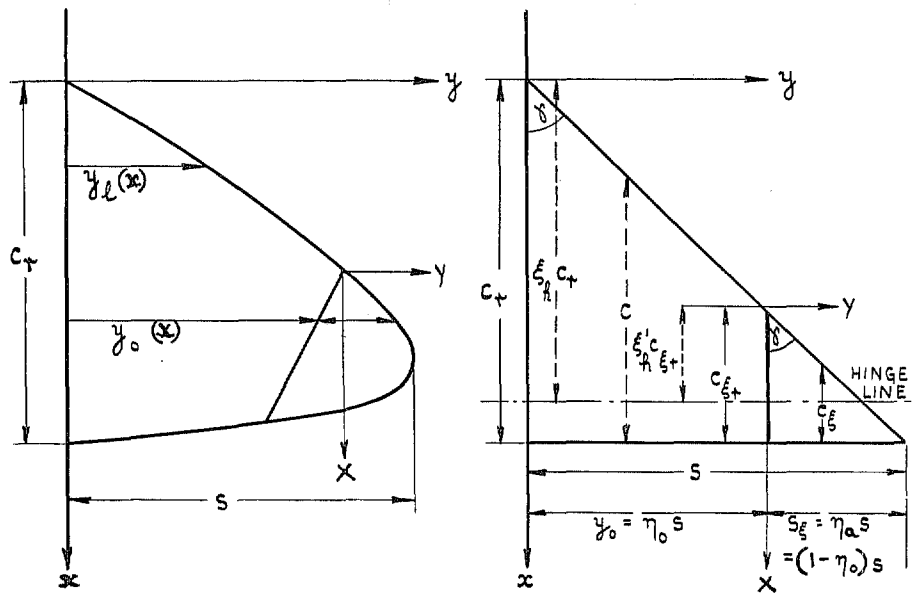
FIG. 1a.   An all-moving wing-tip control fitted to typical wings, the sections of which consist of one segment only.
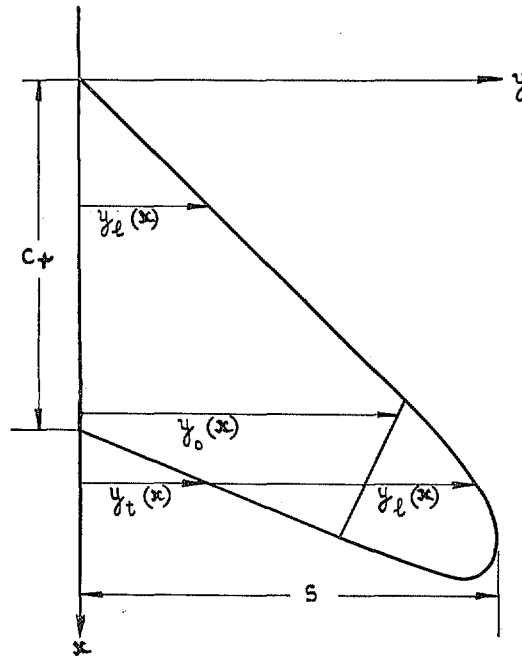
FIG. 1b.   An all-moving wing-tip control fitted to a wing, the spanwise sections of which consist, in part, of two segments.
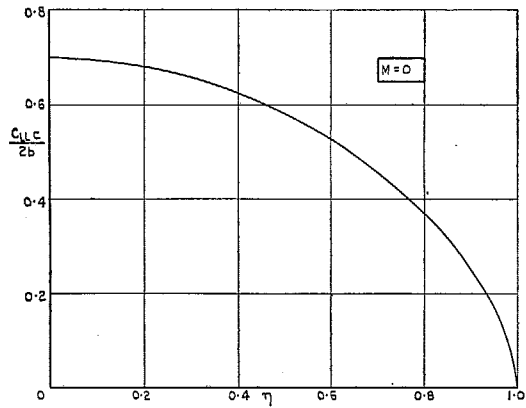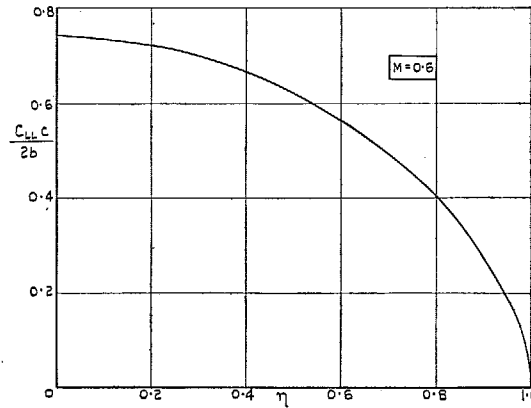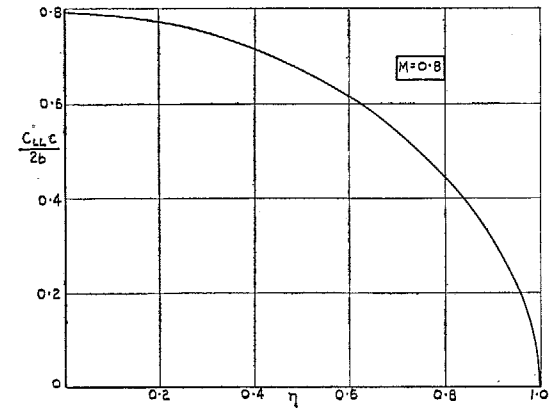
46

$M = 0$

$\dfrac{c_{LL}\,c}{2b}$

(a) SPANWISE LIFT DISTRIBUTION.

$M = 0.6$

$\dfrac{c_{LL}\,c}{2b}$

(a) SPANWISE LIFT DISTRIBUTION.

$M = 0.8$

$\dfrac{c_{LL}\,c}{2b}$

(a) SPANWISE LIFT DISTRIBUTION.

$M = 0$

h

(b) POSITION OF AERODYNAMIC CENTRE.

$M = 0.6$

h

(b) POSITION OF AERODYNAMIC CENTRE.

$M = 0.8$

h
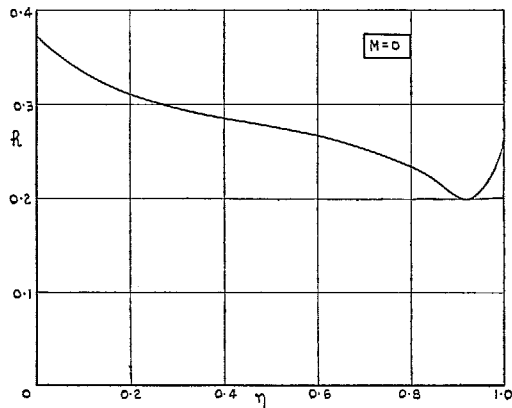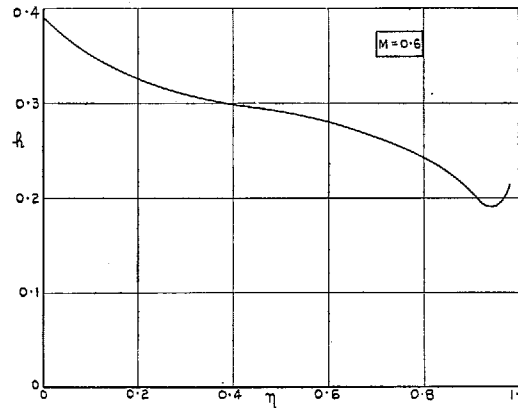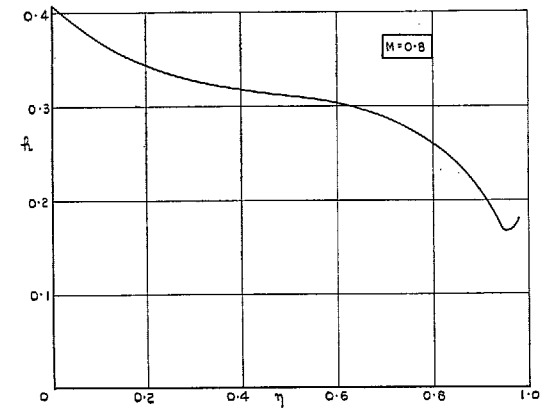
(b) POSITION OF AERODYNAMIC CENTRE.

FIGS. 2a and 2b. The span loading and aerodynamic-centre locus for a delta wing ($A = 2\cdot31$ at incidence at zero Mach number).

FIGS. 3a and 3b. The span loading and aerodynamic-centre locus for a delta wing ($A = 2\cdot31$, $M = 0\cdot6$ or $A = 1\cdot848$, $M = 0$) at incidence.

FIGS. 4a and 4b. Span loading and aerodynamic-centre locus for a delta wing ($A = 2\cdot31$, $M = 0\cdot8$ or $A = 1\cdot386$, $M = 0$) at incidence.
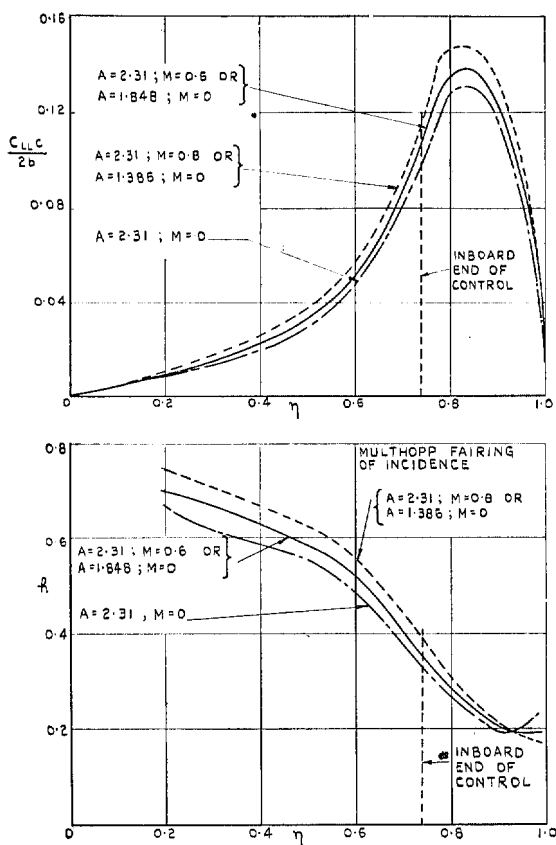
FIG. 5. Comparison of spanwise loading and aerodynamic-centre locus due to antisymmetric control deflection for a delta wing $(A = 2 \cdot 31)$ at $M = 0$, $0 \cdot 6$ and $0 \cdot 8$ or for three delta wings $(A = 2 \cdot 31, 1 \cdot 848,$ and $1 \cdot 386)$ at low speed $(M = 0)$ (Control span ratio $0 \cdot 261$).
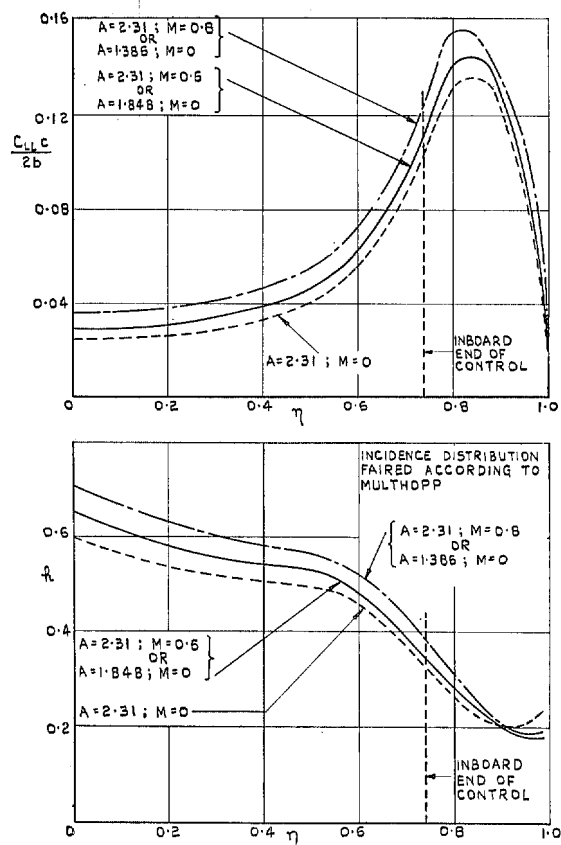
FIG. 6. Spanwise loading and aerodynamic-centre locus for a delta wing $(A = 2 \cdot 31)$ at $M = 0$, $0 \cdot 6$ and $0 \cdot 8$ or three delta wings $(A = 2 \cdot 31, 1 \cdot 848$ and $1 \cdot 386)$ at $M = 0$ fitted with controls of span ratio $0 \cdot 261$ deflected symmetrically.
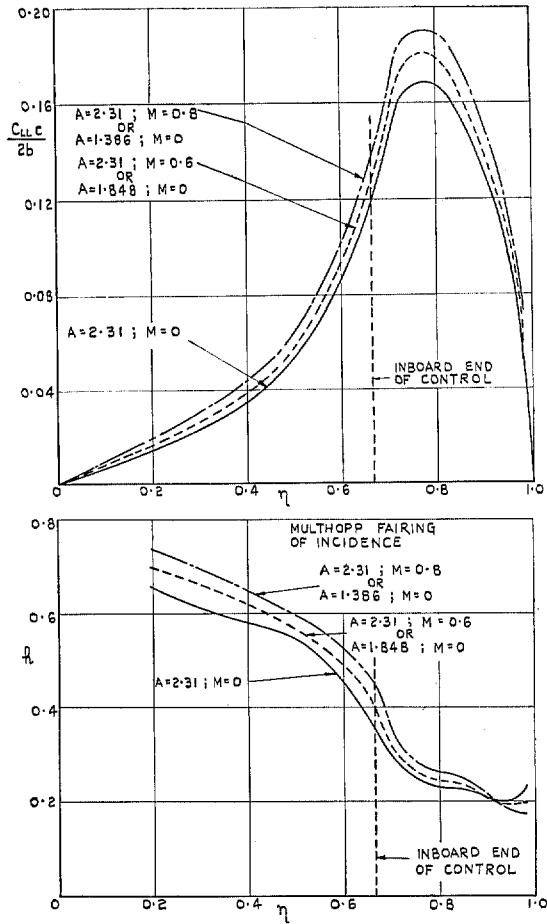
FIG. 7. Comparison of the span loading
and aerodynamic-centre locus for a delta
wing $(A = 2 \cdot 31)$ at $M = 0$, $0 \cdot 6$ and $0 \cdot 8$
or for three delta wings $(A = 2 \cdot 31, 1 \cdot 848$
and $1 \cdot 386)$ at $M = 0$ with controls of span
ratio $0 \cdot 335$ deflected antisymmetrically.
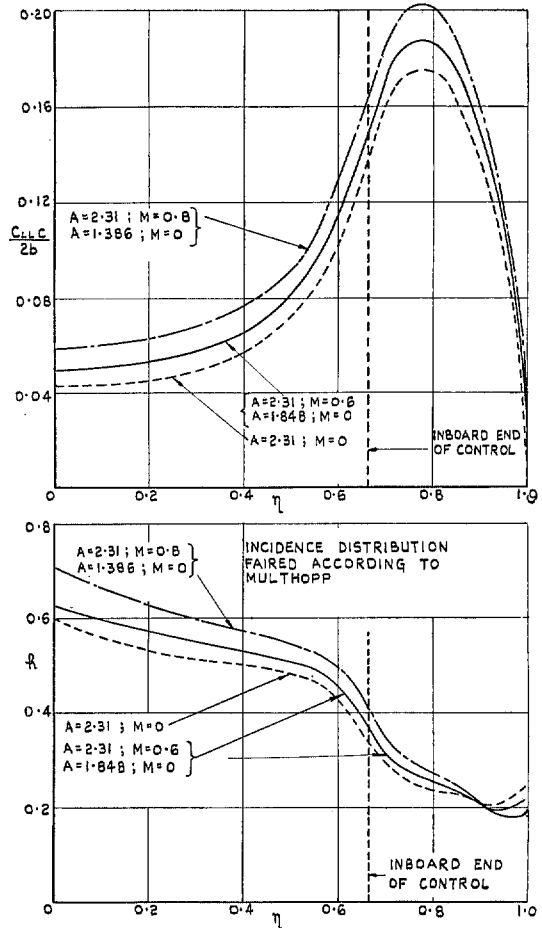
FIG. 8. Comparison of spanwise loading
and aerodynamic-centre locus due to
symmetric deflection of control or span
ratio $0 \cdot 335$ for a delta wing $(A = 2 \cdot 31)$ at
$M = 0$, $0 \cdot 6$ and $0 \cdot 8$, or for three delta
wings $(A = 2 \cdot 31, 1 \cdot 848,$ and $1 \cdot 386)$ at low
speed $(M = 0)$.

49
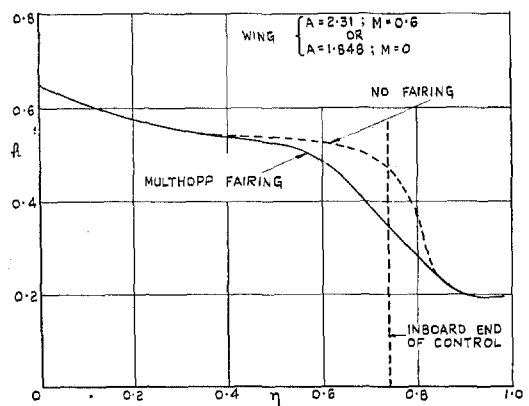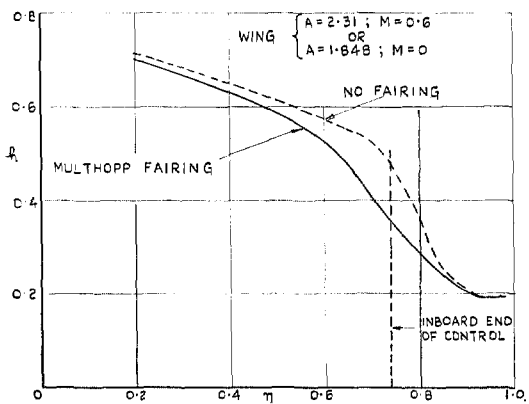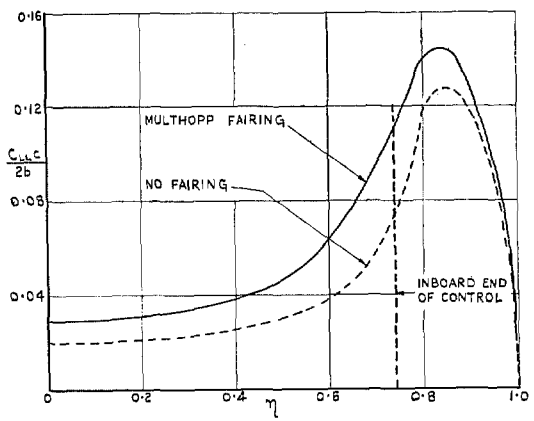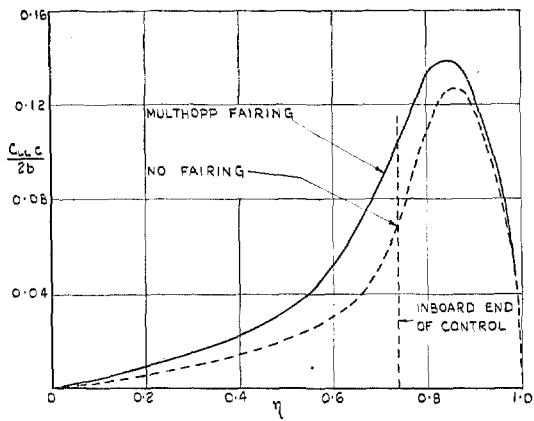
FIG. 9. Effect of method of fairing the discontinuity in incidence on the span loading and aerodynamic-centre locus due to antisymmetric deflection of controls of span ratio 0·261.

FIG. 10. Effect of method of fairing the discontinuity in incidence on the span loading and aerodynamic-centre locus due to symmetric deflection of controls of span ratio 0·261.
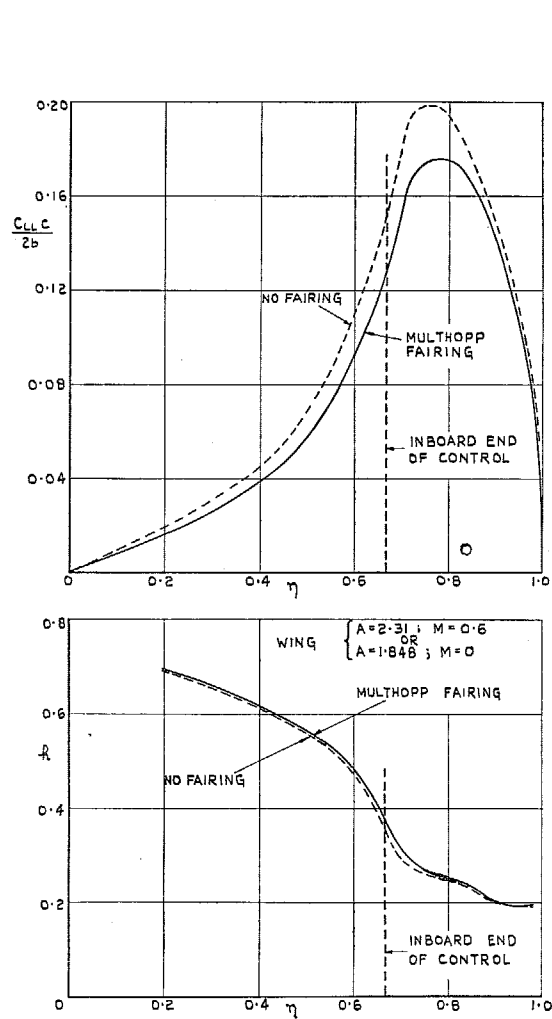
FIG. 11. Effect of fairing the incidence distribution on the span loading and aerodynamic-centre locus for antisymmetrical deflection of the controls of span ratio 0·335.
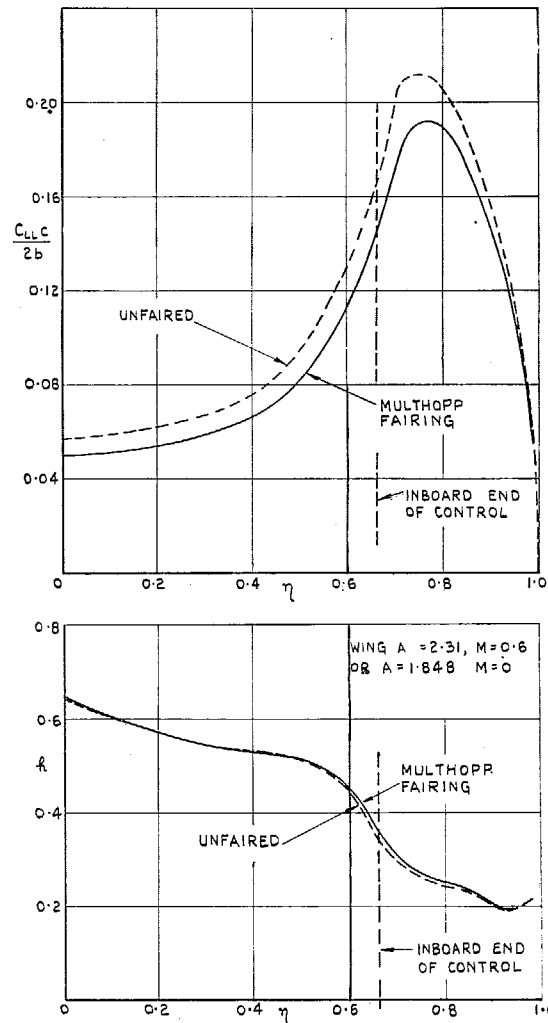
FIG. 12. Effect of fairing the incidence on the span loading and aerodynamic-centre locus for symmetrical deflection of controls of span ratio 0·335.
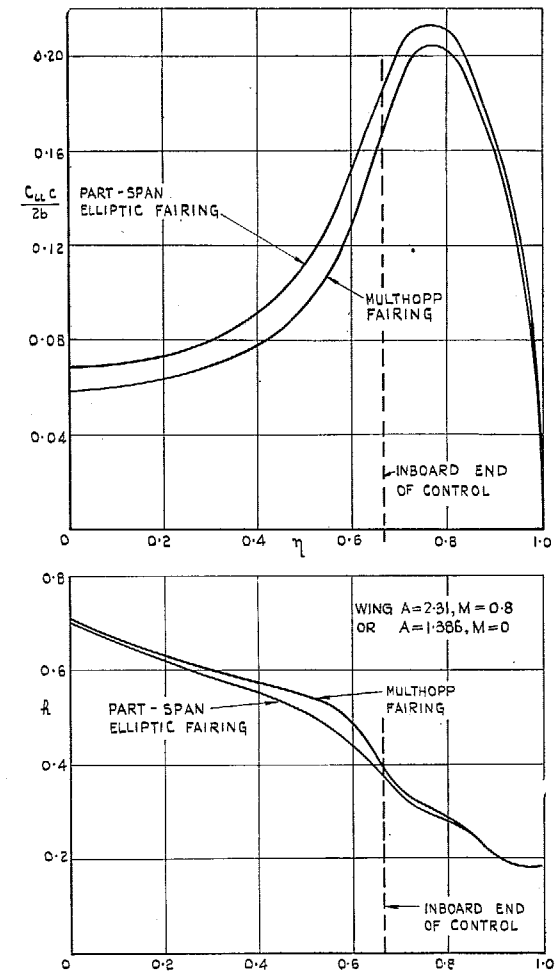
FIG. 13. Comparison of two methods of fairing the discontinuity in incidence for symmetrical deflection of a tip control of span ratio 0·335 on a delta wing.
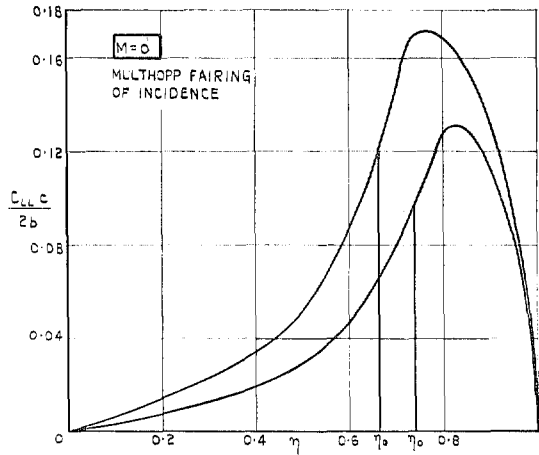
(a) SPANWISE LIFT DISTRIBUTION.
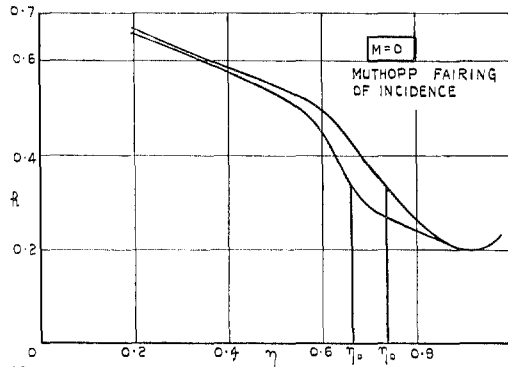
(b) POSITION OF AERODYNAMIC CENTRE.

FIGS. 14a and 14b. Effect of control span ratio on the span loading and aerodynamic-centre locus (Antisymmetrical deflection at $M = 0$).
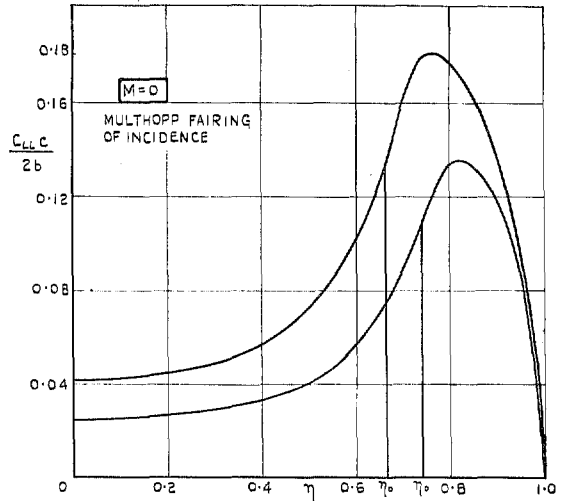
(a) SPANWISE LIFT DISTRIBUTION.
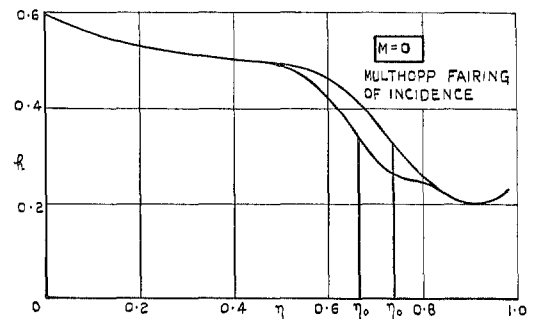
(b) POSITION OF AERODYNAMIC CENTRE.

FIGS. 15a and 15b. Effect of control span ratio on the span loading and aerodynamic-centre locus (Symmetrical deflection).

52

$$\frac{C_{LL}}{\xi A} \cdot \frac{c}{c_r}$$

$$= \frac{a_2(1-\eta)}{A}$$
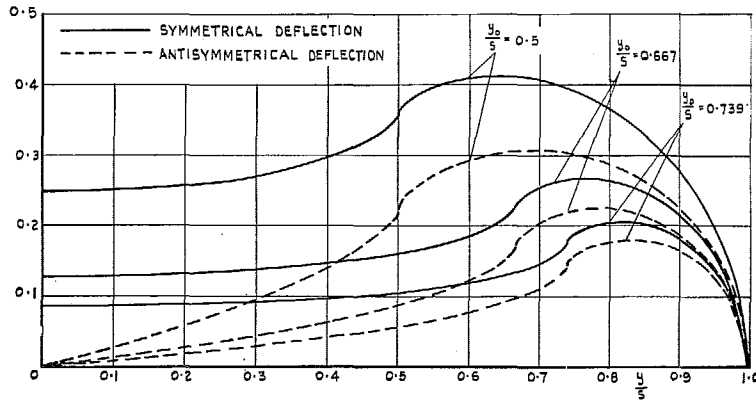
FIG. 16. Spanwise loadings due to symmetrical and antisymmetrical deflection of controls of various span ratio, fitted to a delta wing, at sonic speed.
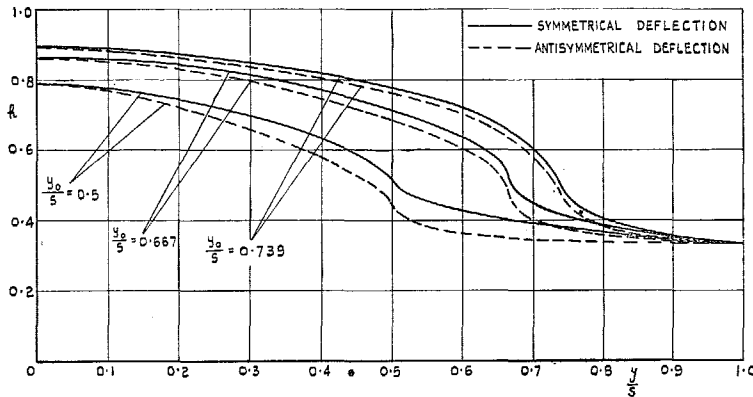
FIG. 17. Aerodynamic-centre locus for symmetrical and antisymmetrical deflection of controls of various span ratio, fitted to a delta wing, at sonic speed.
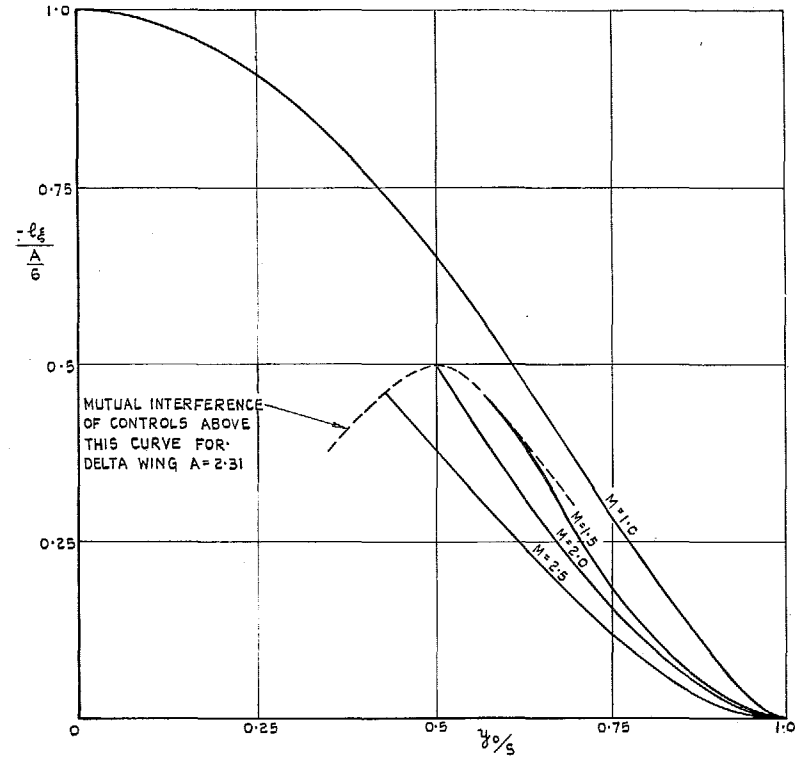
FIG. 18. Variation of rolling moment with control span for outboard controls at sonic and supersonic speeds.
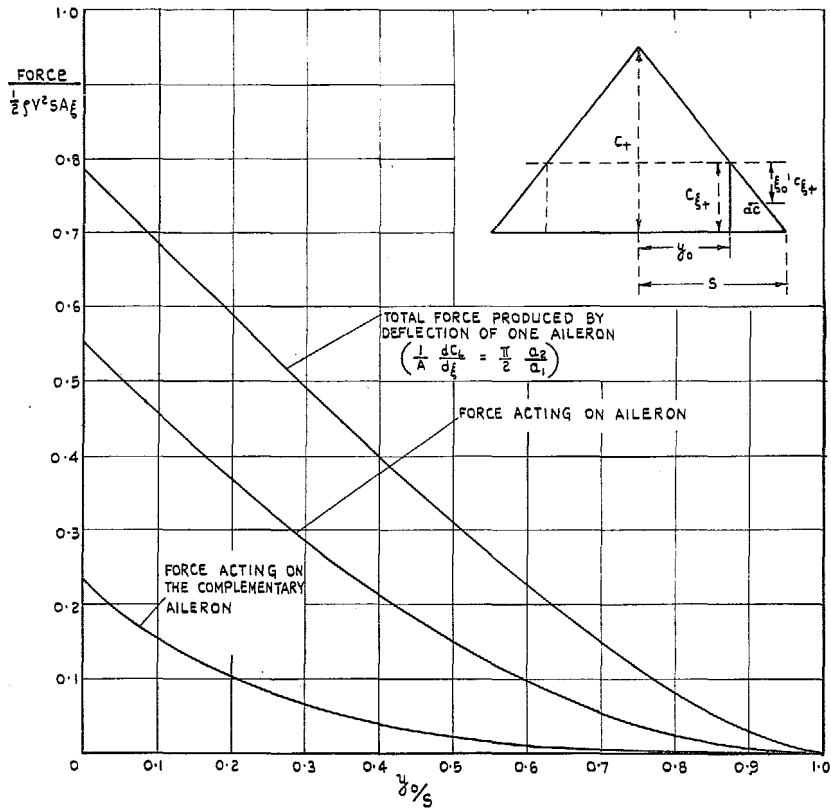
FIG. 19. Lift produced on the various parts of the wing by deflection of the control on one side only (Sonic speed).
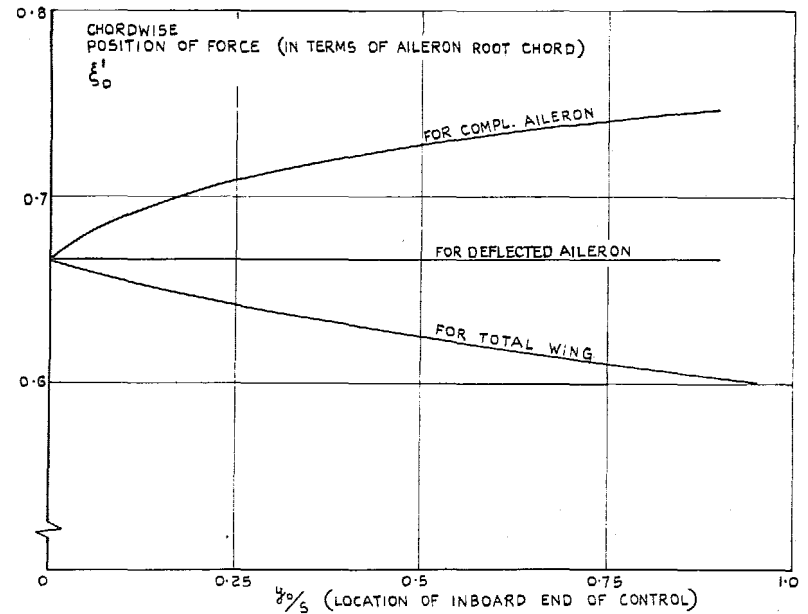
FIG. 20. Chordwise position of the aerodynamic centres of the loads on various parts of the wing due to deflection of the control on one side only (Sonic speed).
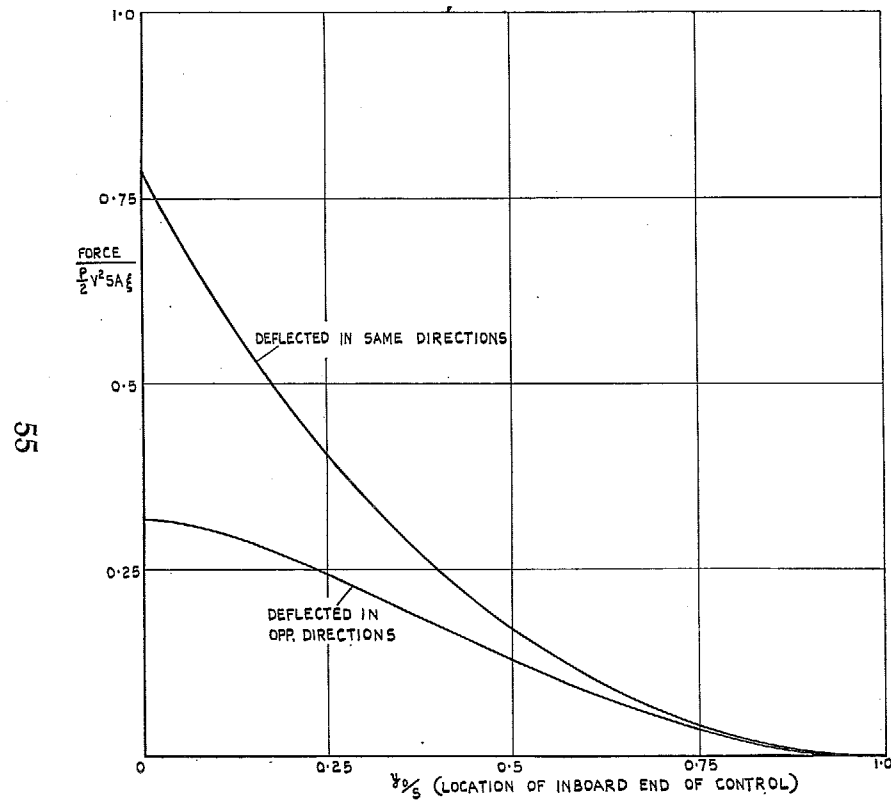
FIG. 21. Force on each control for symmetrical and antisymmetrical deflection of the controls (Sonic speed).
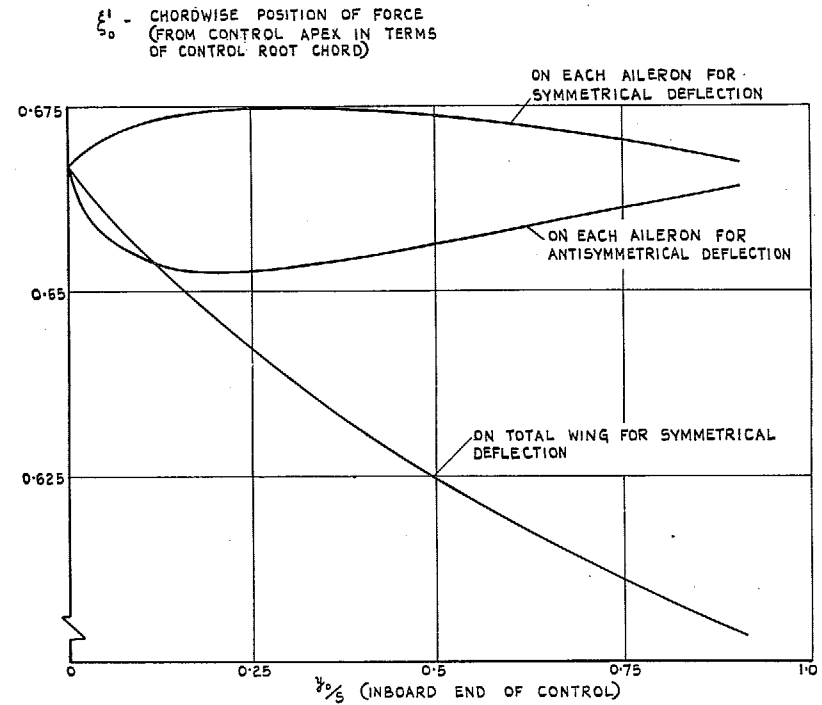
FIG. 22. Chordwise location of aerodynamic centres of the loads on each control and on total wing for symmetrical and antisymmetrical deflection of the controls (Sonic speed).

M = 0

M = 0·8

M = 1·0

M = 2·0

M = 2·5
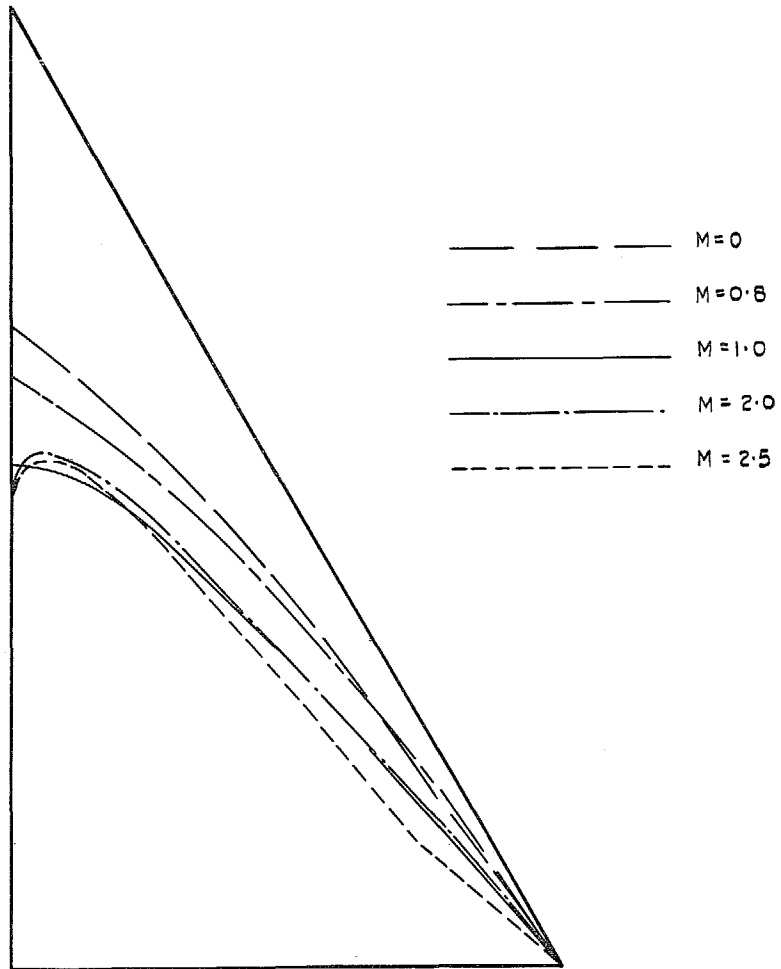
FIG. 23. Drift of the aerodynamic-centre locus
with increase of speed on control of span
ratio 0·261 deflected antisymmetrically.

M = 0

M = 0·8

M = 1·0

M = 2·0

M = 2·5
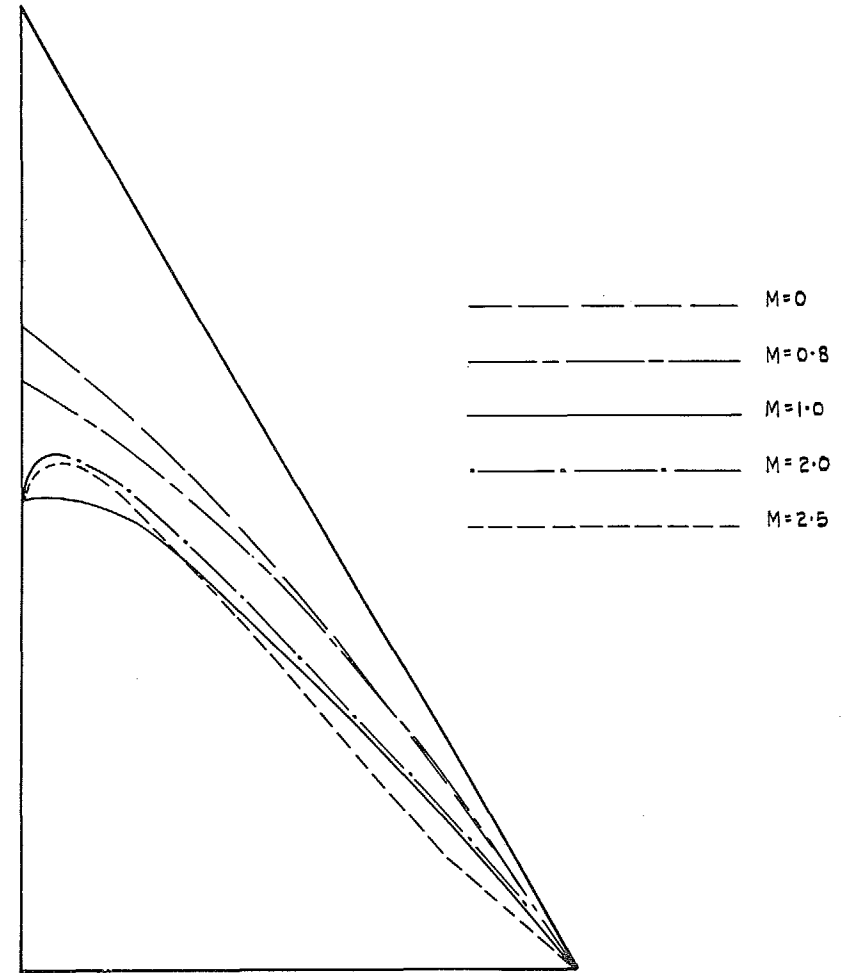
FIG. 24. Drift of the aerodynamic-centre locus
with increase of speed on a control of span
ratio 0·261 deflected symmetrically.
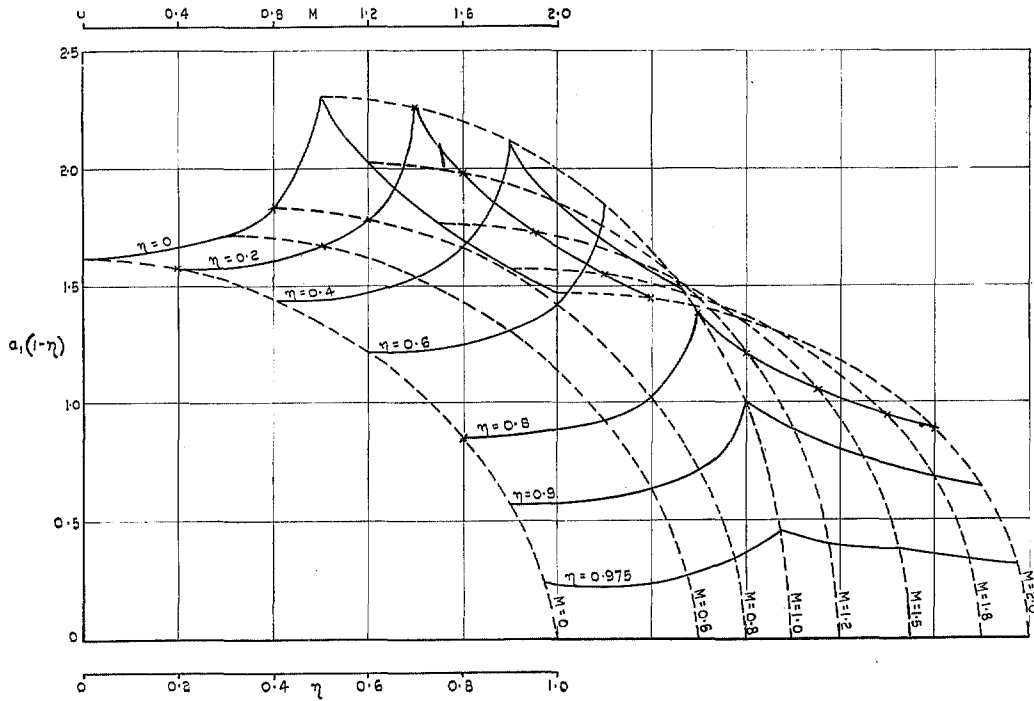
FIG. 25.   Variation of the local lift-coefficient slope with spanwise location and Mach number for a delta wing of aspect ratio 2·31.
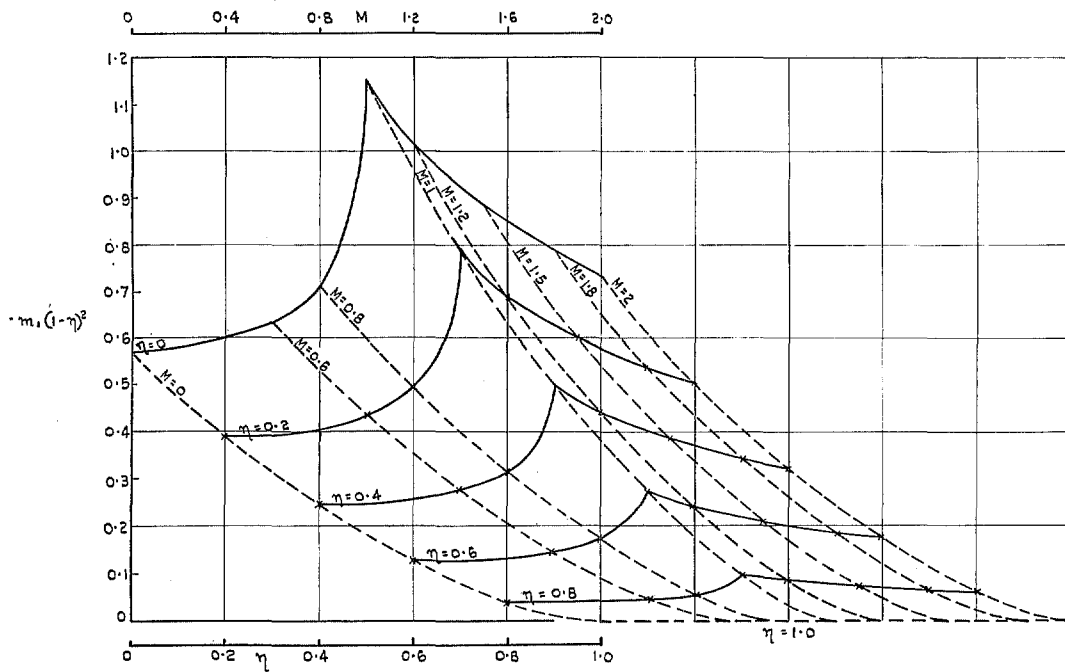
FIG. 26.   Variation of the local pitching moment due to incidence with spanwise location and Mach number for a delta wing of aspect ratio 2·31.
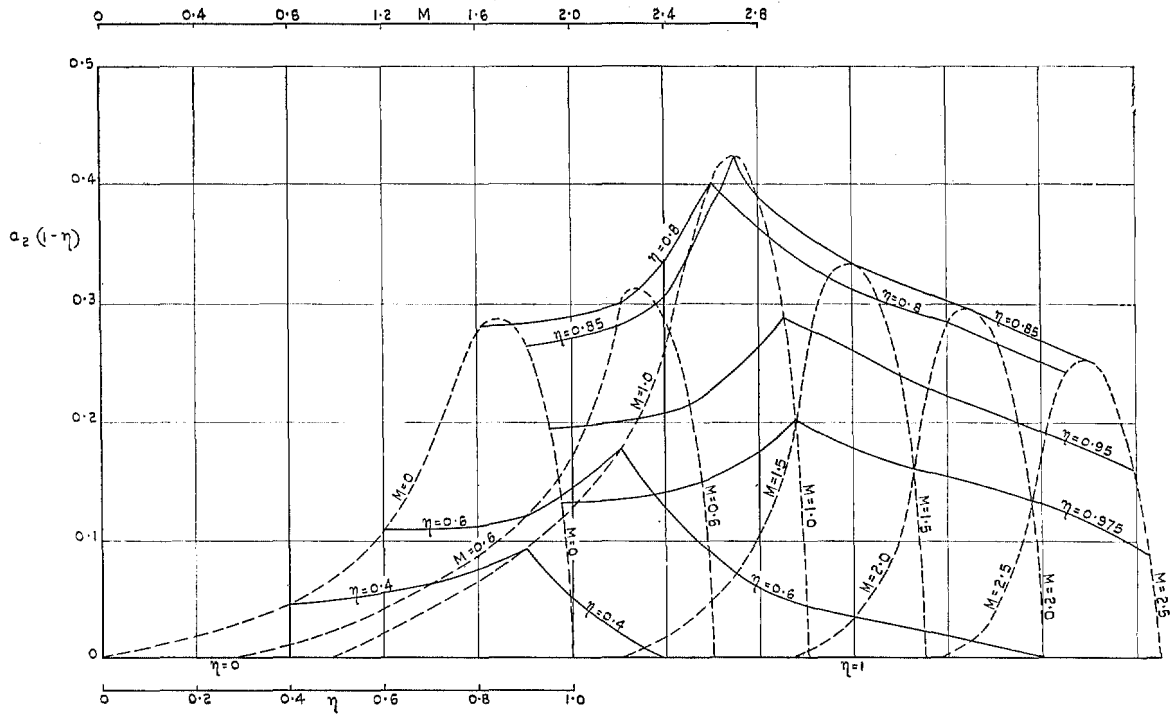
FIG. 27. Variation of the local lift coefficient due to antisymmetrical control deflection with spanwise location and Mach number for a delta wing, $A = 2 \cdot 31$, with controls of span ratio $0 \cdot 261$.
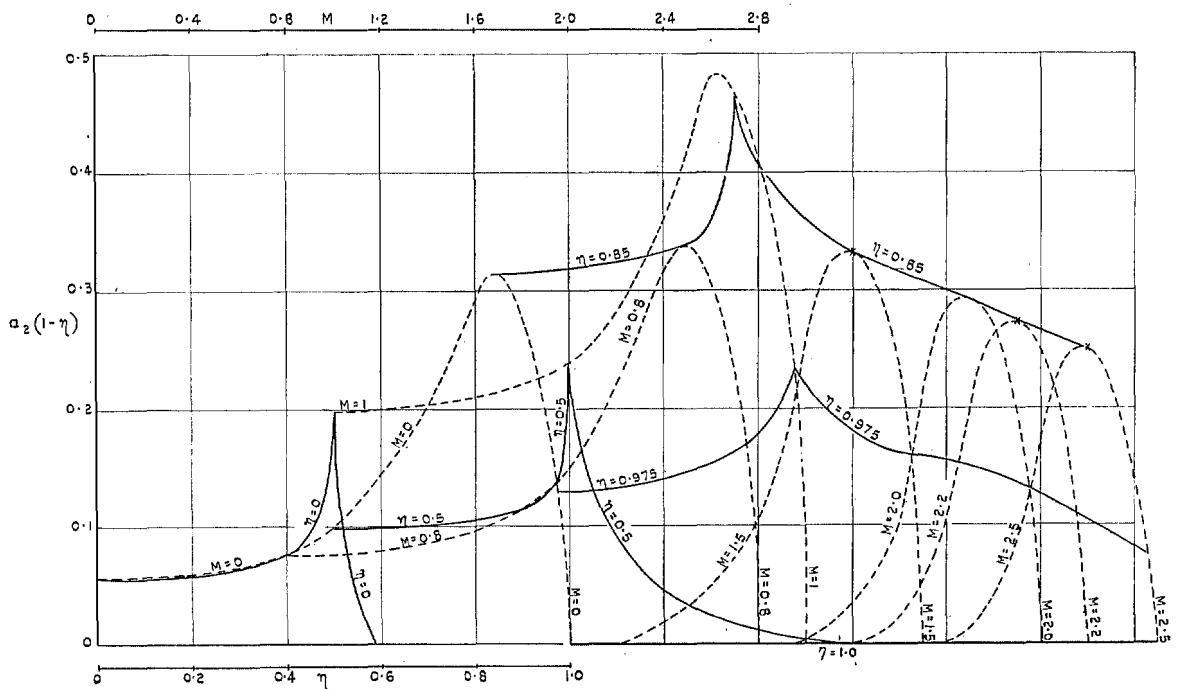
FIG. 28. Variation of the local lift coefficient due to symmetrical deflection of controls of span ratio $0 \cdot 261$ with spanwise location and Mach number for a delta wing $A = 2 \cdot 31$.

58
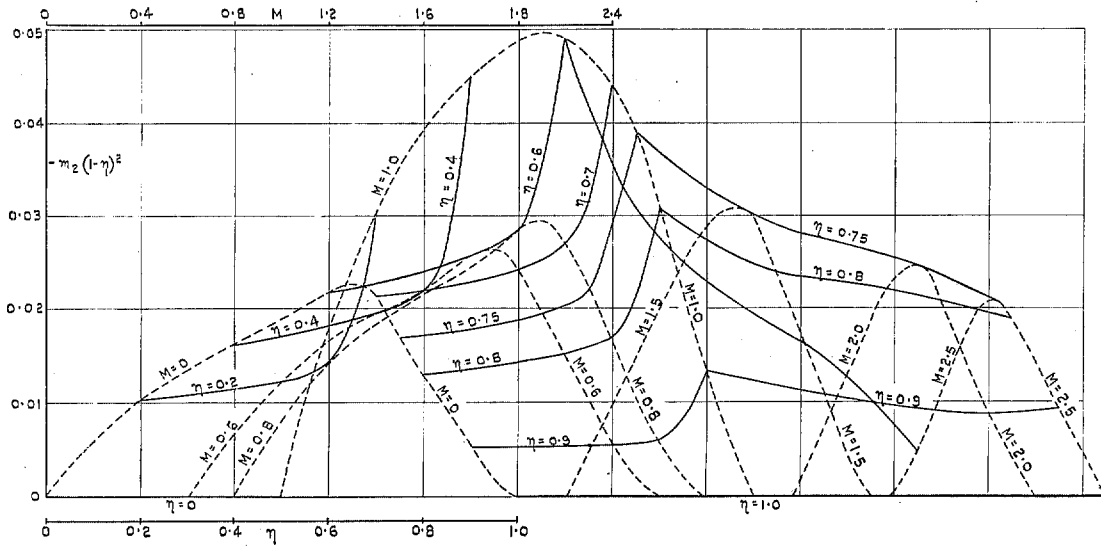
FIG. 29. Variation of the local pitching-moment coefficient with spanwise location and Mach number for antisymmetrical deflection of controls of span ratio 0·261 fitted to a delta wing of aspect ratio 2·31.
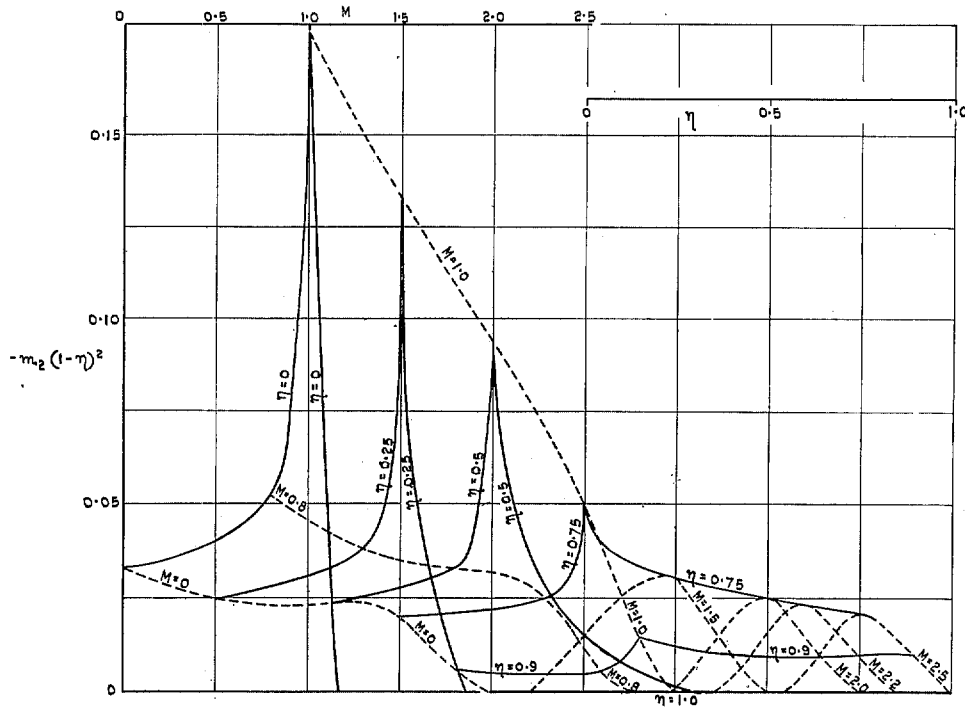
FIG. 30. Variation of the local pitching-moment coefficient due to symmetrical deflection of controls of span ratio 0·261 with spanwise location and Mach number for a delta wing $A = 2·31$.

59

(a) VARIATION OF ℓ_ξ WITH MACH. NUMBER

(b) VARIATION OF ℓ_ξ WITH WING ASPECT RATIO AT M=0.
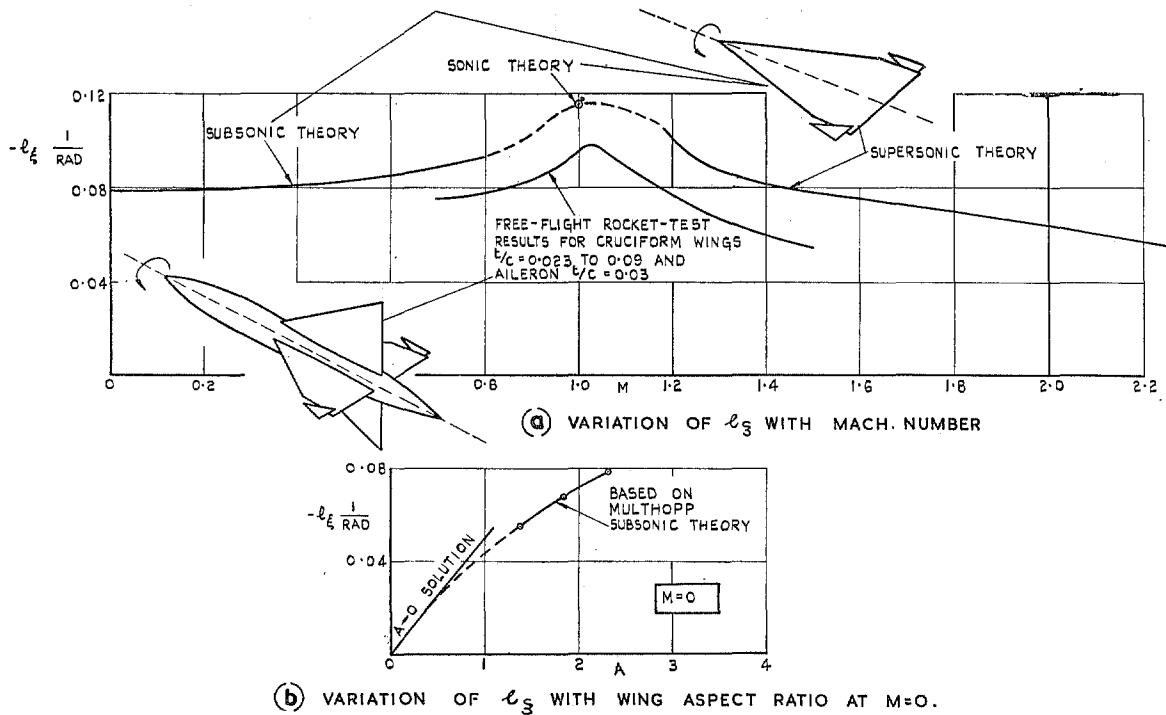
FIGS. 31a and 31b.   Rolling moment produced by deflection of half-delta ailerons of span
ratio 0·261 (Theory and experiment).
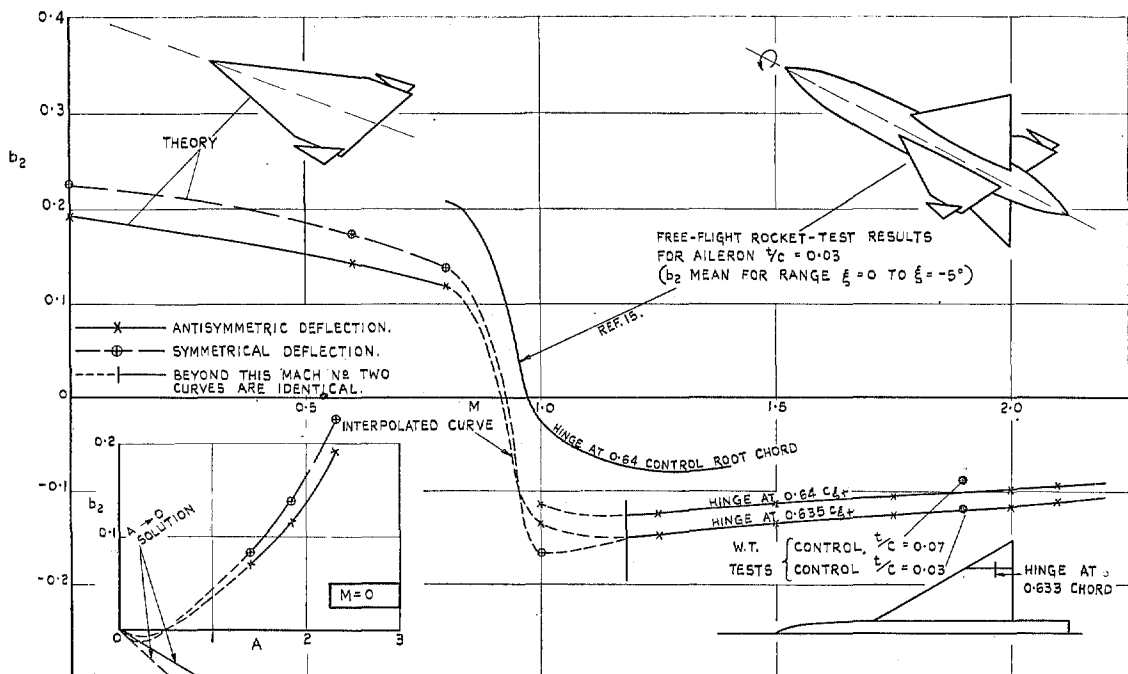
FIG. 32.   Variation of the hinge-moment derivative b_2 with Mach number for half-delta controls
on a delta wing of aspect ratio 2·31, and the variation of b_2 with wing aspect ratio at $M = 0$
(Control span ratio 0·261).
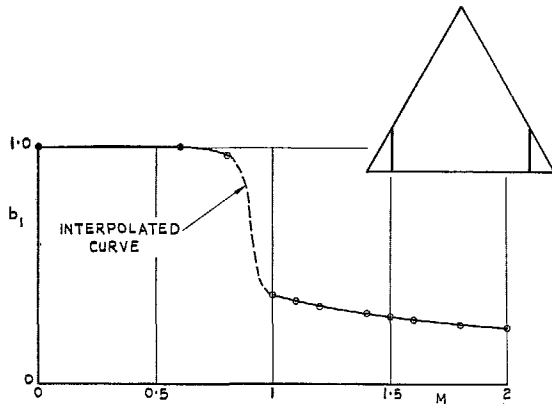
(a) VARIATION OF b_1 WITH MACH NUMBER.
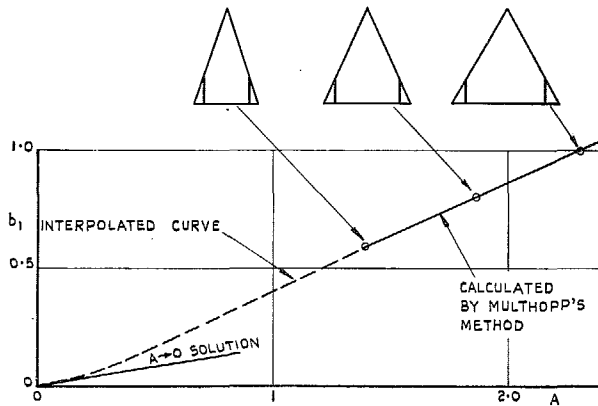
(b) VARIATION OF b_1 WITH ASPECT RATIO AT M = O.

FIGS. 33a and 33b. Effect of variation of Mach number and aspect ratio ($M = 0$) on b_1 for half-delta controls, span ratio $0 \cdot 261$, fitted to delta wings.

X THEORETICAL HINGE LINE FOR ZERO $C_H/_\xi$
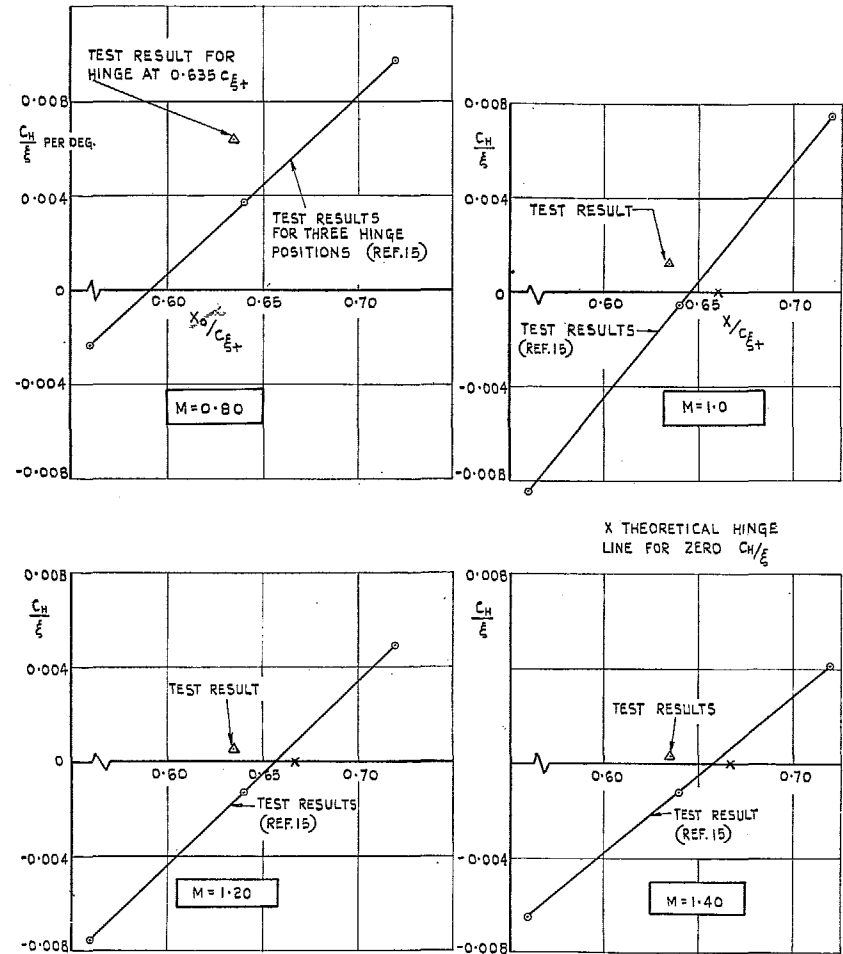
FIG. 34. Variation of mean slope of hinge-moment coefficient (per degree) over control-angle range 0 to −5-deg. at various Mach numbers.
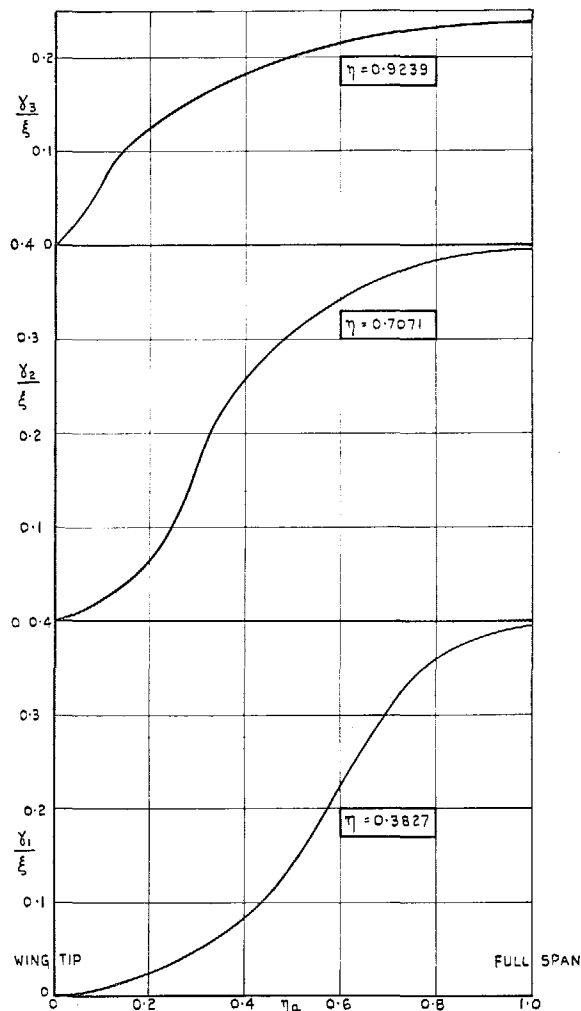
FIG. 35. Variation of span-loading co-
efficients (γ/ξ) at three spanwise stations
for the limit $A \rightarrow 0$ with aileron span ratio
$(\eta_a = 1 - \eta_0)$ for antisymmetrical deflection.
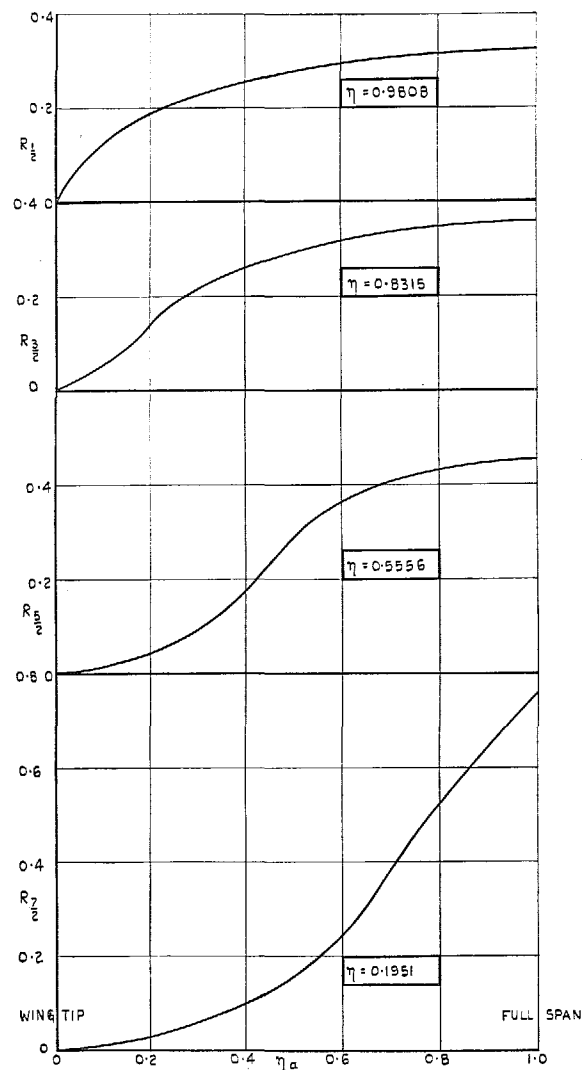
FIG. 36. Interpolation functions for use in
evaluating the loading at the intermediate
stations indicated (Antisymmetrical con-
trol deflection).
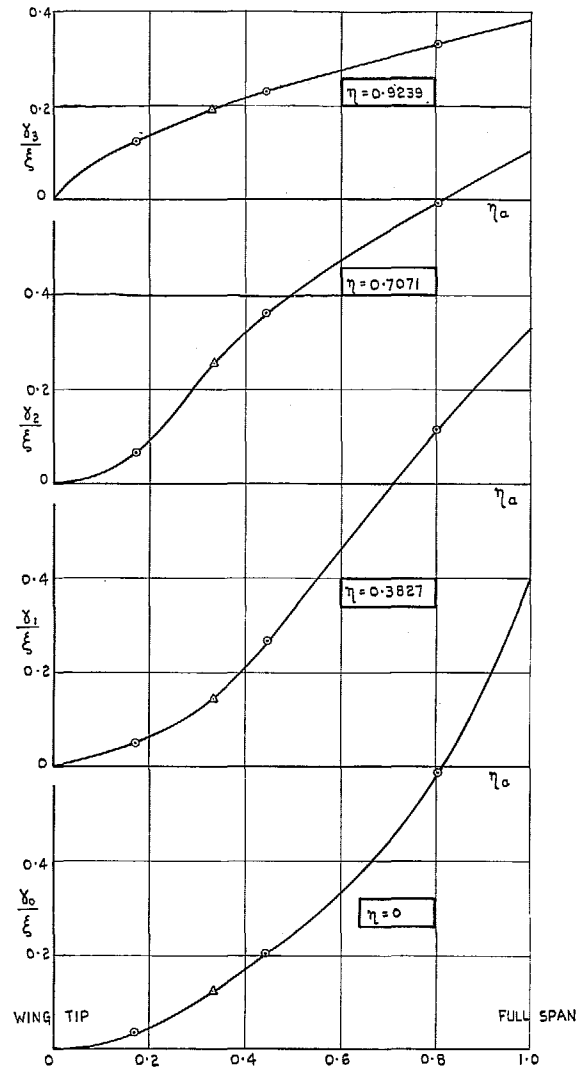
FIG. 37. Variation of span loading co-
efficients (γ/ξ) at the pivotal stations, for
$A \to 0$ and symmetrical deflection, with
control span ratio $(\eta_a = 1 - \eta_0)$.
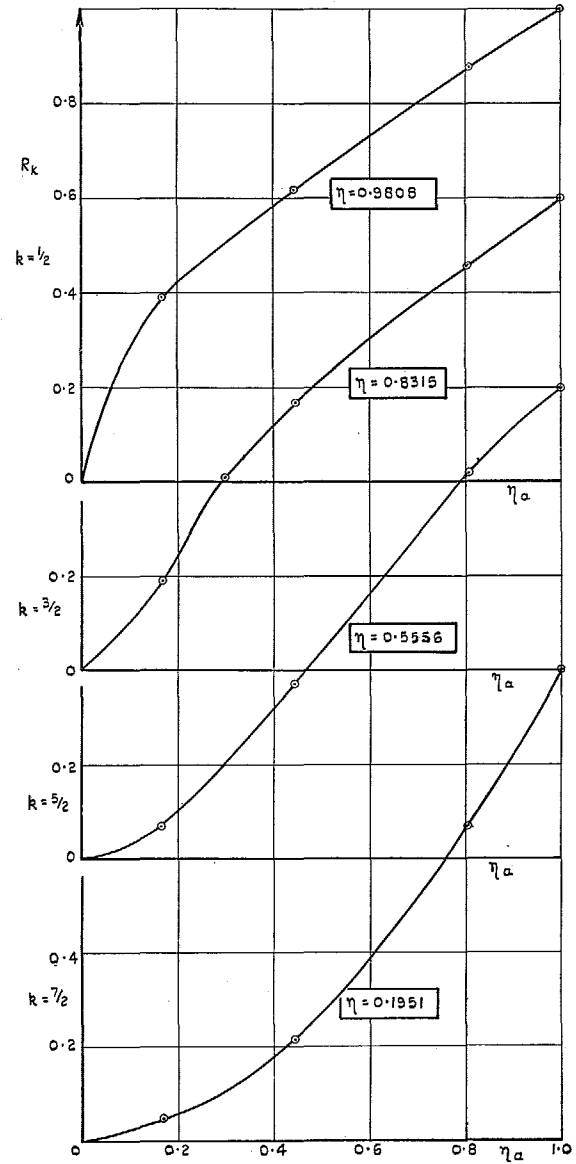
FIG. 38. Interpolation functions for use in
evaluating the loading at the intermediate
stations indicated (Symmetrical control
deflection).
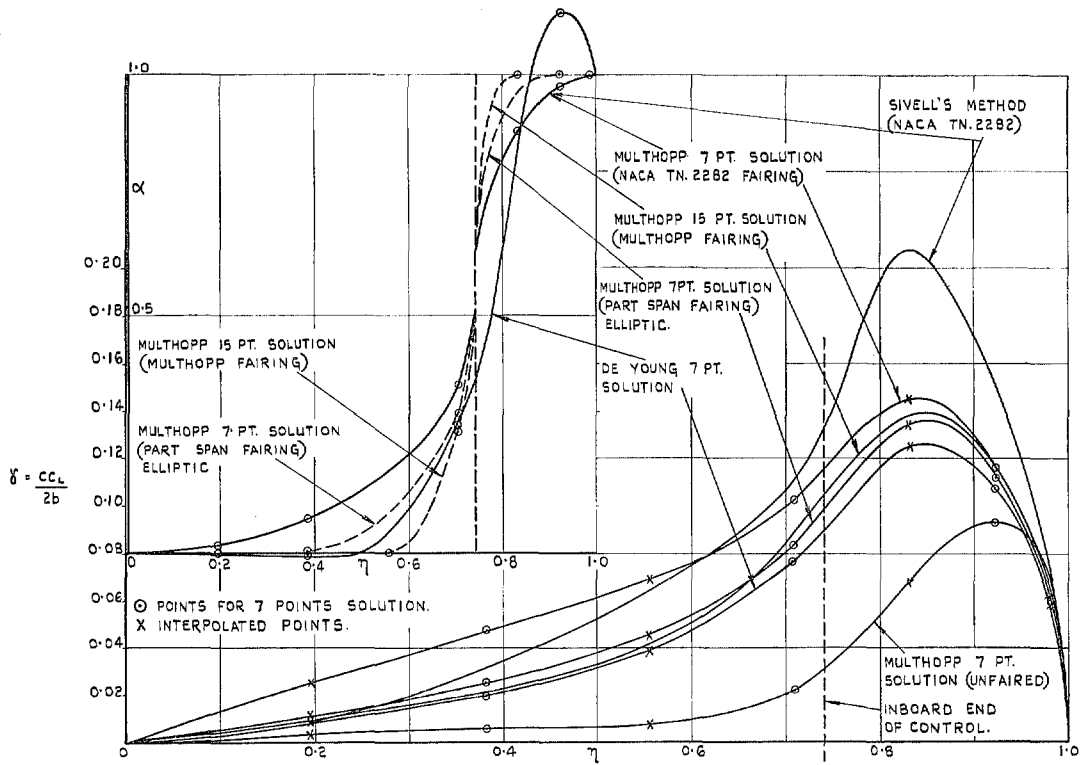
FIG. 39. Comparison of three methods of calculating the spanwise loading due to antisymmetric deflection of half-delta controls, span ratio 0·261, on wing of aspect ratio 1·848.

Publications of the Aeronautical Research Council